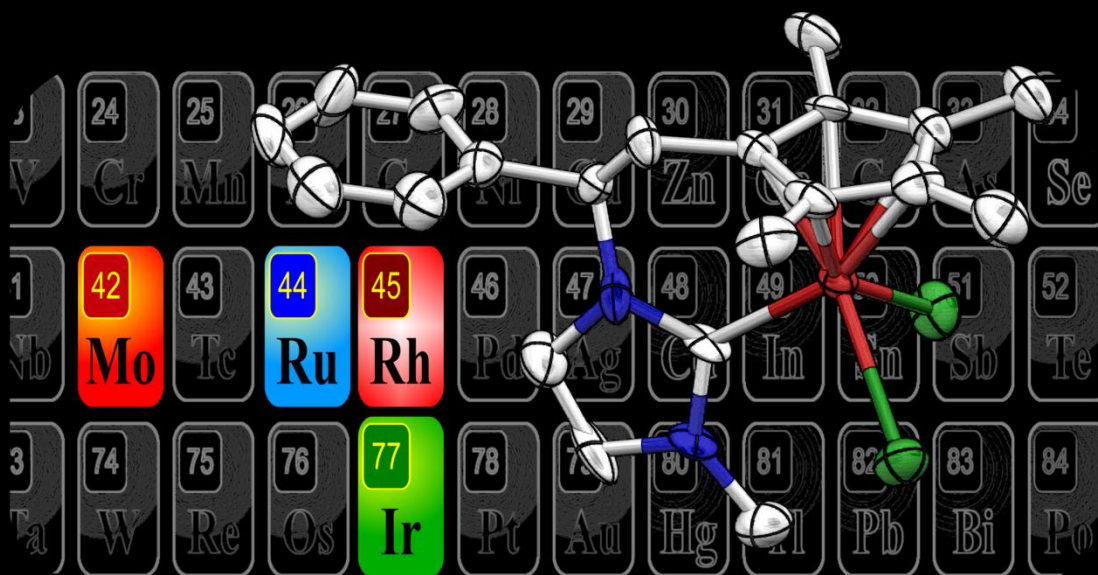


# Cyclopentadienyl-Functionalised N-Heterocyclic Carbenes:

Synthesis, Coordination to Mo, Ru, Rh  
and Ir and Catalytic Applications.

André Pontes da Costa



Dissertation presented to obtain the Ph.D degree in Chemistry  
Instituto de Tecnologia Química e Biológica | Universidade Nova de Lisboa

Oeiras,  
June, 2011



INSTITUTO  
DE TECNOLOGIA  
QUÍMICA E BIOLÓGICA  
/UNL



Knowledge Creation



# Cyclopentadienyl-Functionalised N-Heterocyclic Carbenes:

Synthesis, Coordination to Mo, Ru, Rh  
and Ir and Catalytic Applications.

André Pontes da Costa

Supervisor: Dr. Beatriz Royo

Instituto de Tecnologia Química e Biológica | Universidade Nova de Lisboa

Co-supervisor: Prof. Dr. Eduardo Peris

Departament de Química Inorgànica i Orgànica | Universitat Jaume I

Dissertation presented to obtain the Ph.D degree in Chemistry

Instituto de Tecnologia Química e Biológica | Universidade Nova de Lisboa

Apoio financeiro da FCT e do FSE no âmbito do Quadro Comunitário de Apoio:  
SFRH/BD/28490/2006



UNIÃO EUROPEIA

Fundo Social Europeu

Oeiras,  
June, 2011

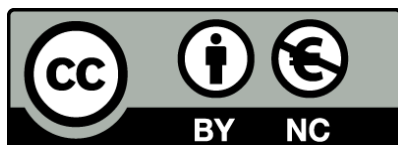


INSTITUTO  
DE TECNOLOGIA  
QUÍMICA E BIOLÓGICA  
/UNL

Knowledge Creation



Copyright © 2011 André Pontes da Costa



Esta obra foi licenciada com uma Licença Creative Commons  
Atribuição-Usó Não-Comercial 3.0 Unported.  
<http://creativecommons.org/licenses/by-nc/3.0/>

This work is licensed under a Creative Commons  
Attribution-NonCommercial 3.0 Unported License.  
<http://creativecommons.org/licenses/by-nc/3.0/>

Title: *Cyclopentadienyl-Functionalised N-Heterocyclic Carbenes: Synthesis,  
Coordination to Mo, Ru, Rh and Ir and Catalytic Applications.*

Author: *André Pontes da Costa*

Supervisor: *Dr. Beatriz Royo*

Co-supervisor: *Prof. Dr. Eduardo Peris*

Cover: *ITQB-UNL, André Pontes da Costa and Leonardo Mendes*

Picture: *Mo, Ru, Rh and Ir atoms highlighted in a partial periodic table and the  
molecular diagram of the first reported Cp\*-functionalised NHC complex (10).*

ISBN: 978-989-20-2413-4

1<sup>st</sup> edition, Oeiras, June, 2011

1<sup>st</sup> edition (revised), Oeiras, December, 2011

# CONTENTS

|                                   |       |
|-----------------------------------|-------|
| List of Abbreviations and Symbols | vii   |
| List of Figures                   | ix    |
| List of Schemes                   | xiii  |
| List of Tables                    | xv    |
| Acknowledgements                  | xvii  |
| Sumário                           | xxiii |
| Abstract                          | xxvii |

---

|           |  |          |
|-----------|--|----------|
| <b>1.</b> | <b>INTRODUCTION</b>                          | <b>1</b> |
| 1.1.      | N-Heterocyclic Carbenes                      | 3        |
| 1.2.      | The nature of NHCs                           | 5        |
| 1.3.      | NHCs as ligands                              | 5        |
|           | 1.3.1. Steric properties of NHCs,            | 7        |
|           | 1.3.2. Electronic properties of NHCs,        | 8        |
| 1.4.      | Donor functionalised NHCs                    | 10       |
|           | 1.4.1. NHCs with neutral chelates,           | 10       |
|           | 1.4.2. Cyclopentadienyl-functionalised NHCs, | 11       |
| 1.5.      | References                                   | 13       |

---

## 2.

OBJECTIVES 19

---

## 3.

### SYNTHESIS OF CYCLOPENTADIENYL-FUNCTIONALISED IMIDAZOLIUM SALTS 23

---

|      |  |    |
|------|--|----|
| 3.1. | Abstract   | 25 |
| 3.2. | Introduction   | 26 |
| 3.3. | Results and discussion                               | 27 |
|      | 3.3.1. Synthesis of the imidazolium salts, 27        |    |
|      | 3.3.2. Characterisation of the imidazolium salts, 31 |    |
| 3.4. | Conclusions  | 33 |
| 3.5. | Experimental procedures                              | 34 |
|      | 3.5.1. Materials and methods, 34                     |    |
|      | 3.5.2. Synthesis and characterisation of 1-5, 34     |    |
| 3.6. | Acknowledgments                                      | 37 |
| 3.7. | References   | 38 |
| 3.8. | Supporting Information                               | 39 |

---

## 4.

### COORDINATION TO Mo AND APPLICATION IN OLEFIN EPOXIDATION 41

---

|      |   |    |
|------|---|----|
| 4.1. | Abstract  | 43 |
| 4.2. | Introduction  | 43 |
| 4.3. | Results and discussion                                | 45 |
|      | 4.3.1. Synthesis of the molybdenum complexes 6-9, 45  |    |
|      | 4.3.2. Characterisation of complexes 6-9, 46          |    |
|      | 4.3.3. Olefin epoxidation by complexes 6, 8 and 9, 49 |    |
| 4.4. | Conclusions   | 52 |
| 4.5. | Experimental procedures                               | 53 |
|      | 4.5.1. Materials and methods, 53                      |    |
|      | 4.5.2. Synthesis and characterisation of 6-9, 53      |    |
|      | 4.5.3. X-ray diffraction studies, 55                  |    |
| 4.6. | Acknowledgments                                       | 56 |
| 4.7. | References  | 56 |

---

|           |  |           |
|-----------|--|-----------|
| <b>5.</b> | <b>COORDINATION TO Rh AND Ir, APPLICATIONS IN HYDROGEN BORROWING CATALYSIS</b> | <b>59</b> |
| 5.1.      | Abstract   | 61        |
| 5.2.      | Introduction   | 62        |
| 5.3.      | Results and discussion   | 64        |
|           | 5.3.1. Coordination of Cp*-NHC ligands to Rh and Ir, 64                        |           |
|           | 5.3.2. Characterisation of the metal complexes, 66                             |           |
|           | 5.3.3. Intramolecular C-H activation studies, 71                               |           |
|           | 5.3.4. Catalysis, 75   |           |
| 5.4.      | Conclusions  | 82        |
| 5.5.      | Experimental procedures  | 82        |
|           | 5.5.1. Materials and methods, 82   |           |
|           | 5.5.2. Synthesis and characterisation, 83                                      |           |
|           | 5.5.3. Catalysis - standard procedures, 87                                     |           |
|           | 5.5.4. X-Ray diffraction studies, 87   |           |
| 5.6.      | Acknowledgments  | 88        |
| 5.7.      | References   | 88        |
| 5.8.      | Supporting Information   | 91        |

---

|           |  |           |
|-----------|--|-----------|
| <b>6.</b> | <b>COORDINATION TO Ru, RESOLUTION OF CHIRAL-AT-METAL COMPLEXES AND ISOMERISATION OF ALLYLIC ALCOHOLS</b> | <b>93</b> |
| 6.1.      | Abstract   | 95        |
| 6.2.      | Introduction   | 96        |
| 6.3.      | Results and discussion   | 97        |
|           | 6.3.1. Synthesis of ruthenium complexes, 97  |           |
|           | 6.3.2. Characterisation of <b>17</b> and <b>18</b> , 98  |           |
|           | 6.3.3. Enantiomeric resolution of chiral-at-metal complexes, 102   |           |
|           | 6.3.4. Catalysis, 104  |           |
| 6.4.      | Conclusions  | 107       |
| 6.5.      | Experimental procedures  | 108       |
|           | 6.5.1. Materials and methods, 108  |           |
|           | 6.5.2. Synthesis and characterisation, 109   |           |
|           | 6.5.3. X-Ray diffraction studies, 113  |           |
| 6.6.      | Acknowledgments  | 113       |

|      |                        |     |
|------|------------------------|-----|
| 6.7. | References             | 113 |
| 6.8. | Supporting information | 115 |

---

## **7. ENANTIOMERICALLY PURE CP-FUNCTIONALISED NHC LIGAND: SYNTHESIS AND COORDINATION TO Rh AND Ir** **119**

---

|      |   |     |
|------|---|-----|
| 7.1. | Abstract  | 121 |
| 7.2. | Introduction  | 122 |
| 7.3. | Results and discussion  | 123 |
|      | 7.3.1. Synthesis and characterisation of an enantiomerically pure Cp-imidazolium salt, 123                |     |
|      | 7.3.2. Synthesis and characterisation of Rh and Ir complexes containing the Cp-NHC ligand <b>21</b> , 124 |     |
| 7.4. | Conclusions   | 128 |
| 7.5. | Experimental procedures   | 129 |
|      | 7.5.1. Materials and methods, 129   |     |
|      | 7.5.2. Synthesis and characterisation, 129  |     |
| 7.6. | Acknowledgments   | 131 |
| 7.7. | References  | 132 |
| 7.8. | Supporting Information  | 132 |

---

## **8. FINAL DISCUSSION** **133**

---

|      |   |     |
|------|---|-----|
| 8.1. | Overview  | 135 |
| 8.2. | Synthesis of Cp-NHC proligands  | 137 |
| 8.3. | Synthesis of metal complexes and their applications in catalysis                      | 139 |
|      | 8.3.1. Synthesis of metal complexes containing the Cp-functionalised NHC ligands, 139 |     |
|      | 8.3.2. Synthesis of chiral-at-metal complexes, 142                                    |     |
|      | 8.3.3. Catalysis, 143   |     |
| 8.4. | Conclusions and outlook   | 148 |



## LIST OF ABBREVIATIONS AND SYMBOLS

|                       |  |
|-----------------------|--|
| $\%V_{\text{Bur}}$    | Buried volume  |
| [ ]                   | Encloses complexes or ions                                   |
| $\pm$                 | Racemic  |
| Bu                    | Butyl  |
| Cat                   | Catalyst   |
| cod                   | 1,5-cyclooctadiene   |
| Cp                    | $C_5H_5$   |
| Cp*                   | $C_5(CH_3)_5$  |
| Cp'-NHC               | Cp'-functionalized N-heterocyclic carbene                    |
| Cp <sup>Bz</sup>      | $C_5(CH_2Ph)_5$  |
| Cp <sup>x</sup> , Cp' | generic Cp type ligand (eg. Indenyl, Cp*, $C_5H_4R, \dots$ ) |
| Cy                    | Cyclohexyl   |
| D                     | Generalized neutral 2-electron donor ligand                  |
| DCE                   | 1,2-dichloroethane   |
| DFT                   | Density functional theory                                    |
| EA                    | Elemental analysis   |
| ESI                   | Electron-spray ionization (MS)                               |
| Flu                   | Fluorenyl  |
| HOMO                  | Highest occupied molecular orbital                           |
| <i>i</i> -            | <i>iso</i> -   |
| Imid                  | Imidazol   |

|            |   |
|------------|---|
| Ind        | Indenyl   |
| IR         | Infra red spectroscopy                          |
| <i>J</i>   | Coupling constant (NMR)                         |
| L          | Generalized ligand (either neutral or anionic)  |
| LUMO       | Lowest unoccupied molecular orbital             |
| Me         | Methyl  |
| Mes        | Mesityl   |
| MS         | Mass spectrometry                               |
| NHC        | N-heterocyclic carbene                          |
| NMR        | Nuclear Magnetic resonance                      |
| OAc, AcO   | Acetate   |
| Ox         | Oxidation                                       |
| Ph         | Phenyl  |
| Pr         | Propyl  |
| Red        | Reduction                                       |
| <i>t</i> - | <i>tert</i>                                     |
| TEP        | Tolman electronic parameter (cm <sup>-1</sup> ) |
| TfO        | Triflate  |
| THF        | Tetrahydrofurane                                |
| TON        | Turn over number                                |
| X          | Generalized anionic ligand (usually halogen)    |
| δ          | Chemical shift in ppm (NMR)                     |
| η          | Ligand hapacity                                 |
| μ          | Bridge ligand                                   |
| ν          | Frequency (cm <sup>-1</sup> )                   |
| Δ          | Reflux temperature                              |

# LIST OF FIGURES

|  |       |
|--|-------|
| <b>Figura 1.</b> Cp'-NHCs: coordenação a Mo, Ru, Rh e Ir.  | xxiii |
| <b>Figure 1.</b> Cp'-functionalised NHCs: coordination to Mo, Ru, Rh and Ir.   | xxv   |
| <b>Figure 1.1.</b> Space fill drawing of the X-ray structure of the first isolated free carbene, 1,3-di-1-adamantylimidazol-2-ylidene. | 3     |
| <b>Figure 1.2.</b> First metal-NHC complexes used in catalysis.  | 4     |
| <b>Figure 1.3.</b> Grubbs catalyst, from 1 <sup>st</sup> to 2 <sup>nd</sup> generation.  | 4     |
| <b>Figure 1.4.</b> Inductive (-I) and mesomeric (+M) effects in the stabilisation of NHCs.   | 5     |
| <b>Figure 1.5.</b> NHCs (A), phosphines (B).   | 6     |
| <b>Figure 1.6.</b> Schematic representation of %V <sub>Bur</sub> .   | 7     |
| <b>Figure 1.7.</b> Qualitative series of NHCs based on basicity.   | 8     |
| <b>Figure 1.8.</b> Schematic representation of the effect in $\nu_{CO}$ by introducing a more $\sigma$ -donor ligand.                  | 9     |
| <b>Figure 1.9.</b> Schematic draw of donor-functionalised NHC.   | 10    |
| <b>Figure 1.10.</b> Possible architectures with bis-NHCs ligands.  | 11    |
| <b>Figure 1.11.</b> First indenyl- and fluorenyl-functionalised NHCs.  | 11    |
| <b>Figure 3.1.</b> Cp'-functionalised imidazolium salts proligands 1-5.  | 25    |
| <b>Figure 3.2.</b> <sup>1</sup> H NMR spectrum of 1.   | 31    |
| <b>Figure 3.3.</b> <sup>1</sup> H NMR spectrum of 2.   | 32    |
| <b>Figure 3.4.</b> <sup>1</sup> H NMR spectrum of 3.   | 32    |
| <b>Figure 3.5.</b> <sup>1</sup> H NMR spectrum of 5.   | 33    |

|  |     |
|--|-----|
| <b>Figure 3.6.</b> $^{13}\text{C}$ NMR spectrum of <b>1</b> .  | 39  |
| <b>Figure 3.7.</b> $^{13}\text{C}$ NMR spectrum of <b>2</b> .  | 39  |
| <b>Figure 3.8.</b> $^{13}\text{C}$ NMR spectrum of <b>3</b> .  | 39  |
| <b>Figure 3.9.</b> $^1\text{H}$ NMR and $\{^1\text{H}\}$ $^{13}\text{C}$ NMR spectra of <b>4</b> .   | 40  |
| <b>Figure 3.10.</b> $^{13}\text{C}$ NMR spectrum of <b>5</b> .   | 40  |
| <b>Figure 4.1.</b> $(\text{Cp}^X\text{-NHC})\text{Mo}(\text{CO})_2\text{I}$ complexes.   | 43  |
| <b>Figure 4.2.</b> $\text{Cp}^*\text{MoO}_2\text{X}$ ( <b>A</b> ) and $\text{Cp}^*\text{Mo}(\text{CO})_3\text{X}$ ( <b>B</b> ).  | 44  |
| <b>Figure 4.3.</b> Some chiral $\text{Cp}^*\text{Mo}(\text{CO})_3\text{X}$ ( <b>C</b> and <b>D</b> ) and <i>ansa</i> - $\text{Cp}^*\text{Mo}(\text{CO})_3$ ( <b>E</b> and <b>F</b> ) used as pre-catalysts for olefin epoxidation. | 45  |
| <b>Figure 4.4.</b> Possible isolated isomers of complex <b>9</b> .   | 47  |
| <b>Figure 4.5.</b> Molecular diagram of complex <b>6</b> .   | 49  |
| <b>Figure 5.1.</b> Examples of “ $\text{Cp}^*\text{IrNHC}$ ” complexes.  | 63  |
| <b>Figure 5.2.</b> Dynamic kinetic resolution of alcohols mediated by “ $\text{Cp}^*\text{IrNHC}$ ” fragment.  | 64  |
| <b>Figure 5.3.</b> Examples of homo- and hetero-bimetallic complexes containing the “ $\text{Cp}^*\text{IrNHC}$ ” fragment.  | 64  |
| <b>Figure 5.4.</b> $\text{Cp}^*$ -functionalised NHC complexes of Rh and Ir.   | 65  |
| <b>Figure 5.5.</b> $^1\text{H}$ NMR and $\{^1\text{H}\}$ $^{13}\text{C}$ NMR spectra of complex <b>10</b> .  | 68  |
| <b>Figure 5.6.</b> $^1\text{H}$ NMR and $\{^1\text{H}\}$ $^{13}\text{C}$ NMR spectra of complex <b>15</b> .  | 69  |
| <b>Figure 5.7.</b> Molecular diagrams of (a) complex <b>10</b> , (b) complex <b>12</b> , (c) complex <b>13</b> , (d) complex <b>14</b> .   | 70  |
| <b>Figure 5.8.</b> Top view of the molecular diagrams of complexes <b>10</b> (a) and <b>12</b> (b).  | 72  |
| <b>Figure 5.9.</b> $^1\text{H}$ NMR and $\{^1\text{H}\}$ $^{13}\text{C}$ NMR spectra of complex <b>16</b> .  | 72  |
| <b>Figure 5.10.</b> Two perspectives of the molecular diagram of <b>16</b> .   | 74  |
| <b>Figure 5.11.</b> $^1\text{H}$ NMR and $\{^1\text{H}\}$ $^{13}\text{C}$ NMR spectra of complex <b>11</b> .   | 85  |
| <b>Figure 5.12.</b> $^1\text{H}$ NMR and $\{^1\text{H}\}$ $^{13}\text{C}$ NMR spectra of complex <b>12</b> .   | 86  |
| <b>Figure 5.13.</b> $^1\text{H}$ NMR and $\{^1\text{H}\}$ $^{13}\text{C}$ NMR spectra of complex <b>13</b> .   | 86  |
| <b>Figure 5.14.</b> $^1\text{H}$ NMR and $\{^1\text{H}\}$ $^{13}\text{C}$ NMR spectra of complex <b>14</b> .   | 87  |
| <b>Figure 6.1.</b> Possible topologies for diastereomeric half-sandwich complexes.   | 96  |
| <b>Figure 6.2.</b> “(Ind-NHC)Ru” complexes reported in the literature.   | 97  |
| <b>Figure 6.3.</b> Molecular diagrams of complexes <b>17</b> and <b>18</b> .   | 100 |
| <b>Figure 6.4.</b> Deviation from an ideal parallel alignment of the azole plane and the vertical axis in complexes (a) <b>17</b> and (b) <b>18</b> compared to (c) complex <b>10</b> .  | 101 |

|  |     |
|--|-----|
| <b>Figure 6.5.</b> Region of the imidazolylidene and <i>CHPh</i> protons of the $^1\text{H}$ NMR spectra of: a) <b>17</b> , b) <b>19A</b> and <b>19B</b> , and c) <b>19A</b> , d) <b>19B</b> . | 104 |
| <b>Figure 6.6.</b> $^1\text{H}$ NMR and $\{^1\text{H}\}$ $^{13}\text{C}$ NMR spectra of complex <b>17</b> .  | 115 |
| <b>Figure 6.7.</b> $^1\text{H}$ NMR and $\{^1\text{H}\}$ $^{13}\text{C}$ NMR spectra of complex <b>18</b> .  | 116 |
| <b>Figure 6.8.</b> $^1\text{H}$ NMR and $\{^1\text{H}\}$ $^{13}\text{C}$ NMR spectra of complex <b>19A</b> .   | 116 |
| <b>Figure 6.9.</b> $^1\text{H}$ NMR and $\{^1\text{H}\}$ $^{13}\text{C}$ NMR spectra of complex <b>19B</b> .   | 117 |
| <b>Figure 6.10.</b> $^1\text{H}$ NMR and $\{^1\text{H}\}$ $^{13}\text{C}$ NMR spectra of complex <b>20A</b> .  | 117 |
| <b>Figure 6.11.</b> $^1\text{H}$ NMR and $\{^1\text{H}\}$ $^{13}\text{C}$ NMR spectra of complex <b>20B</b> .  | 118 |
| <b>Figure 7.1.</b> $^1\text{H}$ NMR and $\{^1\text{H}\}$ $^{13}\text{C}$ NMR spectra of ( <i>R</i> )- <b>21</b> .  | 124 |
| <b>Figure 7.2.</b> $^1\text{H}$ NMR and $\{^1\text{H}\}$ $^{13}\text{C}$ NMR spectra of complex ( <i>R</i> )- <b>22</b> .  | 126 |
| <b>Figure 7.3.</b> Molecular diagram of ( <i>R</i> )- <b>22</b> .  | 127 |
| <b>Figure 7.4.</b> Molecular diagram of ( <i>R</i> )- <b>24</b> .  | 128 |
| <b>Figure 7.5.</b> (a) Simulated and (b) experimental MS spectra of $[\text{M-I}]^+$ ion corresponding to the ionization of complex ( <i>R</i> )- <b>24</b> .                                  | 128 |
| <b>Figure 7.6.</b> $^1\text{H}$ NMR and $\{^1\text{H}\}$ $^{13}\text{C}$ NMR spectra of complex ( <i>R</i> )- <b>23</b> .  | 132 |
| <b>Figure 8.1.</b> Cp'-functionalised imidazolium salts.   | 135 |
| <b>Figure 8.2.</b> Organometallic complexes synthesised.   | 136 |
| <b>Figure 8.3.</b> Isomers of the molybdenum complexes.  | 142 |
| <b>Figure 8.4.</b> Cyclooctene catalytic epoxidation with complexes <b>6</b> , <b>8</b> and <b>9</b> .   | 144 |
| <b>Figure 8.5.</b> Cp'-functionalised NHCs: coordination to Mo, Ru, Rh and Ir.   | 149 |



## LIST OF SCHEMES

|  |    |
|--|----|
| <b>Scheme 3.1.</b> Synthesis of indenyl- and fluorenyl-functionalised NHC ligands.   | 26 |
| <b>Scheme 3.2.</b> Examples of synthesis of donor-functionalised Cp* ligands.  | 27 |
| <b>Scheme 3.3.</b> Synthetic routes towards Cp*-NHC explored during this thesis.   | 28 |
| <b>Scheme 3.4.</b> Synthesis of proligands <b>1-4</b> .  | 29 |
| <b>Scheme 3.5.</b> Regio-isomers of substituted Cp*.   | 29 |
| <b>Scheme 3.6.</b> Synthesis of <b>5</b> .   | 30 |
| <b>Scheme 4.1.</b> Synthesis of (Cp <sup>X</sup> -NHC)Mo(CO) <sub>2</sub> I complexes <b>6-9</b> .   | 46 |
| <b>Scheme 4.2.</b> Conversion of <i>trans-7</i> to <i>cis-7</i> .  | 47 |
| <b>Scheme 5.1.</b> Cp*-functionalized NHC complexes of Rh and Ir.  | 61 |
| <b>Scheme 5.2.</b> Synthesis of complex <b>10</b> .  | 65 |
| <b>Scheme 5.3.</b> Synthesis of complexes <b>11</b> and <b>12</b> .  | 65 |
| <b>Scheme 5.4.</b> Synthesis of complexes <b>13 – 15</b> .   | 66 |
| <b>Scheme 5.5.</b> Intramolecular C-H activation reactivity of complexes <b>10</b> and <b>11</b> .   | 71 |
| <b>Scheme 5.6.</b> Catalytic reactions studied.  | 75 |
| <b>Scheme 5.7.</b> Transfer hydrogenation.   | 75 |
| <b>Scheme 5.8.</b> β-alkylation of alcohols.   | 78 |
| <b>Scheme 5.9.</b> N-alkylation of amines.   | 80 |
| <b>Scheme 6.1.</b> Synthesis of (Cp <sup>X</sup> -NHC)Ru(CO)I and [(Cp <sup>X</sup> -NHC)Ru(CO)(S-PhCH(NH <sub>2</sub> )CH <sub>3</sub> )]OTf complexes. | 95 |
| <b>Scheme 6.2.</b> Synthesis of (Cp <sup>X</sup> -NHC)Ru(CO)I complexes <b>17</b> and <b>18</b> .  | 98 |

|  |     |
|--|-----|
| <b>Scheme 6.3.</b> Preparation of organometallic salts <b>19</b> and <b>20</b> .                                       | 102 |
| <b>Scheme 6.4.</b> Catalytic isomerisation of allylic alcohols <i>versus</i> conventional two-step organic procedures. | 105 |
| <b>Scheme 6.5.</b> Catalytic isomerisation of allylic alcohols, <b>Cat</b> = <b>17</b> and <b>18</b> .                 | 105 |
| <b>Scheme 6.6.</b> Catalytic isomerisation of 3-buten-2-ol in D <sub>2</sub> O.  | 107 |
| <b>Scheme 7.1.</b> Synthesis of enantiomerically pure Cp-functionalised NHC ligand.                                    | 121 |
| <b>Scheme 7.2.</b> Synthesis of enantiomerically pure iridium and rhodium complexes <b>22</b> and <b>23</b> .          | 121 |
| <b>Scheme 7.3.</b> Direct alkylation of Cp anions.   | 122 |
| <b>Scheme 7.4.</b> Synthesis of enantiomerically pure donor-functionalised Cp ligands.                                 | 122 |
| <b>Scheme 7.5.</b> Synthesis of enantiomerically pure bis-NHC ligands.   | 122 |
| <b>Scheme 7.6.</b> Synthesis of enantiomerically pure Cp-functionalised NHC ligand <b>21</b> .                         | 123 |
| <b>Scheme 7.7.</b> Synthesis of enantiomerically pure iridium and rhodium complexes <b>22</b> and <b>23</b> .          | 125 |
| <b>Scheme 7.8.</b> Synthesis of monometallic and bimetallic iridium complexes <b>22</b> and <b>24</b> , respectively.  | 127 |
| <b>Scheme 8.1.</b> Synthesis of proligands <b>1-4</b> .  | 137 |
| <b>Scheme 8.2.</b> Synthesis of <b>5</b> .   | 138 |
| <b>Scheme 8.3.</b> Synthesis of ( <i>R</i> )- <b>21</b> .  | 138 |
| <b>Scheme 8.4.</b> Synthesis of complexes <b>6-9</b> .   | 139 |
| <b>Scheme 8.5.</b> Synthesis of the Ir complex <b>10</b> .   | 140 |
| <b>Scheme 8.6.</b> Synthesis of complexes <b>11-15</b> and <b>22-24</b> .  | 141 |
| <b>Scheme 8.7.</b> Synthesis of complexes <b>17</b> and <b>18</b> .  | 142 |
| <b>Scheme 8.8.</b> Intramolecular C-H activation reactivity of complexes <b>10</b> and <b>11</b> .                     | 143 |
| <b>Scheme 8.9.</b> Synthesis of enantiomerically pure ruthenium complexes.   | 143 |



## LIST OF TABLES

|  |     |
|--|-----|
| <b>Table 1.1.</b> $\eta^5$ -Indenyl- and fluorenyl-functionalised NHC metal complexes.   | 12  |
| <b>Tabel 4.1.</b> Selected IR frequencies and $^{13}\text{C}$ and $^{95}\text{Mo}$ NMR chemical shifts of complexes <b>6-9</b> .                                       | 46  |
| <b>Table 4.2.</b> Catalytic epoxidation of <i>cis</i> -cyclooctene.  | 50  |
| <b>Tabel 5.1.</b> Selected chemical shifts for $^1\text{H}$ and $^{13}\text{C}$ NMR of complexes <b>10-14</b> .  | 67  |
| <b>Tabel 5.2.</b> Selected bond distances and angles of complexes <b>10, 12, 13</b> and <b>14</b> .  | 69  |
| <b>Table 5.3.</b> Selected $^{13}\text{C}$ NMR chemical shifts of complex <b>16</b> and analogs.   | 73  |
| <b>Tabel 5.4.</b> Selected bond length and angles of complex <b>16</b> and analogs.  | 74  |
| <b>Table 5.5.</b> Catalytic transfer hydrogenation.  | 76  |
| <b>Table 5.6.</b> $\beta$ -alkylation of secondary alcohols with primary alcohols.   | 79  |
| <b>Table 5.7.</b> N-alkylation of aniline with primary alcohols.   | 81  |
| <b>Table 6.1.</b> Selected IR frequencies, $^1\text{H}$ and $^{13}\text{C}$ NMR chemical shifts of complexes <b>17</b> and <b>18</b> .                                 | 99  |
| <b>Table 6.2.</b> Selected distances and angles of complexes <b>17</b> and <b>18</b> .   | 100 |
| <b>Table 6.3.</b> Selected IR frequencies, $^1\text{H}$ and $^{13}\text{C}$ NMR chemical shifts of complexes <b>19</b> and <b>20</b> .                                 | 103 |
| <b>Table 6.4.</b> Catalytic isomerisation of allylic alcohols.   | 106 |
| <b>Table 7.1.</b> Selected $^1\text{H}$ and $^{13}\text{C}$ NMR chemical shifts of iridium and rhodium complexes ( <i>R</i> )- <b>22</b> and ( <i>R</i> )- <b>23</b> . | 125 |
| <b>Table 8.1.</b> Catalytic isomerisation of allylic alcohols.   | 145 |
| <b>Table 8.2.</b> Catalytic transfer hydrogenation.  | 146 |
| <b>Table 8.3.</b> $\beta$ -alkylation of secondary alcohols with primary alcohols.   | 147 |
| <b>Table 8.4.</b> N-alkylation of aniline with primary alcohols.   | 148 |



## ACKNOWLEDGEMENTS

First I would like to express my gratitude to my supervisors, Dr. Beatriz Royo at ITQB and Prof. Eduardo Peris at UJI, for giving me the opportunity to pursue research at the highest level. Also for their constant support and trust allowing me to grow not just as a chemist but also as a man.

I wish to acknowledge Dr. José A. Mata (Universidad Jaume I) and Dr. Mercedes Sanaú (Universidad Valencia) for solving the X-ray structures; M. C. Almeida and Dr. A. Coelho for providing data from the Elemental Analyses and Mass Spectrometry Services at ITQB; Dr. Cristian Vicent (Universidad Jaume I) for the Mass Spectrometry and Gabriel Peris (Universidad Jaume I) for acquiring the X-ray data.

I would like to thank Fundação para a Ciência e Tecnologia from Portugal for my PhD fellowship, SFRH/BD/28490/2006.

Aos meus colegas do grupo de Catálise Homogénea do ITQB, com quem tive o privilégio de trabalhar no Lab 7.15: Patrícia Reis, Krishna Mohan, Carla Gamelas, João Cardoso e José Brito. Não posso deixar de agradecer especialmente à Patrícia, não só por me ter recebido no laboratório enquanto ainda era *verdinho*, mas também por todos os momentos que partilhamos fora do dia-a-dia do laboratório! ☺ E ao Krishna pela ajuda no trabalho experimental com os complexos de molibdénio!

A mis compañeros en el grupo de Química Organometálica de la UJI: José Mata, Macarena Poyatos, Miriam Benitez, Sérgio Sanz, Alessandro Zanardi (el Grande), Mónica Viciano, Rosa Corberán, Amparo Prades, Candela Segarra y Sergio “2” Gonell. Por me recibieren muy bien en Castellón, y seren capaces de lidar con el hecho de yo no dominar el castellano. Todo mundo me trató muy bien en CS, dentro y fuera del labo! Especialmente me gustaría de dejar un saludo especial a Alex... El Grande Alex... sabiendo que hay pocas personas como tu en el mundo fue un privilegio conocerte y compartir todos esos momentos... Envía un saludo a Eu y a Andrea! ☺ A Mónica por ser la primera persona que conocí en CS, y según mi teoría *si la primera persona que conoces en una ciudad es buena, entonces seguirás conociendo gente buena...* Muchas gracias por todo... A José por ser José... en primero por la paciencia que tienes conmigo... luego, por ser una de las únicas personas que se ríe de mis bromas... *hehehe* y por siempre tener una palabra de ánimo! Y a Sergio, el aragonés! Espero que tu aventura en las highlands te vaya bien! Y claro, a Maca... por los momentos esos en el 1001... *hehehehe* ya no pregunto por Laura! ☺ A Elena, José y Maca por la revisión del manuscrito de la tesis! Muchas gracias! Y invito a la cena en el próximo congreso! ☺

Não podia deixar de agradecer o companheirismo de todas as pessoas no ITQB, especialmente aos do sétimo piso: Alfama, grupo de Química Organometálica, grupo de Química Bioinorgânica e grupo de Química de Coordenação! E claro, à São! ☺... Não só por serem os que estão mais perto, mas também por serem aqueles com quem partilhei mais experiências no ITQB, e que certamente me ficaram gravados na memória! Um abraço especial aos participantes do ITQ*Beer* e do ITQ*Binho*... Ainda devíamos fazer pelo um último, não? ☺

A la gente del QIO... Por el buen ambiente de trabajo y fuera del... Especialmente Javi por ser el motor de las actividades extra-curriculares! Y a Santi por las charlas introspectivas...

Às pessoas dos Serviços Académicos do ITQB, em especial à Ana Maria Portocarrero, não só pelo excelente trabalho e apoio, mas também pela paciência e dedicação. À Biblioteca do ITQB pela disponibilização de um gabinete aquando do início da escrita, e à Susana Lopes por ter sempre uns *minutinhos* para falar sobre os mais variados assuntos. Ao pessoal da Manutenção, Oficina de Vidro e Economato pela eficaz e rápida ajuda na resolução dos mais variados problemas.

A mis compañeros de los cursos doctorados! Castellón no es lo mismo sin vosotros! En especial a mis *hermanitos pequeños* Pilar y Sergí (no me olvidaré del acento en cuchara ☺) A Isrrrrrael - Un portugués, un catalán y un andaluz van a Villa Real.... *hehehehe*...

Y también a las personas con quien tuve el placer de compartir piso en CS: los hermanos Figols (Patri y Gaspar), el relajado (si eres tu Marcos ☺), las psicólogas (Eva y Elena), el *penetra* (no lo sé si existe en castellano esta palabra, pero eres tu Victor, así que a buscarla en el diccionario! ☺) y claro el loco de Albertyzz!

A todos os meus amigos que me acompanharam nestes últimos anos, tanto em Guimarães como em Lisboa! E que me ajudaram sempre que necessitei! Ao Vítor, por tudo o que vivemos juntos e, ainda assim, seres uma lufada de ar fresco na ociente Lisboa... Ao Leo pela enorme pessoa que és e por ainda me conseguires aturar ao final destes anos todos! ☺ À Raquel por todo o apoio e compreensão nesta fase final! ☺ Ao Artur por muitas coisas, mas principalmente pelo *Catalunya tour*... A Couto por *incendiar* uma parte do meu ser! À Sofia pela enorme amizade e carinho... À Diana pelo sempre presente apoio! Ao Quaresma pelos

*desatrofios...* ☺ Ao Prenda e à Daniela por terem ensinado tanto, e por continuar a aprender convosco cada vez que *revisito* as nossas conversas! E ainda faltam muitos, e agora saem por ordem alfabética para não dar confusão: Alex, Ana Lucena, André, Carlão, Carlos, Celso, Lopes, Luís, Pedro, Rita e Vaz... Acho que nem preciso dizer porquê!!!!..... e à Inês P. e Ana Elisa por me terem arranjado uma tonelada e meia de artigos a que eu não tinha acesso! ☺

Aos meu pais por me deixarem crescer, compreendendo e apoiando as minhas decisões! Por se preocuparem como só os pais o sabem fazer... E por me darem sempre tudo e mais um pouco! Ao meu irmão e à minha cunhada, por não deixarem que a distância nos separe! E por terem sempre tempo para partilhar comigo os escasos momentos que passo em casa!

Por último, aos meus dois sobrinhos, a Ana Margarida e o Francisco, por toda a alegria e energia que me transmitem a cada momento... Pelo calor do vosso sorriso e por terem sempre uma nova aventura para partilhar comigo! Mas acima de tudo, por serem os melhores sobrinhos do mundo!

E claro, a todos com quem me cruzei no caminho e não referi!

muito obrigado – thank you very much –

muchas gracias – grazie mille

*à Ana e ao Francisco,*





## SUMÁRIO

Esta tese trata da síntese de uma série de sais de imidazólio funcionalizados com grupos ciclopentadieno e da sua coordenação a Mo, Ru, Rh e Ir. Um dos objectivos foi adquirir conhecimento químico sobre a reactividade destes complexos, e explorar as suas potenciais aplicações em catalise.

Os sais de imidazólio sintetizados durante esta tese representam uma série contendo diferentes substituintes tanto no anel de ciclopentadienilo como na ponte entre as duas funcionalidades.

Os novos complexos organometálicos obtidos foram utilizados como catalisadores em várias reacções orgânicas: epoxidação de olefinas (Mo); transferência de hidrogénio, N-alkilação de aminas e  $\beta$ -alkilação de álcoois (Ir) e isomerização de álcoois alílicos (Ru).

Uma introdução sobre carbenos N-heterociclicos (NHCs) é apresentada no Capítulo 1. O objectivo deste capítulo é evidenciar o papel dos NHCs como ligandos espectadores em química organometálica, particularmente aqueles contendo uma funcionalidade dadora de electrões. Actualmente, os NHCs estão entre os mais úteis grupos de ligandos em catalise homogénea, devido à sua excelente capacidade dadora- $\sigma$ . O seu potencial levou ao desenvolvimento de um quase ilimitado número de arquitecturas contendo NHCs. No entanto, aquando do início desta tese, ligandos de NHC contendo grupos

ciclopentadienilo eram desconhecidos. A síntese de ligandos similares, descrita por outros grupos de investigação durante o período desta tese, também está revista neste capítulo.

O Capítulo 3 descreve as sínteses dos sais de imidazólio funcionalizados com grupos  $Cp^X$  ( $Cp^X$  = ciclopentadienilo, pentametilciclopentadienilo e pentabenzilciclopentadienilo) desenvolvidas durante a tese. Os sais de imidazólio funcionalizados com grupos ciclopentadieno foram obtidos por duas rotas sintéticas. A primeira, permite a introdução de diferentes tipos de anel ciclopentadieno. Enquanto, a segunda, é um método simples e de grande rendimento para obtenção de sais de imidazólio funcionalizados com grupos ciclopentadieno.

Os sais de imidazólio funcionalizados com grupos  $Cp^X$  ( $Cp^X$  = ciclopentadienilo, pentametilciclopentadienilo e pentabenzilciclopentadienilo) obtidos foram coordenados a molibdénio, e estes resultados estão descritos no Capítulo 4. Os novos complexos organometálicos foram estudados como catalisadores em epoxidação do *cis*-cicloocteno com *t*-butylhidroperóxido. A natureza do anel de ciclopentadienilo tem importantes implicações na performance catalítica dos complexos estudados. Um dos principais objectivos deste capítulo foi o estudo do comportamento e reactividade química dos complexos de Mo-NHC em alto estado de oxidação.

O Capítulo 5 lida com a coordenação dos os sais de imidazólio funcionalizados com pentametilciclopentadienilo ( $Cp^*$ ) a irídio e ródio. Os complexos obtidos foram estudados como catalisadores em processos homogéneos envolvendo uma metodologia do tipo borrowing-hydrogen. Discute-se, também, a activação intramolecular de ligações C-H dos

complexos de irídio. O principal objectivo deste capítulo foi comparar a actividade catalítica destes complexos com complexos semelhantes sem ponte entre os ligandos Cp\* e NHC.

A coordenação a ruténio dos sais de imidazólio funcionalizados com grupos Cp<sup>x</sup> (Cp<sup>x</sup> = pentametilcyclopentadienilo e pentabenzilciclopentadienilo) é descrita no Capítulo 6. Os complexos de ruténio (quirais-no-metal) foram estudados como catalizadores na isomerização de álcoois alílicos. Os resultados do isolamento e resolução dos complexos quirais-no-metal é descrita detalhadamente neste capítulo.

O Capítulo 7 descreve os resultados preliminares obtidos na síntese do primeiro ligando do tipo Cp\_NHC enantiomericamente puro e a sua coordenação a irídio e ródio.

Finalmente, as principais conclusões e perspectivas futuras são descritas no Capítulo 8.



## ABSTRACT

This thesis deals with the synthesis of cyclopentadienyl-functionalised N-heterocyclic carbenes and its coordination to both middle and late transition metals. One of the goals was to gain chemical knowledge on the reactivity patterns of these complexes, and explore their potential applications in catalysis.

The imidazolium salts synthesised in the course of this thesis represent a series containing changes in the electronic and steric parameters. The ligand precursors were coordinated to molybdenum, ruthenium, rhodium and iridium. These organometallic complexes were studied in homogeneous catalysis processes such as: olefin epoxidation (Mo), isomerisation of allylic alcohols (Ru),  $\beta$ -alkylation of alcohols, N-alkylation of amines and transfers hydrogenation of ketones (Ir).

An introduction to N-heterocyclic carbenes (NHCs) chemistry is given in Chapter 1. The aim of this chapter is to highlight the role of NHCs as spectator ligands in organometallic chemistry, particularly those containing a donor functionality. Nowadays, NHCs are amongst the most useful ligands in homogenous catalysis, due to their excellent  $\sigma$ -donor properties. Their potential has led to a rapid growth and development of almost an unlimited number of NHC-containing architectures. However, when this thesis started cyclopentadienyl-functionalised N-heterocyclic

carbenes were unknown. The analogous ligands reported by other groups during the course of this thesis are also reviewed in this chapter.

Chapter 3 describes the synthesis of Cp<sup>X</sup>-functionalised imidazolium salts (Cp<sup>X</sup> = cyclopentadienyl, pentamethylcyclopentadienyl and pentabenzylcyclopentadienyl) developed during this thesis. The cyclopentadienyl-functionalised N-heterocyclic carbenes precursors were obtained following two synthetic approaches. The first, allows for the introduction of a variety of substituted cyclopentadienyl rings. While, the second, is a simple and high yielding method towards pentamethylcyclopentadienyl-functionalised imidazolium salts.

The Cp<sup>X</sup>-functionalised imidazolium salts (Cp<sup>X</sup> = cyclopentadienyl, pentamethylcyclopentadienyl and pentabenzylcyclopentadienyl) obtained were coordinated to molybdenum, and these results are described in Chapter 4. The new organometallic complexes were studied as catalysts in the epoxidation of *cis*-cyclooctene with *t*-butyl hydroperoxide. The nature of the Cp<sup>X</sup>-NHC ligand has important implications in the catalytic performance of their molybdenum complexes. One of the main objectives of this chapter was to study the chemistry of high oxidation state Mo-NHC complexes.

Chapter 5 deals with the coordination of Cp<sup>\*</sup>-functionalised imidazolium salts (Cp<sup>\*</sup> = pentamethylcyclopentadienyl) to both rhodium and iridium. These half-sandwich complexes were studied in homogenous catalysis involving a borrowing-hydrogen methodology. The intra-molecular C-H activation of the iridium complexes is also discussed. The main goal of the work described in this chapter was to compare the catalytic performance of the new complexes with non-bridged related systems.

The coordination of Cp<sup>X</sup>-functionalised imidazolium salts (Cp<sup>X</sup> = pentamethylcyclopentadienyl and pentabenzylcyclopentadienyl) to ruthenium is described in Chapter 6. The chiral-at-metal ruthenium complexes obtained were studied as catalysts in the isomerisation of allylic alcohols. The results concerning the isolation and resolution of chiral-at-metal ruthenium (Cp<sup>X</sup>-NHC)RuICO complexes are described and thoroughly discussed in this chapter.

Chapter 7 describes the preliminary results obtained in the synthesis of the first enantiomerically pure Cp-functionalised imidazolium salt and its coordination to iridium and rhodium.

Finally, the main conclusions and perspectives are outlined in chapter 8.





---

# 1.

## INTRODUCTION

---

|      |  |    |
|------|--|----|
| 1.1. | N-Heterocyclic Carbenes                      | 3  |
| 1.2. | The nature of NHCs                           | 5  |
| 1.3. | NHCs as ligands                              | 5  |
|      | 1.3.1. Steric properties of NHCs,            | 7  |
|      | 1.3.2. Electronic properties of NHCs,        | 8  |
| 1.4. | Donor functionalised NHCs                    | 10 |
|      | 1.4.1. NHCs with neutral chelates,           | 10 |
|      | 1.4.2. Cyclopentadienyl-functionalised NHCs, | 11 |
| 1.5. | References                                   | 13 |

Cyclopentadienyl-Functionalised N-Heterocyclic Carbenes:  
Synthesis, Coordination to Mo, Ru, Rh and Ir and Catalytic Applications.

---

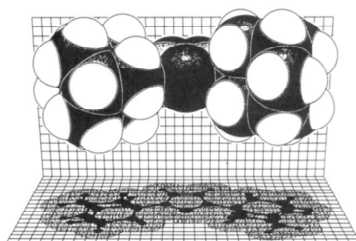
## 1.1. N-Heterocyclic Carbenes

N-Heterocyclic carbenes (NHCs) have run a long way since they were first introduced to chemistry by the pioneering work of Öfele<sup>[1,2]</sup> and Wanzlick,<sup>[3]</sup> in the late 60s. Chemical stability and coordination versatility are two of the many properties of NHCs that may have helped their great development. The easy preparation of NHC-precursors has allowed an almost infinite access to new organometallic topologies, in which the only limitation seems to be the imagination of the researchers.<sup>[4]</sup> During the last decade, NHCs have found a manifold of applications, including organometallic catalysis,<sup>[4-7]</sup> organocatalysis,<sup>[8-10]</sup> pharmaceuticals<sup>[11-13]</sup> or material science.<sup>[12]</sup> It is now clear that NHCs present extraordinary chemical properties, surpassing their initial comparison with phosphines.<sup>[14]</sup>

Four milestone achievements are on the foundation of NHC chemistry:

- (i) The isolation of a thermally stable free-carbene:

Until the 90s, carbenes were regarded as reactive and elusive intermediates.<sup>[15]</sup> When Arduengo *et al.*<sup>[16]</sup> published the isolation of a stable free NHC, it prompted the interest in this new class of ligands.<sup>[15]</sup> The colorless crystals of 1,3-di-1-adamantylimidazol-2-ylidene were remarkably stable and could be analyzed by X-ray diffraction, Figure 1.1.



**Figure 1.1.** Space fill drawing of the X-ray structure of the first isolated free carbene, 1,3-di-1-adamantylimidazol-2-ylidene.

(ii) The first use of NHC complexes in catalysis:

NHCs debut as ligands in homogenous catalysis in a seminal paper by Herrmann *et al.*,<sup>[17]</sup> which described the use of a series of palladium NHC complexes (Figure 1.2) in the Heck reaction.

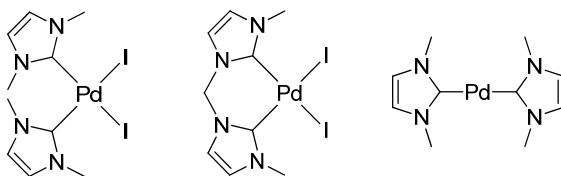


Figure 1.2. First metal-NHC complexes used in catalysis.

(iii) Easy access to NHC-metal-based complexes:

A series of simple and highly efficient methods for the coordination of NHCs to metals are now available.<sup>[18,19]</sup> This fact, together with the simple preparation of a variety of NHC precursors (mainly imidazolium salts) has allowed the preparation of hundreds of new catalysts with improved properties.

(iv) Second generation Grubb's olefin metathesis catalyst:

The advances leading to the second generation of Grubb's catalyst,<sup>[20-22]</sup> (Figure 1.3) have firmly established NHCs as a class of catalytically useful spectator ligands, which can be compared with cyclopentadienyls and phosphines.<sup>[14]</sup>

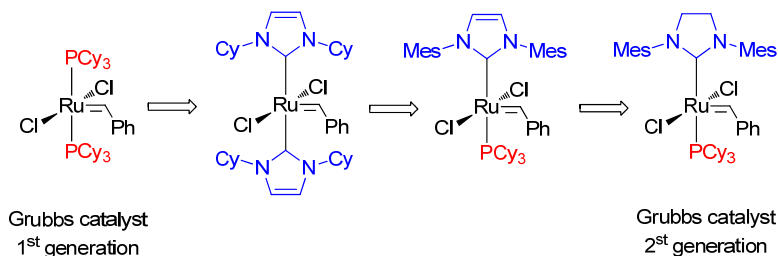


Figure 1.3. Grubbs catalyst, from 1<sup>st</sup> to 2<sup>nd</sup> generation.

## 1.2. The nature of NHCs

From an organic chemistry point of view, a carbene is a neutral divalent carbon atom with six electrons in its valence shell. In NHCs, the carbene centre is bent by virtue of its incorporation into a ring, usually five membered, such as imidazolylidene in Figure 1.4. The two  $\alpha$ -nitrogens stabilize the NHC singlet state by increasing the energy gap between the HOMO and LUMO orbitals. Firstly, they stabilize the filled HOMO orbital increasing its  $s$ -character by electron-withdrawing inductive effect. Secondly, the vacant  $p$ -orbital is destabilized, by a mesomeric effect, through the donation of the  $\alpha$ -amino lone pairs.<sup>[23, 24]</sup> Therefore, NHCs (and other diamino carbenes) are kinetically stable in solution or solid state at room temperature, and can be conveniently prepared by deprotonation of the corresponding salt. Although aromaticity on the heterocyclic ring only provides a marginal effect in the bonding nature of the NHC,<sup>[25]</sup> it has a tremendous effect in the stability of the free carbene towards hydrolysis.<sup>[26]</sup>

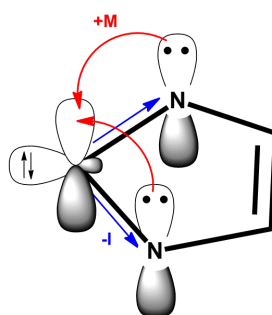
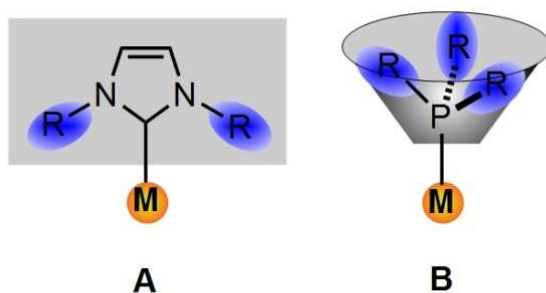


Figure 1.4. Inductive (-I) and mesomeric (+M) effects in the stabilisation of NHCs.

## 1.3. NHCs as ligands

NHCs (A in Figure 1.5) and phosphines (B in Figure 1.5) are two of the most useful classes of ligands in organometallic catalysis, both being

electronically and sterically tunable.<sup>[14]</sup> The seminal work of Tolman<sup>[27]</sup> in documenting the trends of stereoelectronic effects in phosphines, gave a lead start to phosphines.<sup>[14, 28]</sup>



**Figure 1.5.** NHCs (A), phosphines (B).

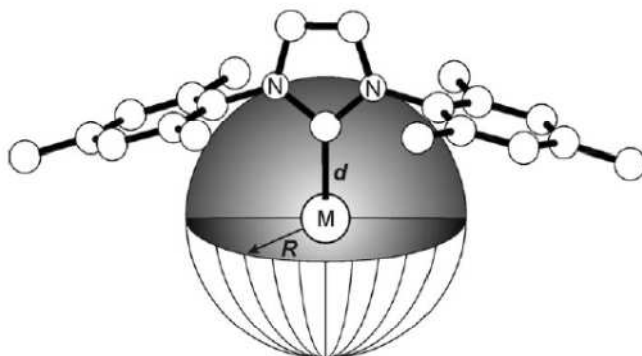
Because NHCs are monodentate two-electron  $\sigma$ -donor ligands, like phosphines, an analogy between the two classes developed.<sup>[23, 25, 28]</sup> However, they are very different both in terms of spatial arrangement and electronic character.<sup>[23]</sup> For example, the steric properties of phosphines reside on their cone angle, while the general principles governing the steric properties of NHCs arise from their fan-shaped profile. When free rotation about the M-C bond is possible (mostly in mono-NHC ligands) the azole ring is expected to orientate its slim axis to the bulky plane of the complex, minimizing the steric repulsions. Moreover, unlike phosphines, due to the fact that in NHCs the wingtips are not directly bonded to the carbene, both steric and electronic properties can be independently tuned.<sup>[14, 29, 30]</sup>

An important part of the art of organometallic chemistry is to pick suitable spectator ligands to elicit the desired properties, by the carefully tuning of their steric and electronic properties.<sup>[31-33]</sup> Therefore the understanding ligand stereoelectronic properties is essential for successful organometallic synthesis and catalyst design.<sup>[29, 30]</sup> In the last

few years a growing amount of information, both experimental and theoretical, dealing with steric and/or electronic properties of NHCs has been reported in the literature.<sup>[24, 30, 34-64]</sup>

### 1.3.1. Steric properties of NHCs

While in phosphines the Tolman cone angle is a logical and natural choice to describe the ligand steric parameters, NHCs cannot be described by the same descriptors. To solve this problem, Cavallo, Nolan and co-workers introduced the concept of buried volume ( $\%V_{\text{Bur}}$ ), see Figure 1.6. The buried volume represents the space occupied by the NHC ligand in the coordination sphere of the metal.<sup>[35, 59, 63, 65]</sup>



**Figure 1.6.** Schematic representation of  $\%V_{\text{Bur}}$ .

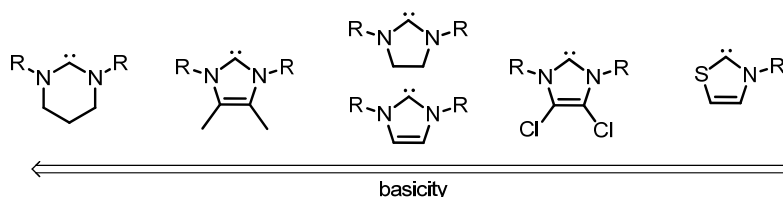
The  $\%V_{\text{Bur}}$  is not limited to a certain class of ligands, but it can be used to compare all kind of ligands. On the other hand, the calculation of this volume only accounts for a snap-shot of the complex geometry.<sup>[62]</sup> Recently, Gusev introduced a new steric parameter – repulsiveness,  $r$  – which represents the direct repulsive interactions of the NHC and the carbonyl ligands in  $\text{Ni}(\text{CO})_3\text{NHC}$ .<sup>[30]</sup> and Cavallo and co-workers reported an initial approach to a dynamic model.<sup>[63]</sup>

### 1.3.2. Electronic properties of NHCs

It is well accepted that NHCs bind strongly to metals centres by  $\sigma$ -bonding, while  $\pi$ -back bonding can be considered negligible. Nevertheless, the bonding between a metal centre and a NHC always presents a  $\pi$ -back bonding component which, while marginal in most cases, becomes significant for Group 11 metals – copper, silver and gold. In addition, contrary to phosphines, NHCs bind to alkaline, lanthanides and high oxidation state metals in which  $\pi$ -back donation is not possible.<sup>[25]</sup> Recently, even  $\pi$ -donor properties of NHCs have been reported.<sup>[43]</sup>

Over the years, many methods have been used to theoretically or experimentally determine the electronic properties of NHCs and compare them with those shown by phosphines. These methods include studies on  $^{13}\text{C}$  NMR chemical shifts of the free ligand or metallic complexes,<sup>[49, 58, 66]</sup> cyclic voltammetry of NHCs complexes,<sup>[51, 60, 64]</sup> basicity of free ligand<sup>[34, 40, 48, 67]</sup> and determination of CO stretching frequencies in FT-IR spectra of NHC organometallic complexes.<sup>[30, 53, 64, 68]</sup>

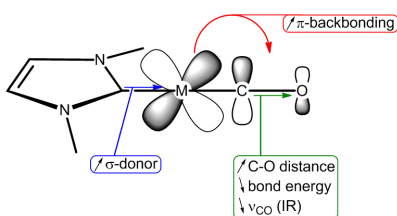
The basicity of the ligand can provide a rough estimation of their  $\sigma$ -donor properties.<sup>[69]</sup> According to both theoretical calculations<sup>[40]</sup> and experimental results,<sup>[67]</sup> it seems clear that generally NHCs ( $\text{p}K_{\text{a}} > 20$ ) are more basic than the most basic phosphines ( $\text{P}(\text{tBu})_3$ ,  $\text{p}K_{\text{a}} = 11.4$ ). These studies also gave some guidelines on how to modulate the basicity of NHCs (Figure 1.7).



**Figure 1.7.** Qualitative series of NHCs based on basicity.<sup>[40, 67]</sup>



In his seminal work, Tolman introduced a single parameter to describe the electronic properties of phosphines. The Tolman electronic parameter – TEP – was determined by looking at the CO stretching frequencies of  $\text{LNi}(\text{CO})_3$  complexes ( $\text{L} = \text{phosphine}$ ), and led to the arrangement of phosphines in a series according to their electron-donating character.<sup>[27]</sup> However, the high toxicity of  $\text{Ni}(\text{CO})_4$  is a major drawback to the use of this complex. Additionally, some bulky  $(\text{NHC})\text{Ni}(\text{CO})_3$  complexes are not stable and readily eliminate CO to afford the corresponding 16 electron complexes  $(\text{NHC})\text{Ni}(\text{CO})_2$ , as a consequence of the high steric hindrance around the tetracoordinated metal center. Tolman already suggested that some other metal-carbonyl compounds could be used to perform these studies, so that IR-spectroscopy may be used as an efficient tool to determine the electron-donor character of NHC ligands (Figure 1.8).



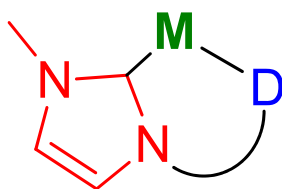
**Figure 1.8.** Schematic representation of the effect in  $\nu_{\text{CO}}$  by introducing a more  $\sigma$ -donor ligand.

The Crabtree<sup>[68]</sup> and Nolan<sup>[53]</sup> groups used  $(\text{NHC})\text{MX}(\text{CO})_2$ , where  $\text{M} = \text{Ir}$  and  $\text{Rh}$ . These studies lead to the development and refinement of a correlation between the TEP and the average CO stretching frequencies in the iridium complexes ( $\overline{\nu_{\text{CO}/\text{Ir}}}$ ), Equation 1. Later, Wolf and Plenio showed that the data obtained in the rhodium system could be easily correlated to the iridium values.<sup>[64]</sup> More recently, Gusev used DFT calculations to calculate the TEP of 76 NHC ligands, some of which had not even been synthesised yet.<sup>[30]</sup>

$$\text{TEP} (\text{cm}^{-1}) = 0.8475 \overline{\nu_{\text{CO}/\text{Ir}}} (\text{cm}^{-1}) + 336.2 (\text{cm}^{-1}) \quad \text{Eq(1)}$$

## 1.4. Donor functionalised NHCs

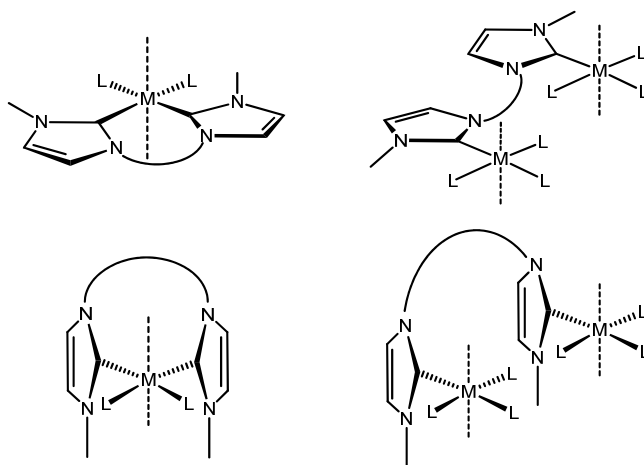
The aim to develop effective new catalysts with increased thermal stability, led to the design of exciting and innovative ligands that included a large amount of donor-functionalised NHCs.<sup>[70]</sup> The introduction of a chelating group (Figure 1.9) is an effective strategy that may introduce features such as lability, chirality and rigidity. Over the past decades, NHCs have shown to be compatible with a wide set of functionalities both neutral and anionic, yielding an extensive array of architectures such as chelate, *pincer* and tripodal.<sup>[4-5, 23, 32, 33, 70-72]</sup>



**Figure 1.9.** Schematic draw of donor-functionalised NHC.

### 1.4.1. NHCs with neutral chelates

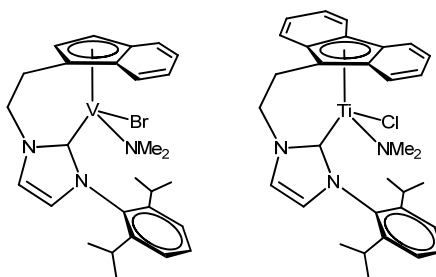
Many chelating NHC-based ligands with neutral functionalities have been reported. In this regard, neutral functionalities such as phosphines, aryls, ethers, oxazolines and amines have been widely used.<sup>[4, 5, 33, 70-72]</sup> Poly-NHC ligands have attracted great attention because they allow the preparation of organometallic compounds with a variety of topologies. A wide set of complexes with bis-, tris- and tetra-NHCs are now available, from which bis-carbenes are the most common. As shown in Figure 1.10, bis-NHCs, may act either as chelating or bridging ligands, affording diverse architectures depending on the orientation of the azole planes with respect to the coordination sphere of the metal.<sup>[4, 5, 71]</sup>



**Figure 1.10.** Possible architectures with bis-NHCs ligands.

#### 1.4.2. Cyclopentadienyl-functionalised NHCs

When this work was started, NHCs tethered to a cyclopentadienyl ring were unknown. During the period of this thesis, Downing and Danopoulos<sup>[73]</sup> reported the synthesis of the first indenyl- and fluorenyl-functionalised NHCs (Ind-NHC and Flu-NHC) and their coordination to Ti and V (Figure 1.11).



**Figure 1.11.** First indenyl- and fluorenyl-functionalised NHCs.

In the following years, the coordination of these ligands to a variety of transition metals, and their application in catalysis proved the versatility of these novel Cp'-NHC ligands. Table 1.1 summarises the isolated Ind-NHC and Flu-NHC organometallic complexes, which range from lanthanides and early transition metals to late transition ones. Some

catalytic properties of these complexes have been reported. For example, Shen and co-workers<sup>[74]</sup> reported the improved activities of (Ind-NHC)NiCl in the polymerization of styrene, when compared with the non-bridged complex. Soon after, Cui and co-workers reported the coordination of this type of ligands to rare earth metals,<sup>[75]</sup> and the catalytic activity of the isolated complexes in the polymerisation of isoprene and copolymerisation of ethylene and norbornene.<sup>[76]</sup> In addition, Danopoulos, Cole-Hamilton and co-workers<sup>[77]</sup> reported (Ind-NHC)Rh (I) and (Ind-NHC)Ir (I) complexes, and their activities in the hydroformilation of 1-octene and carbonylation of methanol.

**Table 1.1.**  $\eta^5$ -Indenyl- and fluorenyl-functionalised NHC metal complexes.

| Cp analog | Bridge (n)     | Metal               | Ref.            |         |      |
|-----------|----------------|---------------------|-----------------|---------|------|
| indenyl   | ethylene (n=2) | K (I)               | [73]            |         |      |
|           |                | Sc (III)            | [75, 76, 79]    |         |      |
|           |                | Y (III)             | [75, 76]        |         |      |
|           |                | Y (III)<br>dimer    | [80]            |         |      |
|           |                | Ho (III)            | [76]            |         |      |
|           |                | Lu (III)            | [75, 76, 79]    |         |      |
|           |                | Ti (IV)             | [80]            |         |      |
|           |                | Zr (IV)             | [80]            |         |      |
|           |                | V(III)              | [73]            |         |      |
|           |                | Rh (I) <sup>a</sup> | [77]            |         |      |
|           |                | Ir (I) <sup>b</sup> | [77]            |         |      |
|           |                | Ru(II)              | [78]            |         |      |
|           |                | Mo(II)              | [81]            |         |      |
|           |                | indenyl             | propylene (n=3) | Ti (IV) | [80] |
|           |                |                     |                 | Zr (IV) | [80] |
| Ni (II)   | [74]           |                     |                 |         |      |
| fluorenyl | ethylene (n=2) | K (I)               | [73]            |         |      |
|           |                | Ti (III)            | [73]            |         |      |
|           |                | Sc (III)            | [76, 79]        |         |      |
|           |                | Y (III)             | [76, 79]        |         |      |
|           |                | Ho (III)            | [76, 79]        |         |      |
|           |                | Lu (III)            | [76, 79]        |         |      |

<sup>a</sup> only one example where the indenyl moiety is chelating in a  $\eta^5$  fashion, others include chelating in a  $\eta^2$  fashion, non-chelating and bimetallic. <sup>b</sup> the indenyl is chelating in a  $\eta^1$  fashion.

## 1.5. References

- [1] K. Öfele, *J. Organomet. Chem.* **1968**, 12, P42.
- [2] K. Öfele, *Angew. Chem. Int. Ed.* **1969**, 8, 916.
- [3] H. W. Wanzlick, H. J. Schonher, *Angew. Chem. Int. Ed.* **1968**, 7, 141.
- [4] M. Poyatos, J. A. Mata, E. Peris, *Chem. Rev.* **2009**, 109, 3677.
- [5] R. Corberán, E. Mas-Marzá, E. Peris, *Eur. J. Inorg. Chem.* **2009**, 1700.
- [6] N. Marion, S. P. Nolan, *Acc. Chem. Res.* **2008**, 41, 1440.
- [7] S. Díez-González, N. Marion, S. P. Nolan, *Chem. Rev.* **2009**, 109, 3612.
- [8] D. Enders, O. Niemeier, A. Henseler, *Chem. Rev.* **2007**, 107, 5606.
- [9] V. Nair, S. Vellalath, B. P. Babu, *Chem. Soc. Rev.* **2008**, 37, 2691.
- [10] N. Marion, S. Díez-González, S. P. Nolan, *Angew. Chem. Int. Ed.* **2007**, 46, 2988.
- [11] K. M. Hindi, M. J. Panzner, C. A. Tessier, C. L. Cannon, W. J. Youngs, *Chem. Rev.* **2009**, 109, 3859.
- [12] L. Mercks, M. Albrecht, *Chem. Soc. Rev.* **2010**, 39, 1903.
- [13] H. G. Raubenheimer, S. Cronje, *Chem. Soc. Rev.* **2008**, 37, 1998.
- [14] R. H. Crabtree, *J. Organomet. Chem.* **2005**, 690, 5451.
- [15] A. J. Arduengo, *Acc. Chem. Res.* **1999**, 32, 913.
- [16] A. J. Arduengo, R. L. Harlow, M. Kline, *J. Am. Chem. Soc.* **1991**, 113, 361.
- [17] W. A. Herrmann, M. Elison, J. Fischer, C. Kocher, G. R. J. Artus, *Angew. Chem. Int. Ed.* **1995**, 34, 2371.
- [18] F. E. Hahn, M. C. Jahnke, *Angew. Chem. Int. Ed.* **2008**, 47, 3122.
- [19] E. Peris, *Top. Organomet. Chem.* **2007**, 21, 83.
- [20] T. M. Trnka, R. H. Grubbs, *Acc. Chem. Res.* **2001**, 34, 18.
- [21] R. H. Grubbs, *Angew. Chem. Int. Ed.* **2006**, 45, 3760.

- [22] C. Samojlowicz, M. Bieniek, K. Grela, *Chem. Rev.* **2009**, *109*, 3708.
- [23] S. T. Liddle, I. S. Edworthy, P. L. Arnold, *Chem. Soc. Rev.* **2007**, *36*, 1732.
- [24] H. Jacobsen, A. Correa, A. Poater, C. Costabile, L. Cavallo, *Coord. Chem. Rev.* **2009**, *253*, 687.
- [25] P. de Fremont, N. Marion, S. P. Nolan, *Coord. Chem. Rev.* **2009**, *253*, 862.
- [26] M. K. Denk, J. M. Rodezno, S. Gupta, A. J. Lough, *J. Organomet. Chem.* **2001**, *617*, 242.
- [27] C. A. Tolman, *Chem. Rev.* **1977**, *77*, 313.
- [28] E. Peris, R. H. Crabtree, *Coord. Chem. Rev.* **2004**, *248*, 2239.
- [29] S. Wurtz, F. Glorius, *Acc. Chem. Res.* **2008**, *41*, 1523.
- [30] D. G. Gusev, *Organometallics* **2009**, *28*, 6458.
- [31] R. H. Crabtree, *The Organometallic Chemistry of the Transition Metals*, 5th ed., John Wiley & Sons, Inc, **2009**.
- [32] O. Kühn, *Chem. Soc. Rev.* **2007**, *36*, 592.
- [33] O. Kühn, *Functionalised N-Heterocyclic Carbene Complexes*, 1st ed., John Wiley & Sons, **2010**.
- [34] Y. J. Kim, A. Streitwieser, *J. Am. Chem. Soc.* **2002**, *124*, 5757.
- [35] R. Dorta, E. D. Stevens, C. D. Hoff, S. P. Nolan, *J. Am. Chem. Soc.* **2003**, *125*, 10490.
- [36] A. C. Hillier, W. J. Sommer, B. S. Yong, J. L. Petersen, L. Cavallo, S. P. Nolan, *Organometallics* **2003**, *22*, 4322.
- [37] X. L. Hu, Y. J. Tang, P. Gantzel, K. Meyer, *Organometallics* **2003**, *22*, 612.
- [38] G. Altenhoff, R. Goddard, C. W. Lehmann, F. Glorius, *J. Am. Chem. Soc.* **2004**, *126*, 15195.
- [39] M. T. Lee, C. H. Hu, *Organometallics* **2004**, *23*, 976.
- [40] A. M. Magill, K. J. Cavell, B. F. Yates, *J. Am. Chem. Soc.* **2004**, *126*, 8717.
- [41] D. Nemcsok, K. Wichmann, G. Frenking, *Organometallics* **2004**, *23*, 3640.

- 
- [42] R. Dorta, E. D. Stevens, N. M. Scott, C. Costabile, L. Cavallo, C. D. Hoff, S. P. Nolan, *J. Am. Chem. Soc.* **2005**, *127*, 2485.
- [43] N. M. Scott, R. Dorta, E. D. Stevens, A. Correa, L. Cavallo, S. P. Nolan, *J. Am. Chem. Soc.* **2005**, *127*, 3516.
- [44] W. A. Herrmann, J. Schutz, G. D. Frey, E. Herdtweck, *Organometallics* **2006**, *25*, 2437.
- [45] M. D. Sanderson, J. W. Kamplain, C. W. Bielawski, *J. Am. Chem. Soc.* **2006**, *128*, 16514.
- [46] H. Turkmen, B. Çetinkaya, *J. Organomet. Chem.* **2006**, *691*, 3749.
- [47] P. Bazinet, T. G. Ong, J. S. O'Brien, N. Lavoie, E. Bell, G. P. A. Yap, I. Korobkov, D. S. Richeson, *Organometallics* **2007**, *26*, 2885.
- [48] Y. Chu, H. Deng, J. P. Cheng, *J. Org. Chem.* **2007**, *72*, 7790.
- [49] S. Fantasia, J. L. Petersen, H. Jacobsen, L. Cavallo, S. P. Nolan, *Organometallics* **2007**, *26*, 5880.
- [50] D. M. Khramov, V. M. Lynch, C. W. Bielawski, *Organometallics* **2007**, *26*, 6042.
- [51] S. Leuthausser, D. Schwarz, H. Plenio, *Chem-Eur. J.* **2007**, *13*, 7195.
- [52] A. Bittermann, P. Harter, E. Herdtweck, S. D. Hoffmann, W. A. Herrmann, *J. Organomet. Chem.* **2008**, *693*, 2079.
- [53] R. A. Kelly, H. Clavier, S. Giudice, N. M. Scott, E. D. Stevens, J. Bordner, I. Samardjiev, C. D. Hoff, L. Cavallo, S. P. Nolan, *Organometallics* **2008**, *27*, 202.
- [54] D. M. Khramov, E. L. Rosen, J. A. V. Er, P. D. Vu, V. M. Lynch, C. W. Bielawski, *Tetrahedron* **2008**, *64*, 6853.
- [55] A. Poater, F. Ragone, S. Giudice, C. Costabile, R. Dorta, S. P. Nolan, L. Cavallo, *Organometallics* **2008**, *27*, 2679.
- [56] G. Y. Song, Y. Zhang, X. W. Li, *Organometallics* **2008**, *27*, 1936.
- [57] D. G. Gusev, *Organometallics* **2009**, *28*, 763.
- [58] H. V. Huynh, Y. Han, R. Jothibas, J. A. Yang, *Organometallics* **2009**, *28*, 5395.

- [59] A. Poater, B. Cosenza, A. Correa, S. Giudice, F. Ragone, V. Scarano, L. Cavallo, *Eur. J. Inorg. Chem.* **2009**, 1759.
- [60] E. L. Rosen, C. D. Varnado, A. G. Tennyson, D. M. Khramov, J. W. Kamplain, D. H. Sung, P. T. Cresswell, V. M. Lynch, C. W. Bielawski, *Organometallics* **2009**, *28*, 6695.
- [61] R. Tonner, G. Frenking, *Organometallics* **2009**, *28*, 3901.
- [62] T. Droge, F. Glorius, *Angew. Chem. Int. Ed.* **2010**, *49*, 6940.
- [63] F. Ragone, A. Poater, L. Cavallo, *J. Am. Chem. Soc.* **2010**, *132*, 4249.
- [64] S. Wolf, H. Plenio, *J. Organomet. Chem.* **2009**, *694*, 1487.
- [65] H. Clavier, S. P. Nolan, *Chem. Commun.* **2010**, *46*, 841.
- [66] D. Tapu, D. A. Dixon, C. Roe, *Chem. Rev.* **2009**, *109*, 3385.
- [67] E. M. Higgins, J. A. Sherwood, A. G. Lindsay, J. Armstrong, R. S. Massey, R. W. Alder, A. C. O'Donoghue, *Chem. Commun.* **2011**, 1559.
- [68] A. R. Chianese, X. Li, M. C. Janzen, J. W. Faller, R. H. Crabtree, *Organometallics* **2003**, *22*, 1663.
- [69] Accurately, the  $pK_a$  corresponds to the acidity constant of the conjugated acid of the ligand – for NHCs, the corresponding imidazolium salt – however it is common practice in organometallic chemistry to refer to the  $pK_a$  of a base when comparing  $\sigma$  donor properties of the ligands, see ref. 39. A higher  $pK_a$  value corresponds to a stronger conjugated base, and therefore a better  $\sigma$ -donating character of the ligand.
- [70] A. T. Normand, K. J. Cavell, *Eur. J. Inorg. Chem.* **2008**, 2781.
- [71] J. A. Mata, M. Poyatos, E. Peris, *Coord. Chem. Rev.* **2007**, *251*, 841.
- [72] D. Pugh, A. A. Danopoulos, *Coord. Chem. Rev.* **2007**, *251*, 610.
- [73] S. P. Downing, A. A. Danopoulos, *Organometallics* **2006**, *25*, 1337.
- [74] H. M. Sun, D. M. Hu, Y. S. Wang, Q. Shen, Y. Zhang, *J. Organomet. Chem.* **2007**, *692*, 903.



- [75] B. L. Wang, D. Wang, D. M. Cui, W. Gao, T. Tang, X. S. Chen, X. B. Jing, *Organometallics* **2007**, *26*, 3167.
- [76] B. L. Wang, D. M. Cui, K. Lv, *Macromolecules* **2008**, *41*, 1983.
- [77] S. P. Downing, P. J. Pogorzelec, A. A. Danopoulos, D. J. Cole-Hamilton, *Eur. J. Inorg. Chem.* **2009**, 1816.
- [78] C. Y. Zhang, F. Luo, B. Cheng, B. Li, H. B. Song, S. S. Xu, B. Q. Wang, *Dalton Trans.* **2009**, 7230.
- [79] B. L. Wang, T. Tang, Y. S. Li, D. M. Cui, *Dalton Trans.* **2009**, 8963.
- [80] S. P. Downing, S. C. Guadano, D. Pugh, A. A. Danopoulos, R. M. Bellabarba, M. Hanton, D. Smith, R. P. Tooze, *Organometallics* **2007**, *26*, 3762.
- [81] D. Takaki, T. Okayama, H. Shuto, S. Matsumoto, Y. Yamaguchi, S. Matsumoto, *Dalton Trans.* **2011**, *40*, 1445.

Cyclopentadienyl-Functionalised N-Heterocyclic Carbenes:  
Synthesis, Coordination to Mo, Ru, Rh and Ir and Catalytic Applications.

---

---

**2.**

**OBJECTIVES**

---

Cyclopentadienyl-Functionalised N-Heterocyclic Carbenes:  
Synthesis, Coordination to Mo, Ru, Rh and Ir and Catalytic Applications.

---

The aim of this thesis was to develop the synthesis of cyclopentadienyl ligands tethered to NHCs and their coordination chemistry to late and middle transition metals. One of the goals was to gain chemical knowledge on the reactivity patterns of these complexes, and explore their potential applications in catalysis.

We thought that the synthesis of cyclopentadienyls bearing NHC ligands (Cp-NHCs) may have important advantages when compared to the non-linked systems. For example, Cp-NHCs, i) may increase complex stability and favour the rigidity required for the preparation of effective asymmetric catalysts; ii) may modify the steric and electronic parameters about the metal; iii) may allow the introduction of chirality on the linker between the Cp and the NHC units; iv) may lead to a versatile coordination chemistry with implications in catalysis due to the different strength of the metal-carbene bond across the periodic table, and v) afford chelation without consuming an extra coordination site, thus leaving the metal complexes with an additional site for catalysis.

With this in mind the following specific aims were considered:

- (i) To design a simple high-yielding method for the synthesis of Cp-NHC ligands, that tolerates changes in the Cp' moiety, allowing for the introduction of smooth modifications in the electronic and steric properties of the ligand.
- (ii) Coordination of the Cp'-functionalised NHC to middle and late transition metals, namely to Mo, Rh, Ir and Ru, thus showing the versatility of the new ligands across the periodic table.
- (iii) Explore the reactivity of the new metal complexes and their potential application in catalysis.

Cyclopentadienyl-Functionalised N-Heterocyclic Carbenes:  
Synthesis, Coordination to Mo, Ru, Rh and Ir and Catalytic Applications.

---

---

# 3.

## SYNTHESIS OF CYCLOPENTADIENYL-FUNCTIONALISED IMIDAZOLIUM SALTS

---

|      |   |    |
|------|---|----|
| 3.1. | Abstract  | 25 |
| 3.2. | Introduction  | 26 |
| 3.3. | Results and discussion                                | 27 |
|      | 3.3.1. Synthesis of the imidazolium salts,            | 27 |
|      | 3.3.2. Characterisation of the imidazolium salts,     | 31 |
| 3.4. | Conclusions   | 33 |
| 3.5. | Experimental procedures                               | 34 |
|      | 3.5.1. Materials and methods,                         | 34 |
|      | 3.5.2. Synthesis and characterisation of <b>1-5</b> , | 34 |
| 3.6. | Acknowledgments                                       | 37 |
| 3.7. | References  | 38 |
| 3.8. | Supporting Information                                | 39 |

---

V. V. K. M. Kandepi, A. P. da Costa, E. Peris and B. Royo\* *Organometallics*, **2009**, *28* (15), 4544-4549.

A. P. da Costa, M. Sanaú, E. Peris\* and B. Royo\* *Dalton Trans.*, **2009**, *35*, 6960-6966.

A. P. da Costa, M. Viciano, M. Sanaú, S. Merino, J. Tejada,\* E. Peris\* and B. Royo\* *Organometallics*, **2008**, *27* (6), 1305-1309.

Cyclopentadienyl-Functionalised N-Heterocyclic Carbenes:  
Synthesis, Coordination to Mo, Ru, Rh and Ir and Catalytic Applications.

---



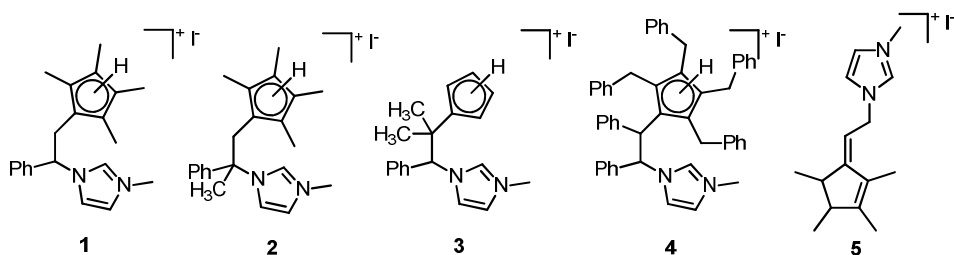
### 3.1. Abstract

This chapter deals with the description of all the Cp-functionalised imidazolium salts that we prepared along the present work.

The proligands depicted in Figure 3.1 were synthesised by two synthetic approaches:

- a) The imidazolium salts **1**, **3** and **4** were synthesised in three steps:
  - i) deprotonation of 1-benzylimidazole with *n*-butyl lithium, ii) reaction with the appropriate fulvene, and iii) quaternization with iodomethane. The imidazolium salt **2** was obtained in a similar way using (*S*)-1-(phenylethyl)imidazole instead of 1-benzylimidazole.
- b) The imidazolium salt **5** was synthesised by condensation between glyoxal, formaldehyde and a Cp\*-functionalised primary amine to afford the imidazole ring followed by quaternisation with iodomethane.

The imidazolium salts were isolated in low to good yields (**1** - 85%, **2** - 43%, **3** - 60%, **4** - 25%, **5** - 66%).



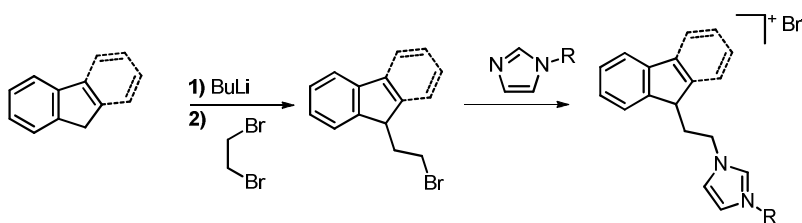
**Figure 3.1.** Cp-functionalised imidazolium salts proligands **1-5**.

All proligands were characterised by mass spectrometry and NMR spectroscopy.

The work reported in this chapter was done by the candidate. The synthesis of imidazolium salts **3** and **4** was done in collaboration with Dr. Krishna Mohan, a postdoc researcher in our research group (ITQB).

## 3.2. Introduction

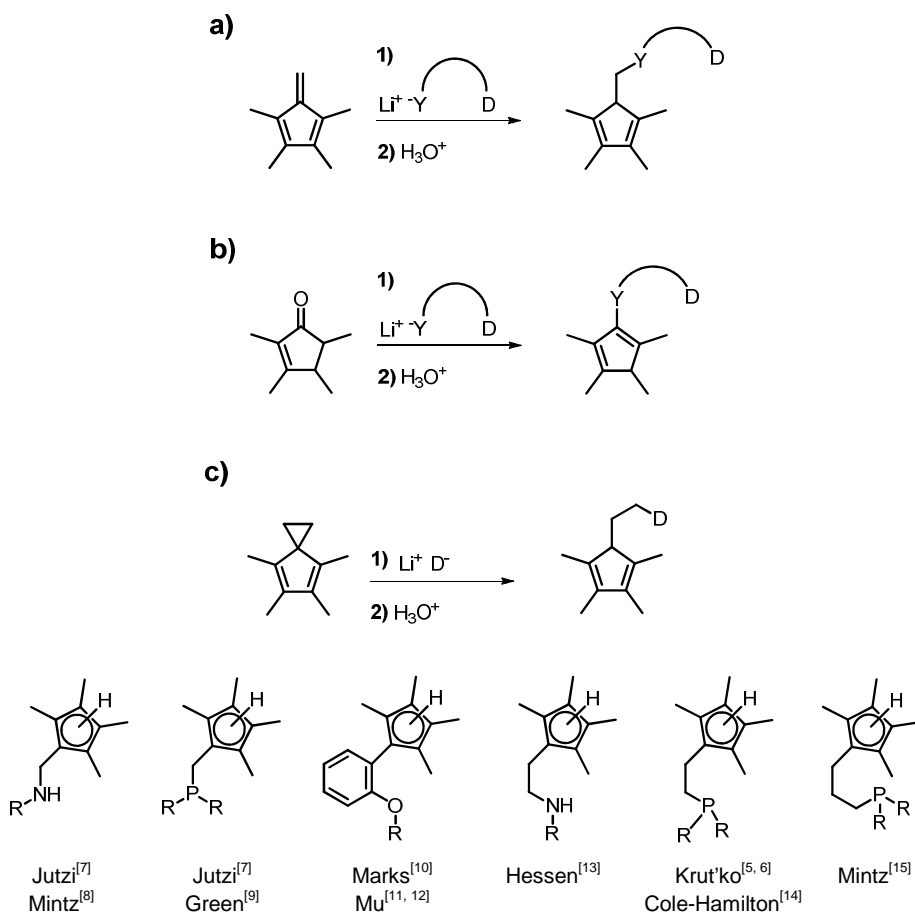
Over the years, many Cp\* ligands with donor functionalities have been synthesised. However, Cp\*-NHC ligands remained elusive. Downing and Danopoulos<sup>[1]</sup> recently described a synthetic pathway for the synthesis of indenyl- and fluorenyl-functionalised NHC ligands in which the first step implies the direct alkylation of the corresponding lithium salt (either lithium indenyl or lithium fluorenyl) with dibromoethane (Scheme 3.1). This strategy was based on previously reported protocols.<sup>[2-3]</sup> The resulting  $\beta$ -bromoethylindene or  $\beta$ -bromoethylfluorene readily reacts with imidazol to afford the desired imidazolium salt.



**Scheme 3.1.** Synthesis of indenyl- and fluorenyl-functionalised NHC ligands.

For the preparation of the related systems containing a Cp\* fragment instead of indenyl (or fluorenyl) some problems arise, the main one being the lack of regioselectivity in the direct alkylation of 1,2,3,4-tetramethylcyclopentadiene,<sup>[4-6]</sup> as previously pointed out by Downing and Danopoulos. In addition, the absence of synthetic methods leading to pure non-geminal-substituted  $\beta$ -haloethyltetramethylcyclopentadienes hampered the access to Cp\*-functionalised NHCs.<sup>[1]</sup>

Some straightforward approaches to Cp\* ligands with donor functionalities are depicted in Scheme 3.2. All these synthetic routes allowed the preparation of a vast variety of donor-functionalised Cp\* ligands, with as N-, O- and P-donor atoms as linkers ranging from methylene to propylene.



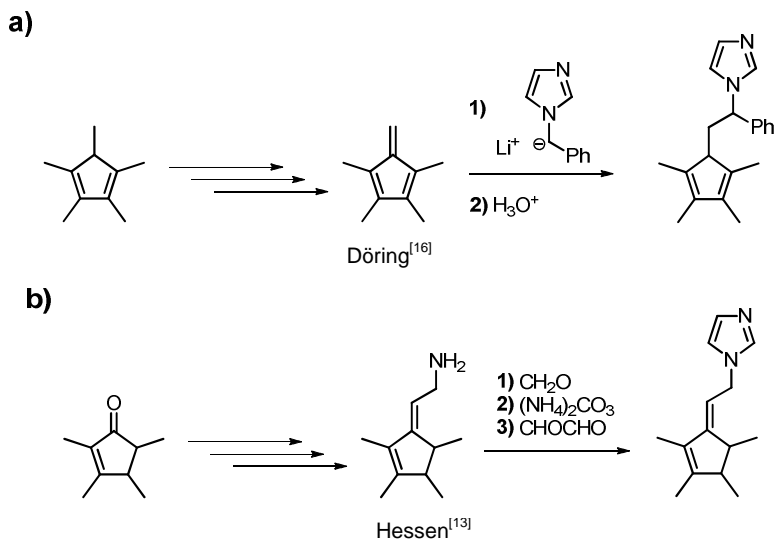
**Scheme 3.2.** Examples of synthesis of donor-functionalised Cp\* ligands.

## 3.3. Results and discussion

### 3.3.1. Synthesis of the imidazolium salts

During this thesis we explored two general strategies for the preparation of Cp\*-functionalised NHCs (Scheme 3.3). Both synthetic approaches share the fact that the starting materials are readily available by simple reactions from commercially available compounds. In route **a)** 1,2,3,4-tetramethylfulvene<sup>[16]</sup> can be prepared in almost quantitative yield in a two steps one-pot reaction from the commercially available 1,2,3,4,5-

pentamethylcyclopentadiene.<sup>[17]</sup> While in route **b**), the exocyclic isomer of 2-(2,3,4,5-tetramethylcyclopentadienyl)ethylamine<sup>[13]</sup> can be easily prepared in good yield and gram scale (~10g in ~70% yield) in three steps from 2,3,4,5-tetramethyl-2-cyclopenten-1-one<sup>[18]</sup> and acetonitrile.

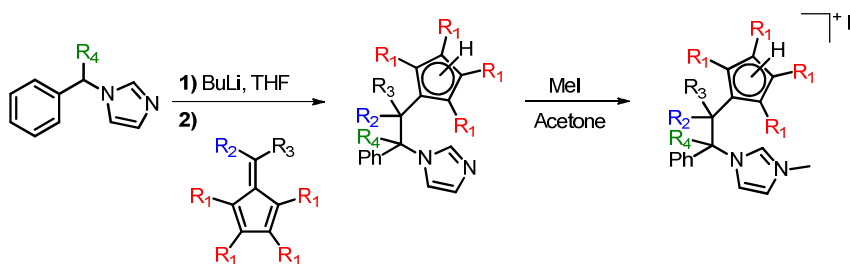


**Scheme 3.3.** Synthetic routes towards Cp\*-NHC explored during this thesis.

### 3.3.1.1. a) The fulvene route

The pro-ligands **1-4** were synthesised following route **a**) as depicted in Scheme 3.4. The imidazolium iodide **1** was synthesised by deprotonation at the methylene group of 1-benzylimidazole with *n*-butyl lithium, followed by reaction with 1,2,3,4-tetramethylfulvene<sup>[16]</sup> and treatment with MeOH. Subsequent reaction with iodomethane affords **1** in 85% overall yield.

In an attempt to obtain an enantiomerically pure chiral Cp\*-NHC ligand, we prepared the imidazolium salt **2** in 43% yield, starting from (*S*)-1-(phenylethyl)imidazole<sup>[19, 20]</sup> as depicted in Scheme 3.4. However, we observed that the final imidazolium proligand **2** is a racemate, probably as a consequence of racemisation during the deprotonation at the chiral carbon (first step of the reaction, Scheme 3.4).

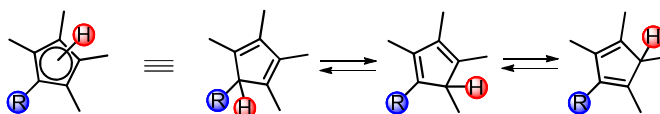


| Ligand | R <sub>1</sub>     | R <sub>2</sub>  | R <sub>3</sub>  | R <sub>4</sub>  | Yield <sup>a</sup> |
|--------|--------------------|-----------------|-----------------|-----------------|--------------------|
| 1      | CH <sub>3</sub>    | H               | H               | H               | 85                 |
| 2      | CH <sub>3</sub>    | H               | H               | CH <sub>3</sub> | 43                 |
| 3      | H                  | CH <sub>3</sub> | CH <sub>3</sub> | H               | 60                 |
| 4      | CH <sub>2</sub> Ph | Ph              | H               | H               | 25                 |

**Scheme 3.4.** Synthesis of pro-ligands **1-4**. <sup>a</sup> Overall yield, based on 1-benzylimidazole or S-1-(phenylethyl)imidazole.

The different stability of the carbanion formed upon reaction of 1-benzylimidazole and 1-(phenylethyl)imidazole with *n*-butyl lithium (secondary and tertiary carbanions, respectively) may explain the different overall yields obtained in the synthesis of **1** and **2**. The tertiary carbanion is less stable and a more hindered nucleophile than the secondary carbanion, thus rendering less efficient deprotonation.

Apart from compound **2**, all other Cp'-functionalised imidazolium salts were isolated as mixtures of regio-isomers, resulting from the different position of the double bonds in the cyclopentadienyl ring, Scheme 3.5. However, this will not interfere with the coordination to the metal centre.

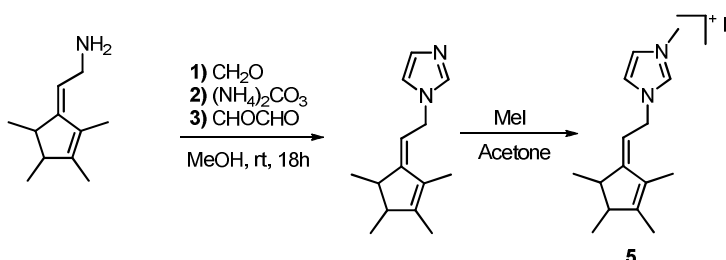


**Scheme 3.5.** Regio-isomers of substituted Cp\*.

This synthetic strategy allowed us to easily modify the substituents on both, the cyclopentadienyl ring and the carbon next to the Cp ring, by choosing the appropriate fulvene fragment. In fact, the unsubstituted Cp-functionalised NHC **3** and the tetrabenzyl-Cp-functionalised NHC **4** were prepared following the same synthetic route (Scheme 3.4).

### 3.3.1.2. *b*) The Cp\*-amine route

The imidazolium iodide **5** was prepared by condensation of glyoxal, formaldehyde and 2-(2,3,4,5-tetramethylcyclopentadienyl)ethylamine<sup>[13]</sup> yielding 2-(2,3,4,5-tetramethylcyclopentadienyl)ethylimidazole. Further quaternization with iodomethane affords the imidazolium iodide **5** with an overall yield of 66% (Scheme 3.6).



**Scheme 3.6.** Synthesis of **5**.

### 3.3.1.3. Route *a*) versus route *b*)

Route **a**) is very versatile allowing the introduction of smooth changes in the electronic and steric properties of the ligands by the carefully choice of the Cp' moiety. Additionally, the bridge has a stereogenic centre, therefore affording a chiral ligand, although we were only able to isolate racemic mixtures of the pro-ligands.

Route **b**) is a one-pot reaction that can be performed in large scale (up to gram scale) and the final product, **5**, is purified by a simple crystallisation without further need of column chromatography, which is required in the purification of **1-4**.

### 3.3.2. Characterisation of the imidazolium salts

The imidazolium salts **1-5** were isolated as yellow solids and were characterised by  $^1\text{H}$  and  $^{13}\text{C}$  NMR spectroscopy and ESI-mass spectrometry.

Compounds **1**, **3** and **4** were isolated as mixtures of regioisomers, but we succeeded to isolate one only regioisomer of the salt **2**. As illustrated in Figure 3.2 ( $^1\text{H}$  spectrum of **1**), most Cp\*-imidazolium salts described in this chapter display complex NMR spectra due to the presence of mixtures of multiple regio-isomers.

Both **1** (Figure 3.2) and **2** (Figure 3.3) showed qualitative similar NMR spectra. On the  $^1\text{H}$  NMR spectra, the more representative signals of this type of imidazolium salts are: (i) the doublet at  $\sim 0.8$  ppm that corresponds to the resonance of the methyl group of the cyclopentadienyl group that couples with the proton of the Cp ring, (ii) the three singlets at  $\sim 2 - 1.5$  ppm due to the protons of the remaining three methyl groups at the Cp\*-ring, (iii) a singlet at  $\sim 4$  ppm assigned to the protons of the methyl group at the imidazolium ring, and (iv) a singlet at  $\sim 10$  ppm due to the acid proton in the imidazolium moiety.

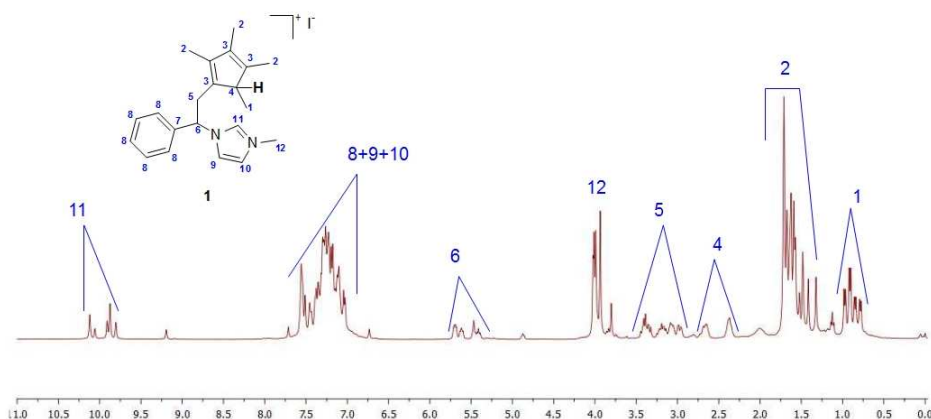
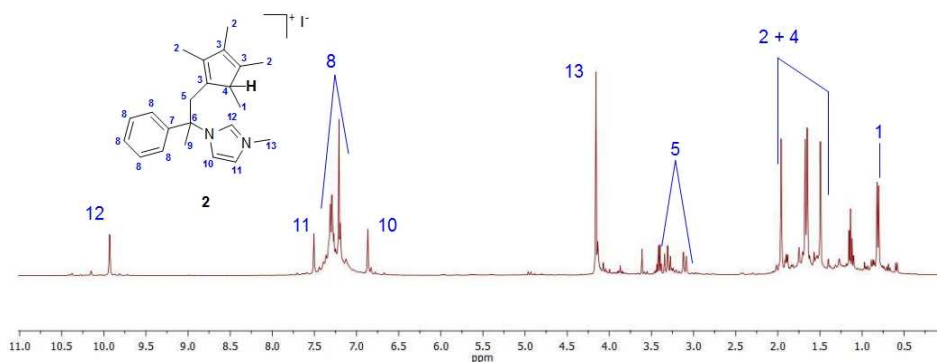


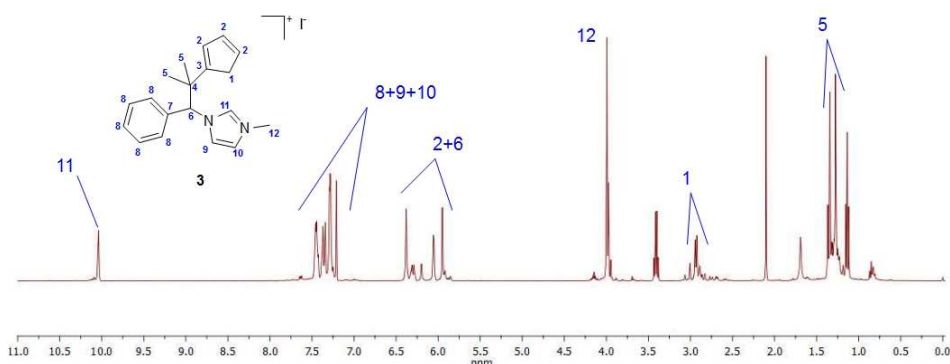
Figure 3.2.  $^1\text{H}$  NMR spectrum of **1** (400 MHz,  $\text{CDCl}_3$ , 300K).



**Figure 3.3.**  $^1\text{H}$  NMR spectrum of **2** (400 MHz,  $\text{CDCl}_3$ , 300K).

The  $^1\text{H}$ -NMR spectrum of **3** (Figure 3.4) displays a resonance at  $\sim 10$  ppm due to the acid proton of the imidazolium salt. A singlet at  $\sim 4$  ppm is attributed to the protons of the N-methyl group at the imidazolium ring. The resonances corresponding to the protons of the cyclopentadienyl ring appear as multiplets at  $\sim 6$  ppm.

The  $^1\text{H}$ -NMR and the  $\{^1\text{H}\}$   $^{13}\text{C}$  NMR spectra of **4** (Figure 3.6 in the supporting information) is rather complex, showing many resonances difficult to fully assign. The characterisation of **4** mainly relies on ESI-mass spectrometry and elemental analysis.

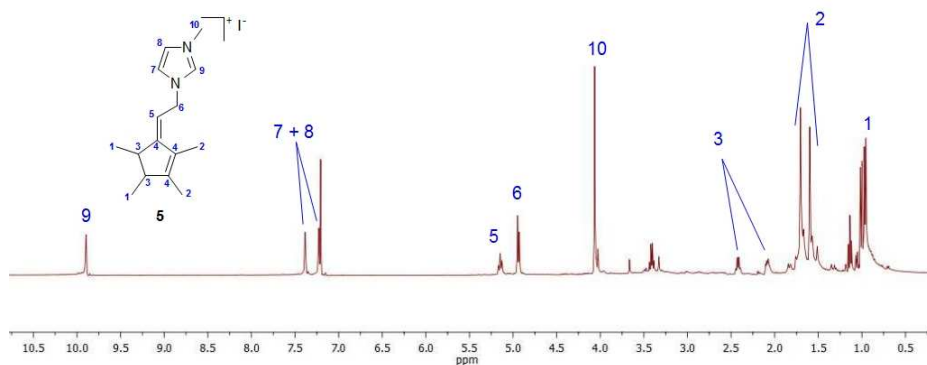


**Figure 3.4.**  $^1\text{H}$  NMR spectrum of **3** (400 MHz,  $\text{CDCl}_3$ , 300K).

The imidazolium salt **5** was synthesised as the exocyclic isomer of the cyclopentadienyl ring, therefore characteristic NMR signals are quite different. The  $^1\text{H}$  NMR spectrum of **5** are shown in Figure 3.5. The



resonances corresponding to the azolium ring display at  $\sim 10$  ppm (acidic proton), 7.47 and 7.28 ppm (protons in the backbone) and a singlet at 4.10 ppm corresponding to the resonance of the N-CH<sub>3</sub> group. The methyl groups in the exocyclic Cp\* functionality resonances as two singlets at  $\sim 1.5 - 2$  ppm corresponding to the methyl groups in the double bond and two doublets at  $\sim 0.8$  ppm for the methyl in single bond, which couple with the endocyclic protons at  $\sim 2 - 2.5$  ppm.



**Figure 3.5.** <sup>1</sup>H NMR spectrum of **5** (400 MHz, CDCl<sub>3</sub>, 300K).

### 3.4. Conclusions

In this chapter, we have described two synthetic pathways for the synthesis of the first Cp<sup>X</sup>-functionalised imidazolium salts (Cp<sup>X</sup> = tetramethylcyclopentadienyl, tetrabenzylcyclopentadienyl and cyclopentadienyl), as precursors of the corresponding Cp<sup>X</sup>-functionalised NHCs.

One of the synthetic pathways provides access to chiral Cp<sup>X</sup>-functionalised NHCs, although these were isolated as racemic mixtures. Nevertheless, the existence of a chiral centre at the bridge can be useful for the preparation of chiral-at-metal complexes.

An alternative synthetic strategy providing a simple and high yielding method to achiral Cp\*<sup>X</sup>-functionalised NHCs has also been developed.

## 3.5. Experimental procedures

### 3.5.1. Materials and methods

All reactions were carried out under inert atmosphere. When required, solvents were dried via standard techniques.

NMR spectra were recorded on a Bruker Avance III 400 MHz spectrometer with CDCl<sub>3</sub> (Cambridge Isotope Laboratories, Inc.) as solvent.

Elemental analyses and Mass Spectrometry were performed in our laboratories at ITQB.

Dimethylfulvene,<sup>[21]</sup> 1-(2,3,4,5-tetramethylcyclopentadienyl)ethylamine,<sup>[13]</sup> (S)-1-(phenylethyl)imidazole<sup>[19, 20]</sup> and 1,2,3,4-tetramethylfulvene,<sup>[16]</sup> were synthesized according to literature procedures. All other reagents are commercially available and were used as received.

### 3.5.2. Synthesis and characterisation of 1-5.

#### Route a) – general procedure

An hexane solution of *n*-BuLi (1.2 eq) was added dropwise to a solution of 1-benzylimidazole or (S)-1-(phenylethyl)imidazole (1 eq) in dried THF at -60 °C. After the solution was stirred for 20 min, the corresponding fulvene (0.8 eq) was added at -60°C, and the reaction mixture was allowed to reach room temperature and stirred for 1 h. Methanol was then added, and the volatiles were evaporated. The crude oil was purified by flash chromatography (hexane/ethyl acetate, 1:4). The Cp'-functionalised imidazole was dissolved in acetone and iodomethane (5 eq) was added to the solution. The reaction was stirred at room temperature for 12 h, and all the volatiles were evaporated affording the tittle compounds as yellow solids which were washed several times with dried diethyl.

**Compound 1**

Yield: 85%.  $^1\text{H}$  NMR (400 MHz,  $\text{CDCl}_3$ )  $\delta$  10.2–9.2 (s, 1H,  $\text{CH}_{\text{imid}}$ ), 7.75–6.76 (m, 7H, PhH,  $\text{CH}_{\text{imid}}$ ), 5.75–4.9 (m, 1H,  $\text{CH}_{\text{linker}}$ ), 4.0–3.8 (s, 3H,  $\text{NCH}_3$ ), 3.44–2.4 (m, 3H,  $\text{CH}_2(\text{linker})$ ,  $\text{Cp}^*\text{H}$ ), 1.74–1.35 (s, 9H,  $\text{CH}_3(\text{Cp}^*)$ ), 1.0–0.8 (d, 3H,  $\text{CH}_3(\text{Cp}^*)$ ). Anal. Calcd for  $\text{C}_{21}\text{H}_{27}\text{IN}_2$ : C, 58.07; H, 6.27; N 6.45. Found: C, 58.46; H, 6.45; N, 6.13.

**Compound 2**

Yield: 43%.  $^1\text{H}$  NMR (400MHz,  $\text{CDCl}_3$ ):  $\delta$  9.96 (br, 1H,  $\text{CH}_{\text{imid}}$ ), 7.53 (br, 1H,  $\text{CH}_{\text{imid}}$ ), 7.39-7.22 (br, 5H, PhH), 6.89 (br, 1H,  $\text{CH}_{\text{imid}}$ ), 4.19 (s, 3H,  $\text{NCH}_3$ ), 3.35 (d, 1H,  $^2J_{\text{H-H}} = 14.2$  Hz,  $\text{CH}_2(\text{linker})$ ), 3.13 (d, 1H,  $^2J_{\text{H-H}} = 14.2$  Hz,  $\text{CH}_2(\text{linker})$ ), 1.70 (s, 3H,  $\text{CH}_3(\text{Cp}^*)$ ), 1.68 (s, 3H,  $\text{CH}_3(\text{Cp}^*)$ ), 1.52 (s, 3H,  $\text{CH}_3(\text{Cp}^*)$ ), 1.19 (s, 3H,  $\text{CH}_3(\text{linker})$ ), 0.84 (d, 3H,  $^3J_{\text{H-H}} = 7.4$  Hz,  $\text{CH}_3(\text{Cp}^*)$ ).  $\{^1\text{H}\}^{13}\text{C}$  NMR (100MHz,  $\text{CDCl}_3$ ):  $\delta$  142.7 ( $\text{C}_{\text{Cp}^*}$ ), 142.0 ( $\text{C}_{\text{Ph}}$ ), 141.4 ( $\text{C}_{\text{Cp}^*}$ ), 136.8 ( $\text{CH}_{\text{imid}}$ ), 134.1 ( $\text{C}_{\text{Cp}^*}$ ), 132.9 ( $\text{C}_{\text{Cp}^*}$ ), 129.2 ( $\text{CH}_{\text{Ph}}$ ), 128.8 ( $\text{CH}_{\text{Ph}}$ ), 125.8 ( $\text{CH}_{\text{Ph}}$ ), 123.7 ( $\text{CH}_{\text{imid}}$ ), 120.9 ( $\text{CH}_{\text{imid}}$ ), 69.1 ( $\text{C}_{\text{linker}}$ ), 50.0( $\text{CH}_{\text{Cp}^*}$ ), 37.6 ( $\text{NCH}_3$ ), 36.8 ( $\text{CH}_2(\text{linker})$ ), 28.4 ( $\text{CH}_3(\text{linker})$ ), 15.3 ( $\text{CH}_3(\text{Cp}^*)$ ), 12.0 ( $\text{CH}_3(\text{Cp}^*)$ ), 11.8 ( $\text{CH}_3(\text{Cp}^*)$ ), 11.0 ( $\text{CH}_3(\text{Cp}^*)$ ). Anal. Calcd for  $\text{C}_{22}\text{H}_{29}\text{IN}_2$ : C, 58.93; H, 6.25; N 6.52. Found: C, 58.46; H, 6.69; N, 6.29.

**Compound 3**

Yield: 60%.  $^1\text{H}$  NMR (400MHz,  $\text{CDCl}_3$ ):  $\delta$  10.2 (s, 1H,  $\text{NCHN}$ ), 7.47-7.20 (m, 7H,  $\text{CH}_{\text{Ph}}+\text{CH}_{\text{imid}}$ ), 6.43-6.06 (m, 4H,  $\text{CH}_{\text{Cp}}$ ), 5.94 (s, 1H,  $\text{CHPh}_{\text{linker}}$ ), 4.02 (s, 3H,  $\text{NCH}_3$ ), 2.96 (d, 2H,  $\text{CH}_2\text{Cp}$ ), 1.38 (s, 3H,  $\text{CH}_3_{\text{linker}}$ ), 1.30 (s, 3H,  $\text{CH}_3_{\text{linker}}$ ).  $\{^1\text{H}\}^{13}\text{C}$  NMR (100 MHz,  $\text{CDCl}_3$ ,  $\delta$ ): 151.7, 150.1 ( $\text{C}_{\text{Phenyl}}$ ), 134.7, 132.97 ( $\text{CH}_{\text{imid}}$ ), 134.6, 134.3 ( $\text{C}_{\text{Cp}}$ ), 132-128 ( $\text{CH}_{\text{Phenyl}} + \text{CH}_{\text{Cp}}$ ), 122.78, 122.71 ( $\text{CH}_{\text{imid}}$ ), 122.4, 122.3 ( $\text{CH}_{\text{imid}}$ ), 72.96, 72.65 ( $\text{CHPh}_{\text{linker}}$ ), 42.06, 41.41 ( $\text{C}(\text{CH}_3)_2\text{linker}$ ), 41.57, 40.64 ( $\text{CH}_2\text{Cp}$ ), 37.09, 37.02 ( $\text{NCH}_3$ ), 27.39, 26.88 ( $\text{CH}_3\text{linker}$ ), 25.38, 24.93 ( $\text{CH}_3\text{linker}$ ). Anal.

Calcd. for  $C_{19}H_{23}N_2I$ : C, 56.16; H, 5.70; N, 6.89. Found: C, 56.27; H, 5.78; N, 6.55. MS (ESI):  $m/z$  407 (100,  $M^+-I$ ).

#### Compound 4

Yield: 25%.  $^1H$  NMR (400MHz,  $CD_2Cl_2$ ):  $\delta$  10.2 (s, 1H, NCHN), 7.47-7.20 (m, 7H,  $CH_{Ph}+CH_{Imid}$ ), 6.43-6.06 (m, 4H,  $CH_{Cp}$ ), 5.94 (s, 1H,  $CHPh_{linker}$ ), 4.02 (s, 3H,  $NCH_3$ ), 1.57 (s, 1H,  $CH_{Cp}$ ), 1.38 (s, 3H,  $CH_3_{linker}$ ), 1.30 (s, 3H,  $CH_3_{linker}$ ).  $\{^1H\}^{13}C$  NMR (100 MHz,  $CDCl_3$ ,  $\delta$ ): 146-134 ( $C_{Phenyl}$ ), 130-125 ( $CH_{Phenyl} + CH_{Imid}$ ), 65.59-64.22 ( $NCHPh_{linker}$ ), 52.46-47.97 ( $CHPhCHPh_{linker}$ ), 36.21, 36.10, 35.81 ( $NCH_3$ ), 35.30-31.23 ( $CH_2Ph_{Cp}$ ). Anal. Calcd. for  $C_{51}H_{45}N_2I$ : C, 75.36; H, 5.58; N, 3.44. Found: C, 75.26; H, 5.92; N, 3.02. MS (ESI):  $m/z$  687 ( $M^+-I$ , 100%).

#### *Preparation of pentabenzylfulvene:*

*n*-BuLi (6.04 mL of 1.6 M in hexane, 9.66 mmol) was added dropwise to a solution of pentabenzylcyclopentadiene (3.60 g, 8.05 mmol) in THF (20 mL) at  $-60$  °C. After being stirred for 20 min, the reaction mixture was allowed to warm to room temperature and it was further stirred for 1 h. Triphenylmethyl chloride (2.69 g, 9.66 mmol) was then added to the reaction mixture at 0 °C. The reaction mixture was allowed to stir for 16h at 4°C and the crude mixture was used without further purification.

#### Route b) – general procedure

#### Compound 5

An aqueous solution of formaldehyde (190  $\mu$ L of 33% wt in water, 2.53 mmol) was added dropwise to neat 2-(2,3,4,5-tetramethylcyclopentadienyl)ethylamine (418 mg, 2.53 mmol) at 0°C. The mixture was stirred until formation of a white solid (10-15 minutes). Ammonium carbonate (121.6 mg, 1.27mmol), an aqueous solution of glyoxal (290  $\mu$ L of 40%wt in water, 2.53 mmol) and 5-10 mL of methanol

were subsequently added and the mixture stirred at room temperature overnight. The reaction mixture was treated with brine and extracted with hexane. The organic layer was dried over sodium sulphate anhydrous and evaporated to dryness. The remaining crude brown oil was redissolved in acetone, and iodomethane (720  $\mu$ L, 11.6 mmol) was added. Stirring was continued for 24 h at room temperature. Solvent was removed under vacuum to yield **5** as a yellow solid. The product was washed several times with diethyl ether and dried under vacuum. Yield: 600 mg (66%).  $^1\text{H}$  NMR (400MHz,  $\text{CDCl}_3$ ):  $\delta$  9.87 (br, 1H,  $\text{CH}_{\text{imid}}$ ), 7.47 (br, 1H,  $\text{CH}_{\text{imid}}$ ), 7.28 (br, 1H,  $\text{CH}_{\text{imid}}$ ), 5.18 (t, 1H,  $^3J_{\text{H-H}} = 7.7$  Hz,  $\text{CH}_{\text{linker}}$ ), 4.97 (d, 2H,  $^3J_{\text{H-H}} = 7.7$  Hz,  $\text{CH}_{2(\text{linker})}$ ), 4.10 (s, 3H, N- $\text{CH}_3$ ), 2.45 (q, 1H,  $^3J_{\text{H-H}} = 7.2$  Hz,  $\text{CH}_{(\text{Cp}^*)}$ ), 2.10 (q, 1H,  $^3J_{\text{H-H}} = 7.0$  Hz,  $\text{CH}_{(\text{Cp}^*)}$ ), 1.73 (s, 3H,  $\text{CH}_3(\text{Cp}^*)$ ), 1.63 (s, 3H,  $\text{CH}_3(\text{Cp}^*)$ ), 1.04 (d, 3H,  $^3J_{\text{H-H}} = 7.2$  Hz,  $\text{CH}_3(\text{Cp}^*)$ ), 0.99 (d, 3H,  $^3J_{\text{H-H}} = 7.0$  Hz,  $\text{CH}_3(\text{Cp}^*)$ ).  $\{^1\text{H}\}^{13}\text{C}$  NMR (100MHz,  $\text{CDCl}_3$ ) d 161.7 ( $\text{C}_{\text{Cp}^*}$ ), 150.3 ( $\text{C}_{\text{Cp}^*}$ ), 136.6 ( $\text{CH}_{\text{imid}}$ ), 130.1 ( $\text{C}_{\text{Cp}^*}$ ), 123.6 ( $\text{CH}_{\text{imid}}$ ), 121.3 ( $\text{CH}_{\text{imid}}$ ), 104.7 ( $\text{CH}_{\text{linker}}$ ), 51.5 ( $\text{CH}_{\text{Cp}^*}$ ), 49.0 ( $\text{CH}_{2(\text{linker})}$ ), 42.41 ( $\text{CH}_{\text{Cp}^*}$ ), 37.38 (N- $\text{CH}_3$ ), 22.2 ( $\text{CH}_3(\text{Cp}^*)$ ), 19.33 ( $\text{CH}_3(\text{Cp}^*)$ ). MS (ESI):  $m/z$  [ $\text{M} - \text{I}$ ] $^+$  calc for  $\text{C}_{15}\text{H}_{23}\text{N}_2$ , 231.2; found, 231.1.

### 3.6. Acknowledgements

We gratefully acknowledge Dr. Juan Tejada (UCLM, Spain) for guidance in the development of the first synthetic route towards  $\text{Cp}^*$ -functionalised NHCs imidazolium salt **1**. We wish to acknowledge M. C. Almeida and Dr. A. Coelho for providing data from the Mass Spectrometry and Elemental Analysis Services at ITQB. The Bruker Avance III 400 MHz spectrometer is part of the National NMR Network and was purchased in the framework of the National Program for Scientific Re-equipment, contract REDE/1517/RMN/2005, with funds from POCI 2010 (FEDER) and Fundação para a Ciência e a Tecnologia (FCT).

### 3.7. References

- [1] S. P. Downing, A. A. Danopoulos, *Organometallics* **2006**, *25*, 1337.
- [2] J. Kukral, P. Lehmus, M. Klinga, M. Leskela, B. Rieger, *Eur. J. Inorg. Chem.* **2002**, 1349.
- [3] M. Deppner, R. Burger, H. G. Alt, *J. Organomet. Chem.* **2004**, 689, 1194.
- [4] P. Jutzi, J. Dahlhaus, *Synthesis* **1993**, 684.
- [5] D. P. Krut'ko, M. V. Borzov, E. N. Veksler, E. M. Myshakin, D. A. Lemenovskii, *Russ. Chem. Bull.* **1998**, *47*, 956.
- [6] D. P. Krut'ko, M. V. Borzov, E. N. Veksler, R. S. Kirsanov, A. V. Churakov, *Eur. J. Inorg. Chem.* **1999**, 1973.
- [7] T. Heidemann, P. Jutzi, *Synthesis* **1994**, 777.
- [8] D. M. Bensley, E. A. Mintz, *J. Organomet. Chem.* **1988**, 353, 93.
- [9] R. M. Bellabarba, G. P. Clancy, P. T. Gomes, A. M. Martins, L. H. Rees, M. L. H. Green, *J. Organomet. Chem.* **2001**, *640*, 93.
- [10] Y. X. Chen, T. J. Marks, *Organometallics* **1997**, *16*, 3649.
- [11] Y. T. Zhang, Y. Mu, C. S. Lu, G. H. Li, J. S. Xu, Y. R. Zhang, D. S. Zhu, S. H. Feng, *Organometallics* **2004**, *23*, 540.
- [12] J. S. Xu, Y. T. Zhang, G. H. Li, Y. Mu, S. H. Feng, *Polyhedron* **2006**, *25*, 3071.
- [13] D. van Leusen, D. J. Beetstra, B. Hessen, J. H. Teuben, *Organometallics* **2000**, *19*, 4084.
- [14] A. C. McConnell, P. J. Pogorzelec, A. M. Z. Slawin, G. L. Williams, P. I. P. Elliott, A. Haynes, A. C. Marr, D. J. Cole-Hamilton, *Dalton Trans.* **2006**, 91.
- [15] D. M. Bensley, E. A. Mintz, S. J. Sussangkarn, *J. Org. Chem.* **1988**, *53*, 4417.
- [16] S. Döring, G. Erker, *Synthesis* **2001**, 43.
- [17] Aldrich catalog number #214027.
- [18] Aldrich catalog number #274658.
- [19] W. A. Herrmann, M. Elison, J. Fischer, C. Kocher, G. R. J. Artus, *Chem-Eur. J.* **1996**, *2*, 772.

- [20] W. A. Herrmann, L. J. Goossen, C. Kocher, G. R. J. Artus, *Angew. Chem. Int. Ed.* **1996**, *35*, 2805.
- [21] J. Thiele, H. Balhorn, *Justus Liebigs Ann. Chem.* **1906**, *348*, 1.

### 3.8. Supporting information

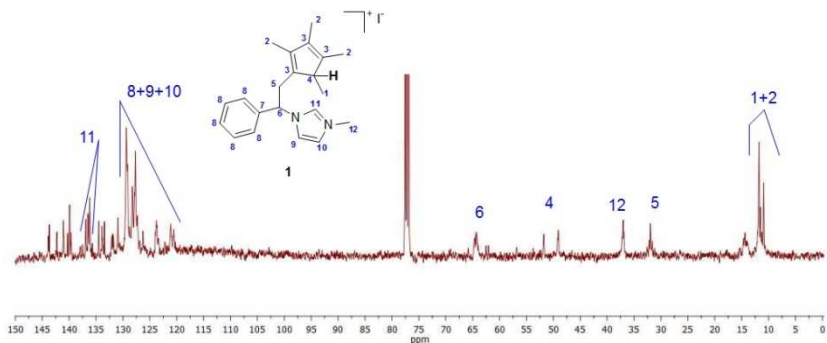


Figure 3.6. <sup>13</sup>C NMR spectrum of **1** (100 MHz, CDCl<sub>3</sub>, 300K).

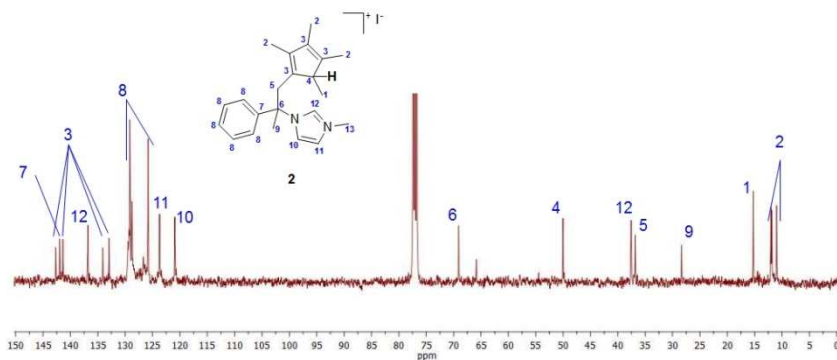


Figure 3.7. <sup>13</sup>C NMR spectrum of **2** (100 MHz, CDCl<sub>3</sub>, 300K).

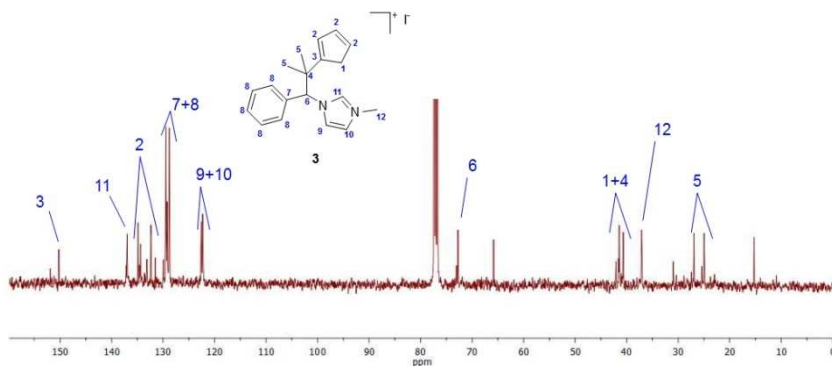
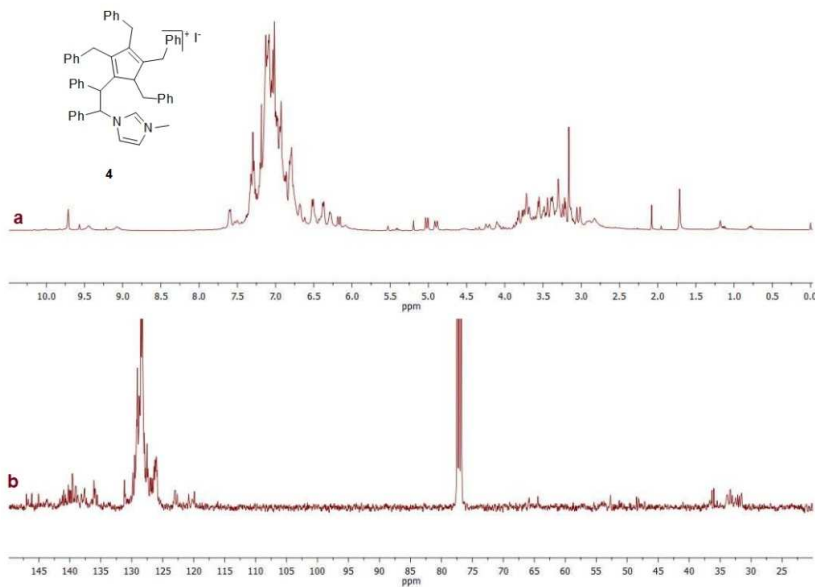
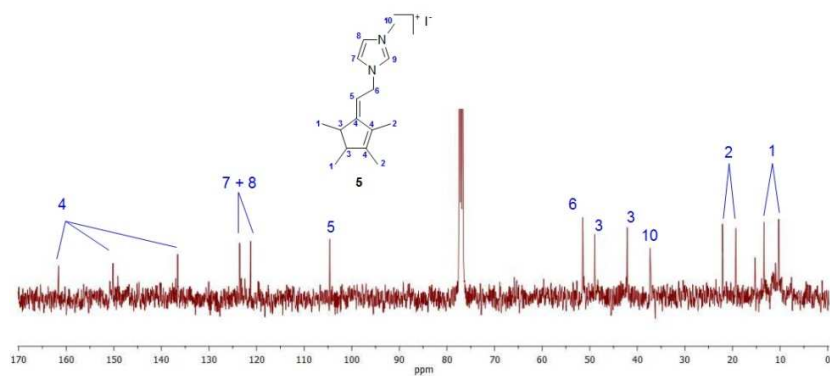


Figure 3.8. <sup>13</sup>C NMR spectrum of **3** (100 MHz, CDCl<sub>3</sub>, 300K).

Cyclopentadienyl-Functionalised N-Heterocyclic Carbenes:  
Synthesis, Coordination to Mo, Ru, Rh and Ir and Catalytic Applications.



**Figure 3.9.**  $^1\text{H}$  NMR and  $\{^1\text{H}\}$   $^{13}\text{C}$  NMR spectra of **4** (400 MHz,  $\text{CDCl}_3$ , 300K).



**Figure 3.10.**  $^{13}\text{C}$  NMR spectrum of **5** (100 MHz,  $\text{CDCl}_3$ , 300K).



---

# 4.

## COORDINATION TO Mo AND APPLICATION IN OLEFIN EPOXIDATION

---

|      |  |    |
|------|--|----|
| 4.1. | Abstract   | 43 |
| 4.2. | Introduction   | 43 |
| 4.3. | Results and discussion   | 45 |
|      | 4.3.1. Synthesis of the molybdenum complexes <b>6-9</b> , 45         |    |
|      | 4.3.2. Characterisation of complexes <b>6-9</b> , 46                 |    |
|      | 4.3.3. Olefin epoxidation by complexes <b>6, 8</b> and <b>9</b> , 49 |    |
| 4.4. | Conclusions  | 52 |
| 4.5. | Experimental procedures  | 53 |
|      | 4.5.1. Materials and methods, 53                                     |    |
|      | 4.5.2. Synthesis and characterisation of <b>6-9</b> , 53             |    |
|      | 4.5.3. X-ray diffraction studies, 55                                 |    |
| 4.6. | Acknowledgments  | 56 |
| 4.7. | References   | 56 |

Cyclopentadienyl-Functionalised N-Heterocyclic Carbenes:  
Synthesis, Coordination to Mo, Ru, Rh and Ir and Catalytic Applications.

---

## 4.1. Abstract

This chapter describes the preparation of a series of molybdenum complexes of general formula  $(Cp^X-NHC)Mo(CO)_2I$ , depicted in Figure 4.1. Complexes **6-9** were synthesised by reaction of  $[MoCl(\eta^3-C_3H_5)(CO)_2(NCCH_3)_2]$  with the corresponding lithium NHC-cyclopentadienides, which were previously prepared by treatment of the corresponding imidazolium proligands with *n*-BuLi. All complexes were isolated as air stable red solids in good yields, and were characterised by NMR and IR spectroscopy, mass spectrometry, and elemental analysis. The structure of complex **6** was determined by X-ray diffraction studies.

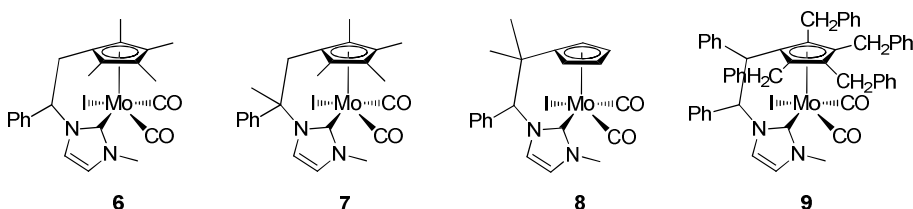


Figure 4.1.  $(Cp^X-NHC)Mo(CO)_2I$  complexes.

Preliminary catalytic studies on the epoxidation of *cis*-cyclooctene with *tert*-butyl hydroperoxide (TBHP) using complexes **6-9** as catalysts showed that their activity clearly depends on the nature of the  $Cp^X-NHC$  ligand.

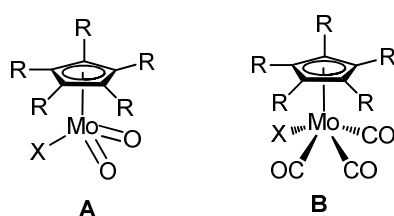
The work described in this chapter was done in collaboration with Dr. Krishna Mohan, a postdoc researcher in our research group, who designed the synthetic strategies for the preparation of **6-9**, and performed the catalytic studies.

## 4.2. Introduction

The study of high oxidation state molybdenum organometallic complexes has influenced both industrial and biochemical research.

Industrially, high oxidation state molybdenum complexes are involved as catalysts in a vast number of important chemical transformations, such as olefin epoxidation<sup>[1-4]</sup> and olefin metathesis.<sup>[5]</sup>

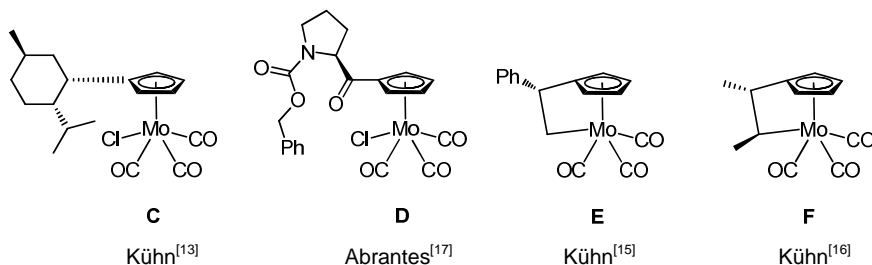
Although the synthesis of the first organo-molybdenum oxo-complex, CpMoO<sub>2</sub>Cl (Cp = cyclopentadienyl, **A**, Figure 4.2) was reported by Green and Cousins in 1963,<sup>[6]</sup> the first application in catalysis was only described thirty years later, when Trost and Bergman reported the excellent catalytic activity of **A** in olefin epoxidation.<sup>[7]</sup> The major limitation to the development and application of these type of complexes was the lack of good yielding synthetic methods. Recent developments enabled the easier synthesis of several Cp'MoO<sub>2</sub>Cl complexes and their application in catalysis. Additionally, it was shown that Cp'Mo(CO)<sub>3</sub>Cl compounds (**B**, Figure 4.2) can be used as olefin epoxidation pre-catalyst. Oxidative decarbonylation of Cp'Mo(CO)<sub>3</sub>Cl with excess of TBHP provides a convenient pathway to generate the dioxomolybdenum(VI) complexes Cp'MoO<sub>2</sub>Cl. During the last ten years important advances have been made in the chemistry of Cp'Mo(CO)<sub>3</sub>X complexes, mainly due to the groups of Romão, Kühn, Poli, and Gonçalves.<sup>[8-21]</sup>



**Figure 4.2.** Cp'MoO<sub>2</sub>X (**A**) and Cp'Mo(CO)<sub>3</sub>X (**B**).

The introduction of chirality into these complexes by using cyclopentadienyls with linked chiral substituents suffers from a major drawback: the free rotation of the cyclopentadienyl ring, yielding negligible asymmetric induction (**C** and **D**, Figure 4.3).<sup>[13, 17]</sup> In order to overcome this problem, Kühn and co-workers developed a series of

catalytically active *ansa*-bridged cyclopentadienyl compounds of molybdenum (**E** and **F**, Figure 4.3).<sup>[15, 16]</sup> However, some of these complexes show low stability under oxidative conditions leading to a significant decomposition of the catalyst during the catalytic cycle.



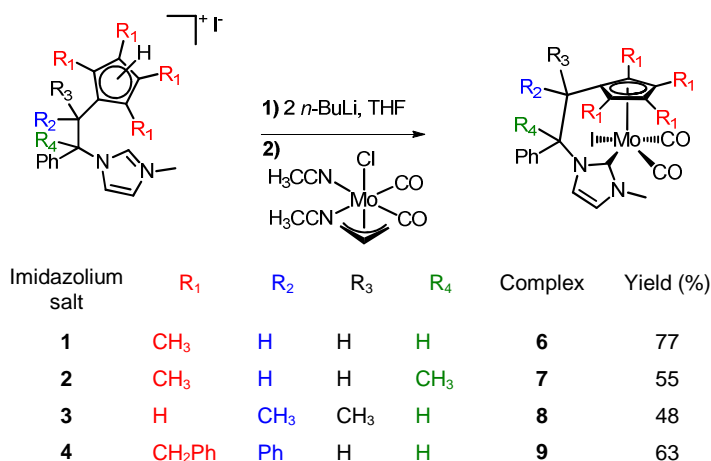
**Figure 4.3.** Some chiral Cp<sup>\*</sup>Mo(CO)<sub>3</sub>X (**C** and **D**) and *ansa*-Cp<sup>\*</sup>Mo(CO)<sub>3</sub> (**E** and **F**) used as pre-catalysts for olefin epoxidation.

The work described in this chapter aims to explore the use of tethered Cp<sup>\*</sup>-NHC ligands in molybdenum chemistry. So far, the chemistry of high-valent molybdenum-NHC is almost unexplored.<sup>[22, 23]</sup> On the other hand, low-valent NHC-based molybdenum carbonyls are known.<sup>[24-29]</sup> We were also interested in studying the potential application of our new complexes in olefin epoxidation, and relating our results with the recently described catalytic outcomes of other NHC-based molybdenum carbonyls obtained in our group.<sup>[27]</sup>

## 4.3. Results and discussion

### 4.3.1. Synthesis of the molybdenum complexes 6-9

The Cp<sup>x</sup>-NHC ligand precursors **1-4** were coordinated to molybdenum(II) as depicted in Scheme 4.1. Treatment of the proligands **1-4** with two equivalents of *n*-BuLi and subsequent reaction with [MoCl(η<sup>3</sup>-C<sub>3</sub>H<sub>5</sub>)(CO)<sub>2</sub>(NCCH<sub>3</sub>)<sub>2</sub>] afforded the corresponding (Cp<sup>x</sup>-NHC)Mo(CO)<sub>2</sub>I complexes **6-9** in moderate to good yields.



**Scheme 4.1.** Synthesis of (Cp<sup>X</sup>-NHC)Mo(CO)<sub>2</sub>I complexes **6-9**.

#### 4.3.2. Characterisation of complexes 6-9

Complexes **6-9** were isolated as red solids that were air- and moisture-stable in the solid state, and quite stable in solution (samples in CD<sub>2</sub>Cl<sub>2</sub> showed trace amounts of degradation after 24h).

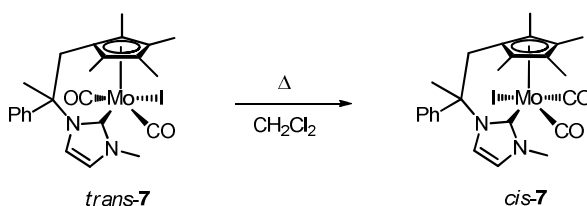
All complexes were characterised by IR, NMR (<sup>1</sup>H, <sup>13</sup>C and <sup>95</sup>Mo) spectroscopy, mass spectrometry and EA. Selected spectroscopic data are summarised in Table 4.1. The crystal structure of **6** was determined by X-ray diffraction analyses.

**Table 4.1.** Selected IR frequencies and <sup>13</sup>C and <sup>95</sup>Mo NMR chemical shifts for complexes **6-9**.

| complex  | IR <sup>a</sup>                     | <sup>13</sup> C NMR  |                      | <sup>95</sup> Mo NMR <sup>b</sup> |
|----------|-------------------------------------|----------------------|----------------------|-----------------------------------|
|          | ν <sub>CO</sub> (cm <sup>-1</sup> ) | C <sub>NHC</sub>     | CO                   |                                   |
| <b>6</b> | 1933/1834                           | 187 <sup>c</sup>     | 260/251 <sup>c</sup> | -741                              |
| <b>7</b> | 1935/1832                           | 188 <sup>c</sup>     | 260/251 <sup>c</sup> |                                   |
| <b>8</b> | 1945/1851                           | 186 <sup>d</sup>     | 247 <sup>d</sup>     | -810                              |
| <b>9</b> | 1941/1883/<br>1860/1819             | 187/185 <sup>d</sup> | 260/248 <sup>d</sup> | -686/-759                         |

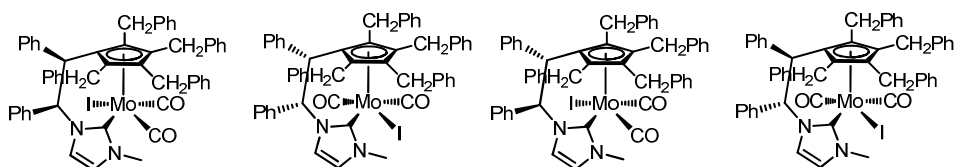
<sup>a</sup> in KBr pellets. <sup>b</sup> in CD<sub>2</sub>Cl<sub>2</sub>, 26 MHz, 298 K. <sup>c</sup> in CD<sub>2</sub>Cl<sub>2</sub>, 125 MHz, 300 K. <sup>d</sup> in CD<sub>2</sub>Cl<sub>2</sub>, 100 MHz, 300 K. All chemical shifts reported in ppm.

Complexes **6** and **9** were isolated as the *cis* isomers (relative to the disposition of the two CO ligands), while compounds **7** and **8** were obtained as a mixture of *cis* and *trans* isomers. We found that *trans*-**7** converted into *cis*-**7** in refluxing dichloromethane (Scheme 4.2).



**Scheme 4.2.** Conversion of *trans*-**7** to *cis*-**7**.

In the preparation of **8**, a mixture of *cis*-**8** and *trans*-**8** was obtained (*cis:trans* = 3:1), probably also as a consequence of the conversion of the *trans* isomer to the *cis* form. The formation of the two isomers contrasts with previously reported non-chelating CpMo(CO)<sub>2</sub>(NHC)X complexes, in which the *cis* isomer is clearly favoured.<sup>[26, 28]</sup> Complex **9** was isolated as a mixture of two distinct diastereoisomers due to the presence of two chiral carbons at the bridge between the cyclopentadienyl and the NHC fragments, the phenyl substituents can either be in *syn* or *anti* configuration, Figure 4.4.



**Figure 4.4.** Possible isolated isomers of complex **9**.

The IR spectrum of **8** shows that the  $\nu(\text{CO})$  absorptions appear in the same range as in other reported CpMo(NHC)(CO)<sub>2</sub>Br complexes (NHC = 1,3-dimethylimidazolyliidene, 1,3-dipropylimidazolyliidene).<sup>[28]</sup> The fact that the Cp-complex **8** shows CO stretching absorptions at higher frequencies

than in the Cp\* and Cp<sup>Bz</sup> analogues indicates the weaker electron donating character of the Cp ring compared to that of Cp\* and Cp<sup>Bz</sup>. The  $\sigma$ -donor character of the NHC fragment has also a clear influence on the CO-frequency, as observed by comparing the IR spectra of **8** and **9** with those shown by CpMo(CO)<sub>3</sub>I ( $\nu(\text{CO})$  2055, 1950 cm<sup>-1</sup>)<sup>[30]</sup> and Cp<sup>Bz</sup>Mo(CO)<sub>3</sub>I ( $\nu(\text{CO})$  2024, 1950 cm<sup>-1</sup>).<sup>[31]</sup> The <sup>1</sup>H NMR spectra of **6-9** show that the signal due to the acidic NCHN protons has disappeared, thus suggesting that the coordination of the NHC had taken place. The {<sup>1</sup>H} <sup>13</sup>C NMR spectra provide clear indication that the coordination has occurred, with resonances at 187 (for **6**), 188 (for **7**) and 185 (for **8**) assigned to the C<sub>NHC</sub>. In complex **9**, the C<sub>NHC</sub> displays two resonances at 187 and 185 ppm indicating the presence of two diastereoisomers (ratio 1:1) due to the existence of two asymmetric carbons in the bridge.

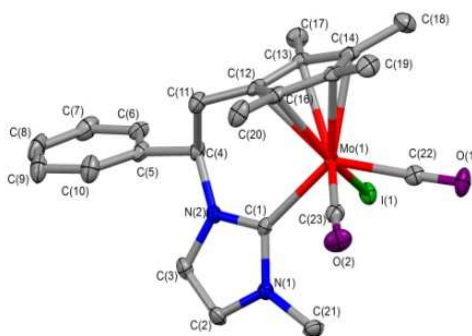
The determination of the *cis/trans* conformation about the metal centre, can be evaluated by the relative intensity of the asymmetric and symmetric stretching frequencies of the CO ligands in the IR spectra.<sup>[32]</sup> Additional evidence is provided by the {<sup>1</sup>H} <sup>13</sup>C NMR spectra. For complexes *cis-6* and *cis-7* the two CO ligands are inequivalent and display <sup>13</sup>C NMR signals at 260 and 251 ppm. *Trans-8* displays a single resonance at 258 ppm for the two inequivalent CO ligands, probably due to accidental degeneration. While two resonances at 247.3 and 247.1 ppm are found for *cis-8*, and are in the same range of previously reported *cis*-[CpMo<sup>II</sup>(NHC)(CO)<sub>2</sub>X] complexes.<sup>[26, 28]</sup> The CO ligands in complex **9** display two pairs of resonances at 259 ppm and 248 ppm, indicating the presence of two diastereoisomers.

The <sup>95</sup>Mo NMR shifts for compounds **6**, **8** and **9** are -741 ppm (**6**), -810 (**8**) and -686 and -759 ppm (**9**), respectively. Given the structural similarity of these complexes, it can be concluded that the electron density around the metal centre is lower in **8**, as expected for the



unsubstituted cyclopentadienyl ring, and this justifies the shifting of the  $^{95}\text{Mo}$  NMR resonance to higher field than for the  $\text{Cp}^x\text{-NHC}$  complexes **6** and **9**. These results are in accordance with both IR and  $^{13}\text{C}$  NMR data.

The crystal structure of **6** was determined by X-ray diffraction studies. The molecular diagram and selected bond lengths and angles are depicted in Figure 4.5. The structure can be described as a distorted four-legged piano-stool. The  $\text{Cp}^*\text{-NHC}$  ligand is chelating through the cyclopentadienyl ring and NHC. An iodide and two CO ligands complete the coordination sphere about the molybdenum centre. Both  $\text{Mo-C}_{\text{NHC}}$  (2.21 Å),  $\text{Mo-CO}$  (1.98 and 1.94 Å) and  $\text{Mo-Cp}_{\text{centroid}}$  (1.99 Å) distances are on the expected range for  $\text{CpMo}^{\text{II}}(\text{NHC})(\text{CO})_2\text{X}$  complexes.<sup>[26, 28]</sup>

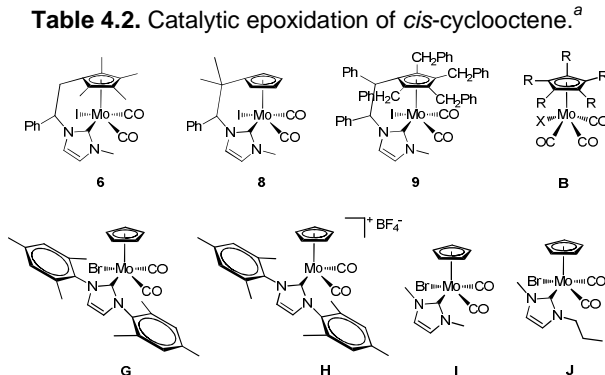


**Figure 4.5.** Molecular diagram of complex **6**. Selected bond lengths (Å) and angles ( $^\circ$ ):  $\text{Mo}(1)\text{-Cp}^*_{\text{centroid}}$  1.989;  $\text{Mo}(1)\text{-I}(1)$  2.8635(3);  $\text{Mo}(1)\text{-C}(1)$  2.207(3);  $\text{Mo}(1)\text{-C}(22)$  1.978(3);  $\text{Mo}(1)\text{-C}(23)$  1.939(3);  $\text{I}(1)\text{-Mo}(1)\text{-C}(1)$  76.91(7);  $\text{I}(1)\text{-Mo}(1)\text{-C}(22)$  77.81(8);  $\text{C}(1)\text{-Mo}(1)\text{-C}(22)$  128.71(11);  $\text{C}(1)\text{-Mo}(1)\text{-C}(23)$  84.19(11);  $\text{C}(22)\text{-Mo}(1)\text{-C}(23)$  76.16(12).

#### 4.3.3. Olefin epoxidation by complexes **6**, **8** and **9**

The catalytic essays were performed in chloroform at 55°C using *tert*-butylhydroperoxide, *cis*-cyclooctene and 1 mol % of precatalyst (**6**, **8** or **9**). These reaction conditions were chosen for comparative purposes with previously reported  $\text{Cp}'\text{Mo}(\text{CO})_3\text{Cl}$  ( $\text{Cp}' = \text{Cp}$ ,  $\text{Cp}^*$  and  $\text{Cp}^{\text{Bz}}$ ),<sup>[8]</sup> and no attempt was made to optimise the catalytic conditions. The catalytic results are summarised in Table 4.2.

**Table 4.2.** Catalytic epoxidation of *cis*-cyclooctene.<sup>a</sup>



| entry | catalyst | X               | R                  | t (h) | % conv | Ref       |
|-------|----------|-----------------|--------------------|-------|--------|-----------|
| 1     | <b>6</b> | I               | CH <sub>3</sub>    | 8     | 19     | this work |
| 2     | <b>6</b> | I               | CH <sub>3</sub>    | 20    | 25     | this work |
| 3     | <b>8</b> | I               | H                  | 8     | 5      | this work |
| 4     | <b>8</b> | I               | H                  | 20    | 11     | this work |
| 5     | <b>9</b> | I               | CH <sub>2</sub> Ph | 5     | 26     | this work |
| 6     | <b>9</b> | I               | CH <sub>2</sub> Ph | 8     | 51     | this work |
| 7     | <b>9</b> | I               | CH <sub>2</sub> Ph | 20    | 91     | this work |
| 8     | <b>B</b> | Cl              | H                  | 4     | 100    | [8]       |
| 9     | <b>B</b> | Cl              | CH <sub>3</sub>    | 4     | 60     | [8]       |
| 10    | <b>B</b> | Cl              | CH <sub>2</sub> Ph | 4     | 100    | [8]       |
| 11    | <b>G</b> | Br              | H                  | 4     | 18     | [28]      |
| 12    | <b>G</b> | Br              | H                  | 24    | 45     | [28]      |
| 13    | <b>H</b> | BF <sub>4</sub> | H                  | 4     | 90     | [28]      |
| 14    | <b>H</b> | BF <sub>4</sub> | H                  | 24    | 99     | [28]      |
| 15    | <b>I</b> | Br              | H                  | 24    | 15     | [28]      |
| 16    | <b>J</b> | Br              | H                  | 24    | 20     | [28]      |

<sup>a</sup> Reaction conditions: 55°C in CHCl<sub>3</sub>. Catalyst : cyclooctene : TBHP ratio of 1 : 100 : 200.

The catalytic reactions selectively produced the epoxide without formation of any other by-products. Both **6** and **8** showed negligible activity after 5 hours of reaction, achieving epoxide yields of 25% (for **6**) and 11% (for **8**) after 20 hours. The Cp<sup>Bz</sup> containing complex (**9**) was the most active catalyst, affording 91% yield of the corresponding epoxide after 20 hours of reaction. The improved catalytic performance of Cp<sup>Bz</sup>

complexes compared to Cp or Cp\* is in accordance with the reported activities for the Cp'MoO<sub>2</sub>Cl and Cp'Mo(CO)<sub>3</sub>Cl (Cp' = Cp, Cp\* and Cp<sup>Bz</sup>) systems, entries 8-9.<sup>[8]</sup>

In 2010, Zhao and co-workers reported a series of CpMo(NHC)(CO)<sub>2</sub>X and their activity as epoxidation catalysts (entries 11-16).<sup>[28]</sup> The best catalytic performances were reported for the more sterically hindered complexes **G** and **H** (NHC = 1,3-bis(2,4,6-trimethylbenzene)-imidazolyliidene). While the electronically neutral complex **G** showed lower activity than complex **9**, the cationic complex **H** showed higher activity at shorter reactions times. The less sterically hindered complexes **I** (NHC = 1,3-dimethylimidazolyliidene) and **J**, (NHC = 1-methyl-3-propyl-imidazolyliidene) showed similar catalytic activity to our complex **8**.

The chemistry of high-valent molybdenum-NHC is almost unexplored. The reaction of imidazolyliidenes with MoO<sub>2</sub>Cl<sub>2</sub>(THF)<sub>2</sub> has been shown to afford Mo-NHC adducts of the type MoO<sub>2</sub>Cl<sub>2</sub>(NHC), MoO<sub>2</sub>Cl<sub>2</sub>(NHC)<sub>2</sub> and [MoO<sub>2</sub>Cl(NHC)<sub>3</sub>]Cl according to the nature of the NHC ligand. However, these complexes rapidly decomposed in solution due to hydrolysis of the Mo-NHC bond.<sup>[22, 23]</sup> We envisioned that the introduction of a chelating functionality, such as cyclopentadienyl, would provide additional stability and allow for the isolation and characterisation of dioxo NHC-Mo(VI) complexes. The protocol reported by Romão and co-workers is one of the most reliable methods for the preparation of Cp'MoO<sub>2</sub>X. The parent carbonyl complex, Cp'Mo(CO)<sub>3</sub>X, smoothly oxidise at room temperature by reaction with excess of TBHP (10 equivalents) to afford the corresponding dioxo species Cp'MoO<sub>2</sub>X in good yields [Cp' = Cp (55%), Cp\* (56%) and Cp<sup>Bz</sup> (75%)].<sup>[8]</sup> With this in mind, we decided to attempt the oxidation of complexes **6** and **9** under similar reaction conditions. The reaction was followed by IR

spectroscopy, and the disappearance of the  $\nu_{\text{CO}}$  was accompanied by the appearance of two new bands at 935 and 905  $\text{cm}^{-1}$ , which might correspond to the symmetric and asymmetric stretching frequencies of a “MoO<sub>2</sub>” fragment. However, we were unable to undoubtedly confirm the presence of the Cp and/or NHC ligands due to difficulties in obtaining pure sample of the oxidised compound.

After our work was published, Zhao and co-workers successfully isolated and characterised the complex [CpMo(NHC)O<sub>2</sub>]BF<sub>4</sub> (NHC=1,3-bis(2,4,6-trimethylbenzene)-imidazolyliene) obtained by oxidation of the cationic complex **H** (Table 4.2), under similar reaction conditions. Moreover, both experimental evidence and theoretical calculations suggest that the halogen atom bonded to the metal centre destabilises the Mo-NHC bond.<sup>[28]</sup>

## 4.4. Conclusions

This chapter describes the coordination of a series of Cp'-functionalised NHC ligands to molybdenum affording complexes of the general type (Cp'-NHC)Mo(CO)<sub>2</sub>I **6 - 9**.

The CO stretching frequencies in the IR spectra, the chemical shifts of the CO ligands in the <sup>13</sup>C NMR and the <sup>95</sup>Mo NMR data consistently indicate that the electron-richness around the metal centre increased in the order **8** << **6** ~ **7** < **9**. Therefore, the careful choice of the Cp' functionality provides for a smooth change in the electronic and steric properties of the ligand with clear influence in the catalytic results.

Complexes **6**, **8** and **9** are active in the epoxidation of cyclooctene with TBHP as oxidant, although activity is much lower compared to other Cp'Mo(CO)<sub>3</sub>X complexes. Among the complexes studied, complex **9** resulted to be the more active catalysts in the epoxidation of *cis*-cyclooctene.

## 4.5. Experimental procedures

### 4.5.1. Materials and methods

All reactions were carried out under inert atmosphere. Solvents were dried via standard techniques. All other reagents are commercially available and were used as received.

$^1\text{H}$  and  $^{13}\text{C}$  NMR spectra were recorded on a Bruker Avance III 400 MHz and Bruker Avance 500 MHz spectrometers.  $^{95}\text{Mo}$  NMR spectra were acquired on a Bruker Avance II spectrometer equipped with a 5 mm z-gradient TXO probe. The chemical shift was referenced to 1 M  $\text{Na}_2\text{MoO}_4$  in  $\text{D}_2\text{O}$  (pH = 11). The  $^{95}\text{Mo}$  NMR experiments were done at University Paul Sabatier in Toulouse following the method developed by S. Massou.<sup>[33]</sup> IR spectra were recorded on samples as KBr pellets using a Mattson 7000 FT-IR spectrometer. Elemental analyses and mass spectrometry were performed in our laboratories at ITQB.

### 4.5.2. Synthesis and characterisation of 6-9

#### Synthesis of complexes: General procedure

To a solution of the appropriate proligand in THF was added *n*-BuLi (1.6 M in hexane, 2 eq) at  $-60\text{ }^\circ\text{C}$ . After stirring for 1 h at room temperature, a solution of  $[\text{MoCl}(\eta^3\text{-C}_3\text{H}_5)(\text{CO})_2(\text{NMe})_2]$  (1 eq) in THF was added dropwise. The mixture was stirred for 12h and volatiles were removed under vacuum. The remaining solid was extracted with diethyl ether yielding the corresponding molybdenum complexes **6-9** as red solids.

#### Complex 6

Yield: 77%.  $^1\text{H}$  NMR (400 MHz,  $\text{CD}_2\text{Cl}_2$ ,  $\delta$ ): 7.13 (m, 5H, Ph), 6.89 (s, 1H,  $\text{CH}_{\text{Imid}}$ ), 6.36 (s, 1H,  $\text{CH}_{\text{Imid}}$ ), 4.97-4.94 (dd, 1H,  $\text{CHPh}_{\text{linker}}$ ), 3.69 (s, 3H,  $\text{NCH}_3$ ), 3.08-2.83 (m, 2H,  $\text{CH}_{2\text{linker}}$ ), 2.43 (s, 3H,  $\text{CH}_{3\text{Cp}^*}$ ), 1.97 (s, 3H,  $\text{CH}_{3\text{Cp}^*}$ ), 1.93 (s, 3H,  $\text{CH}_{3\text{Cp}^*}$ ), 1.73 (s, 3H,  $\text{CH}_{3\text{Cp}^*}$ ).  $\{^1\text{H}\}^{13}\text{C}$  NMR (125 MHz,  $\text{CDCl}_3$ ,  $\delta$ ): 260 (CO), 251 (CO), 187 ( $\text{C}_{\text{carbene-Mo}}$ ), 139 ( $\text{C}_{\text{phenyl}}$ ), 130-128 ( $\text{CH}_{\text{phenyl}}$ ), 123 ( $\text{CH}_{\text{Imid}}$ ), 122 ( $\text{CH}_{\text{Imid}}$ ), 116 ( $\text{C}_{\text{Cp}^*}$ ), 105 ( $\text{C}_{\text{Cp}^*}$ ), 102

(C<sub>Cp</sub><sup>+</sup>), 100 (C<sub>Cp</sub><sup>+</sup>), 99 (C<sub>Cp</sub><sup>+</sup>), 66 (CHPh<sub>linker</sub>), 41 (NCH<sub>3</sub>), 31 (CH<sub>2linker</sub>), 13 (CH<sub>3Cp</sub><sup>+</sup>), 11.3 (CH<sub>3Cp</sub><sup>+</sup>), 11.2 (CH<sub>3Cp</sub><sup>+</sup>), 11 (CH<sub>3Cp</sub><sup>+</sup>). <sup>95</sup>Mo NMR (CD<sub>2</sub>Cl<sub>2</sub>, 26.07 MHz, δ): -741. IR (KBr): ν(Mo-CO), cm<sup>-1</sup> 1933 (vs), 1834 (s). Anal. Calcd for C<sub>23</sub>H<sub>25</sub>N<sub>2</sub>O<sub>2</sub>MoCl(OC<sub>4</sub>H<sub>8</sub>): C, 57.40; H, 5.90; N, 4.96. Found: C, 57.60; H, 6.27; N, 4.56. MS (ESI): *m/z* 459 (100, M<sup>+</sup>-Cl).

### Complex 7

Yield: 55%. <sup>1</sup>H NMR (400 MHz, CD<sub>2</sub>Cl<sub>2</sub>, δ): 7.47 (m, 5H, Ph), 6.94 (s, 1H, CH<sub>Imid</sub>), 6.48 (s, 1H, CH<sub>Imid</sub>), 3.68 (s, 3H, NCH<sub>3</sub>), 3.12-2.87 (m, 2H, CH<sub>2linker</sub>), 2.34 (s, 3H, CH<sub>3Cp</sub><sup>+</sup>), 1.96 (s, 3H, CH<sub>3Cp</sub><sup>+</sup>), 1.92 (s, 3H, CH<sub>3Cp</sub><sup>+</sup>), 1.77 (s, 3H, CH<sub>3Cp</sub><sup>+</sup>), 1.81 (s, 3H, CMePh<sub>linker</sub>). {<sup>1</sup>H}<sup>13</sup>C NMR (125 MHz, CD<sub>2</sub>Cl<sub>2</sub>, δ): 260 (CO), 251 (CO), 188 (C<sub>carbene</sub>-Mo), 147 (C<sub>phenyl</sub>), 130-129 (CH<sub>phenyl</sub>), 123 (CH<sub>Imid</sub>), 123 (CH<sub>Imid</sub>), 117 (C<sub>Cp</sub><sup>+</sup>), 103 (C<sub>Cp</sub><sup>+</sup>), 102 (C<sub>Cp</sub><sup>+</sup>), 100 (C<sub>Cp</sub><sup>+</sup>), 98 (C<sub>Cp</sub><sup>+</sup>), 73 (C(CH<sub>3</sub>)Ph<sub>linker</sub>), 42 (NCH<sub>3</sub>), 30 (CH<sub>2linker</sub>), 38 (C(CH<sub>3</sub>)Ph<sub>linker</sub>), 13 (CH<sub>3Cp</sub><sup>+</sup>), 12 (CH<sub>3Cp</sub><sup>+</sup>), 11.5 (CH<sub>3Cp</sub><sup>+</sup>), 11.2 (CH<sub>3Cp</sub><sup>+</sup>). IR (KBr): ν(Mo-CO), cm<sup>-1</sup> 1935 (vs), 1832 (s). Anal. Calcd for C<sub>24</sub>H<sub>27</sub>N<sub>2</sub>O<sub>2</sub>MoI(OC<sub>4</sub>H<sub>8</sub>)<sub>2</sub>: C, 51.76; H, 5.84; N, 3.77. Found: C, 51.37; H, 5.96; N, 3.83. MS (ESI): *m/z* 473 (100, M<sup>+</sup>-I).

### Complex 8

Yield: 48%. <sup>1</sup>H NMR (400 MHz, CD<sub>2</sub>Cl<sub>2</sub>, δ): 7.46-7.39 (m, 5H, CHPh<sub>linker</sub>), 7.07 (s, 1H, CH<sub>Imid</sub>), 6.87 (s, 1H, CH<sub>Imid</sub>), 5.91 (s, 1H, CH<sub>Cp</sub>), 5.57 (s, 1H, CH<sub>Cp</sub>), 5.26 (s, 1H, CHPh<sub>linker</sub>), 4.71 (s, 1H, CH<sub>Cp</sub>), 4.61 (s, 1H, CH<sub>Cp</sub>), 3.76 (s, 3H, NCH<sub>3</sub>), 1.41 (s, 3H C(CH<sub>3</sub>)<sub>2linker</sub>), 1.38 (s, 3H C(CH<sub>3</sub>)<sub>2linker</sub>). {<sup>1</sup>H}<sup>13</sup>C NMR (100 MHz, CD<sub>2</sub>Cl<sub>2</sub>, δ): 150.3 (C<sub>carbene</sub>-Mo), 124.1 (CH<sub>Imid</sub>), 121.3 (CH<sub>Imid</sub>), 105.1 (C<sub>Cp</sub>), 83.8 (C<sub>Cp</sub>), 77.5 (C<sub>Cp</sub>), 77.2 (C<sub>Cp</sub>), 50.6 (CH<sub>2linker</sub>), 39.8 (NCH<sub>3</sub>), 29.9 (CH<sub>2linker</sub>), 21.2 (CH<sub>3Cp</sub>), 9.88 (CH<sub>3Cp</sub>), 8.7 (CH<sub>3Cp</sub>). IR (KBr): ν(Mo-CO), cm<sup>-1</sup> 1945 (vs), 1851(s), <sup>95</sup>Mo NMR (CD<sub>2</sub>Cl<sub>2</sub>, 26.07 MHz, δ): -810. Anal. Calcd. for C<sub>21</sub>H<sub>21</sub>N<sub>2</sub>O<sub>2</sub>MoCl(C<sub>7</sub>H<sub>8</sub>): C, 60.21; H, 5.19; N, 5.01. Found: C, 60.61; H, 4.89; N, 4.83. MS (ESI): *m/z* 431 (100, M<sup>+</sup>-I).

**Synthesis of **9****

Yield: 63%.  $\{^1\text{H}\}^{13}\text{C}$  NMR (100 MHz,  $\text{CD}_2\text{Cl}_2$ ,  $\delta$ ): 259.58, 259.55 (CO), 247.69, 247.63 (CO), 186.50, 184.67 ( $\text{C}_{\text{carbene}}\text{-Mo}$ ), 141.55, 140.74, 140.64, 140.63, 140.25, 140.08, 140.00, 139.87, 139.62, 139.53, 138.60, 138.10 ( $\text{C}_{\text{isopPh}}$ ), 132.54-122.88 ( $\text{CH}_{\text{Ph}}$  +  $\text{CH}_{\text{Imid}}$ ), 120.91, 118.27, 113.02, 109.70, 109.61, 106.72, 106.48, 104.40, 103.22, 102.17 ( $\text{C}_{\text{Cp}}$ ), 69.83, 68.90 ( $\text{NCHPh}_{\text{linker}}$ ), 48.98, 46.07 ( $\text{CHPhCHPh}_{\text{linker}}$ ), 41.62, 41.47 ( $\text{NCH}_3$ ), 36.68, 35.96, 34.66, 33.61, 33.48, 33.32, 33.28, 33.16 ( $\text{CH}_2\text{Ph}_{\text{Cp}}$ ). IR (KBr):  $\nu(\text{Mo-CO})$ ,  $\text{cm}^{-1}$  1941(vs), 1883(s), 1860(vs), 1819(s).  $^{95}\text{Mo}$  NMR ( $\text{CD}_2\text{Cl}_2$ , 26.07 MHz,  $\delta$ ): -686, -759. Anal. Calcd. for  $\text{C}_{53}\text{H}_{45}\text{N}_2\text{O}_2\text{MoCl}(\text{C}_7\text{H}_8)_2$ : C, 76.08; H, 5.81; N 2.65. Found: C, 75.83; H, 6.25; N, 3.03. MS (ESI):  $m/z$  840 (100,  $\text{M}^+\text{-Cl}$ ).

**Catalytic epoxidation of *cis*-cyclooctene: General procedure**

The catalytic reactions were performed in air, within a reaction vessel equipped with a magnetic stirrer and immersed in a oil bath at 55 °C. A catalyst : cyclooctene : TBHP molar ratio of 1 : 100 : 200 was used with 3 mL of  $\text{CHCl}_3$ . *Cis*-cyclooctene, chloroform, mesitylene (as internal standard), and the catalysts were placed into the reaction vessel, and TBHP was added to the reaction mixture. The course of the reaction was monitored by quantitative GC analysis. Samples taken were diluted in  $\text{CH}_2\text{Cl}_2$  and treated with  $\text{MgSO}_4$  and  $\text{MnO}_2$  to remove water and destroy excess of peroxide. The resulting slurry was filtered, and the filtrate was injected to a GC column (DB5). The conversion of *cis*-cyclooctene and the formation of cyclooctene oxide were calculated from calibration curves ( $r^2=0.999$ ) recorded prior to the reaction course.

**4.5.3. X-ray diffraction studies**

Suitable single crystals of complex **6** for the X-ray diffraction study were grown in  $\text{CH}_2\text{Cl}_2/\text{Et}_2\text{O}$  solutions at 5 °C. Data collection was carried out in a Bruker Kappa-Appex-II diffractometer at 100 K. Space group

assignment was based on systematic absences, E statistics and successful refinement of the structures. The structure was solved by direct methods with the aid of successive difference Fourier maps and were refined using the SHELXTL 6.1 software package.<sup>[34]</sup> All non-hydrogen were refined anisotropically. Hydrogen atoms were assigned to ideal positions and refined using a riding model. The diffraction frames were integrated using the SAINT package.<sup>[35]</sup>

## 4.6. Acknowledgements

Stéphane Massou, Marc Vedrenne and Prof. Montserrat Gómez from University Paul Sabatier (Toulouse, France) are acknowledged for the <sup>95</sup>Mo NMR spectra. Dr. A. L. Llamas-Saiz from University of Santiago de Compostela (Spain) is acknowledged for the X-ray diffraction studies. We wish to acknowledge M. C. Almeida and Dr. A. Coelho for providing data from the Mass Spectrometry and Elemental Analysis Services at ITQB. The Bruker Avance III 400 MHz spectrometer and Bruker Avance 500 MHz spectrometers are part of the National NMR Network and were purchased in the framework of the National Program for Scientific Re-equipment, contract REDE/1517/RMN/2005, with funds from POCI 2010 (FEDER) and Fundação para a Ciência e a Tecnologia (FCT).

## 4.7. References

- [1] F. E. Kühn, A. M. Santos, W. A. Herrmann, *Dalton Trans.* **2005**, 2483.
- [2] Q. H. Xia, H. Q. Ge, C. P. Ye, Z. M. Liu, K. X. Su, *Chem. Rev.* **2005**, *105*, 1603.
- [3] C. Freund, M. Abrantes, F. E. Kühn, *J. Organomet. Chem.* **2006**, *691*, 3718.
- [4] F. E. Kühn, A. M. Santos, M. Abrantes, *Chem. Rev.* **2006**, *106*, 2455.
- [5] R. R. Schrock, *Chem. Rev.* **2009**, *109*, 3211.



- [6] M. Cousins, M. L. H. Green, *J. Chem. Soc.* **1963**, 889.
- [7] M. K. Trost, R. G. Bergman, *Organometallics* **1991**, *10*, 1172.
- [8] M. Abrantes, A. M. Santos, J. Mink, F. E. Kühn, C. C. Romão, *Organometallics* **2003**, *22*, 2112.
- [9] M. Abrantes, S. Gago, A. A. Valente, M. Pillinger, I. S. Gonçalves, T. M. Santos, J. Rocha, C. C. Romão, *Eur. J. Inorg. Chem.* **2004**, 4914.
- [10] J. Zhao, A. M. Santos, E. Herdtweck, F. E. Kühn, *J. Mol. Catal. A-Chem.* **2004**, *222*, 265.
- [11] F. E. Kühn, J. Zhao, M. Abrantes, W. Sun, C. A. M. Afonso, L. C. Branco, I. S. Gonçalves, M. Pillinger, C. C. Romão, *Tetrahedron Lett.* **2005**, *46*, 47.
- [12] A. A. Valente, J. D. Seixas, I. S. Gonçalves, M. Abrantes, M. Pillinger, C. C. Romão, *Catal. Lett.* **2005**, *101*, 127.
- [13] M. Abrantes, A. Sakthivel, C. C. Romão, F. E. Kühn, *J. Organomet. Chem.* **2006**, *691*, 3137.
- [14] S. S. Braga, S. Gago, J. D. Seixas, A. A. Valente, M. Pillinger, T. M. Santos, I. S. Gonçalves, C. C. Romão, *Inorg. Chim. Acta* **2006**, *359*, 4757.
- [15] J. Zhao, E. Herdtweck, F. E. Kühn, *J. Organomet. Chem.* **2006**, *691*, 2199.
- [16] J. Zhao, K. R. Jain, E. Herdtweck, F. E. Kühn, *Dalton Trans.* **2007**, 5567.
- [17] M. Abrantes, F. A. A. Paz, A. A. Valente, C. C. L. Pereira, S. Gago, A. E. Rodrigues, J. Klinowski, M. Pillinger, I. S. Gonçalves, *J. Organomet. Chem.* **2009**, *694*, 1826.
- [18] A. M. Al-Ajlouni, D. Veljanovski, A. Capape, J. Zhao, E. Herdtweck, M. J. Calhorda, F. E. Kühn, *Organometallics* **2009**, *28*, 639.
- [19] A. Capape, A. Raith, F. E. Kühn, *Adv. Synth. Catal.* **2009**, *351*, 66.
- [20] M. Abrantes, P. Neves, M. M. Antunes, S. Gago, F. A. A. Paz, A. E. Rodrigues, M. Pillinger, I. S. Gonçalves, C. M. Silva, A. A. Valente, *J. Mol. Catal. A-Chem.* **2010**, *320*, 19.

- [21] P. Neves, C. C. L. Pereira, F. A. A. Paz, S. Gago, M. Pillinger, C. M. Silva, A. A. Valente, C. C. Romão, I. S. Gonçalves, *J. Organomet. Chem.* **2010**, *695*, 2311.
- [22] W. A. Herrmann, G. M. Lobmaier, M. Alison, *J. Organomet. Chem.* **1996**, *520*, 231.
- [23] E. Mas-Marzá, P. M. Reis, E. Peris, B. Royo, *J. Organomet. Chem.* **2006**, *691*, 2708.
- [24] W. A. Herrmann, K. Öfele, M. Alison, F. E. Kühn, P. W. Roesky, *J. Organomet. Chem.* **1994**, *480*, c7.
- [25] K. Ogata, Y. Yamaguchi, T. Kashiwabara, T. Ito, *J. Organomet. Chem.* **2005**, *690*, 5701.
- [26] F. Wu, V. K. Dioumaev, D. J. Szalda, J. Hanson, R. M. Bullock, *Organometallics* **2007**, *26*, 5079.
- [27] V. Krishna Mohan Kandepi, J. Cardoso, B. Royo, *Catal. Lett.* **2010**, *136*, 222.
- [28] S. Y. Li, C. W. Kee, K. W. Huang, T. S. A. Hor, J. Zhao, *Organometallics* **2010**, *29*, 1924.
- [29] D. Takaki, T. Okayama, H. Shuto, S. Matsumoto, Y. Yamaguchi, S. Matsumoto, *Dalton Trans.* **2011**, *40*, 1445.
- [30] T. E. Sloan, A. Wojcicki, *Inorg. Chem.* **1968**, *7*, 1268.
- [31] L.-C. Song, L.-Y. Zhang, Q.-M. Hu, X.-Y. Huang *Inorg. Chim. Acta* **1995**, *230*, 127.
- [32] M. D. Bala, D. C. Levendis, N. J. Coville, *J. Organomet. Chem.* **2006**, *691*, 1919.
- [33] J. A. Brito, H. Teruel, S. Massoud, M. Gomez, *Magn. Reson. Chem.* **2009**, *47*, 573.
- [34] Sheldrick, G. M., SHELXTL, version 6.1, Bruker AXS, Inc. ed.; Madison, WI, 2000
- [35] SAINT, Bruker Analytical X-ray System, version 5.0. ed.; Madison, WI, 1998.

---

# 5.

## COORDINATION TO Rh AND Ir, APPLICATIONS IN HYDROGEN BORROWING CATALYSIS

---

|      |   |    |
|------|---|----|
| 5.1. | Abstract  | 61 |
| 5.2. | Introduction  | 62 |
| 5.3. | Results and discussion                                  | 64 |
|      | 5.3.1. Coordination of Cp*-NHC ligands to Rh and Ir, 64 |    |
|      | 5.3.2. Characterisation of the metal complexes, 66      |    |
|      | 5.3.3. Intramolecular C-H activation studies, 71        |    |
|      | 5.3.4. Catalysis, 75                                    |    |
| 5.4. | Conclusions   | 82 |
| 5.5. | Experimental procedures                                 | 82 |
|      | 5.5.1. Materials and methods, 82                        |    |
|      | 5.5.2. Synthesis and characterisation, 83               |    |
|      | 5.5.3. Catalysis - standard procedures, 87              |    |
|      | 5.5.4. X-Ray diffraction studies, 87                    |    |
| 5.6. | Acknowledgments   | 88 |
| 5.7. | References  | 88 |
| 5.8. | Supporting Information                                  | 91 |

---

A. P. da Costa, M. Sanaú, E. Peris\* and B. Royo\* *Dalton Trans.*, **2009**, 35, 6960-6966.

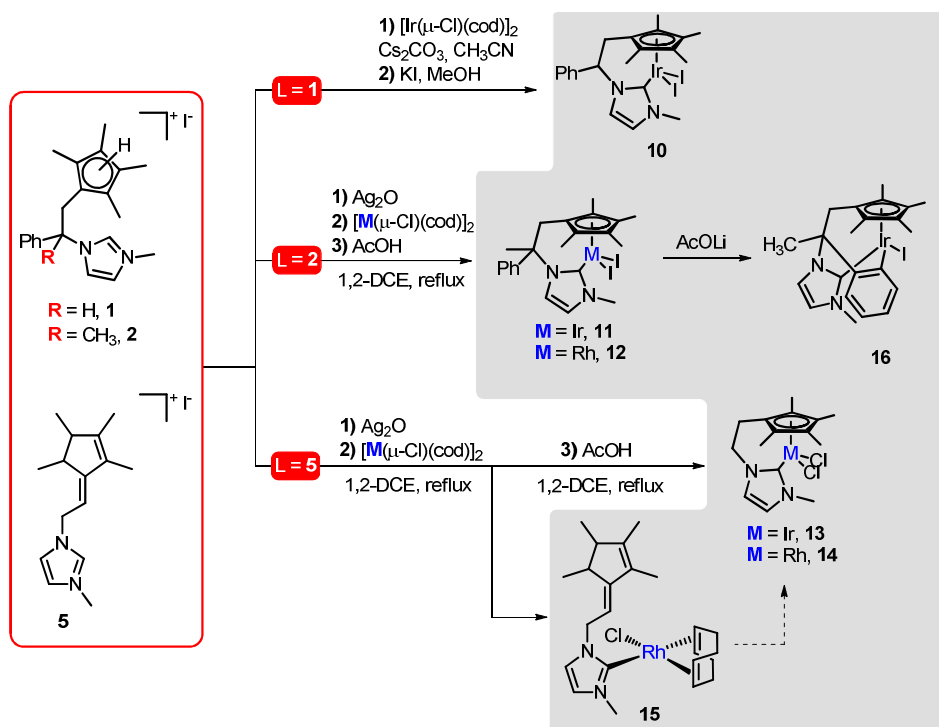
A. P. da Costa, M. Viciano, M. Sanaú, S. Merino, J. Tejada,\* E. Peris\* and B. Royo\* *Organometallics*, **2008**, 27 (6), 1305-1309.

Cyclopentadienyl-Functionalised N-Heterocyclic Carbenes:  
Synthesis, Coordination to Mo, Ru, Rh and Ir and Catalytic Applications.

---

## 5.1. Abstract

This chapter describes the coordination of the Cp\*-imidazolium ligand precursors **1**, **2** and **5** to iridium and rhodium, in order to obtain the complexes depicted in Scheme 5.1.



**Scheme 5.1.** Cp\*-functionalized NHC complexes of Rh and Ir.

Two coordination procedures were employed in the preparation of the iridium and rhodium complexes:

- Complex **10** was obtained in 70% yield from the reaction of the imidazolium salt **1** with  $[\text{Ir}(\mu\text{-Cl})(\text{cod})]_2$  in the presence of  $\text{Cs}_2\text{CO}_3$  in acetonitrile, followed by reflux of the reaction mixture in methanol.
- Complexes **11-14** were synthesised by reaction of the corresponding imidazolium salt with silver oxide, and subsequent transmetalation to the respective metal precursor  $[\text{M}(\mu\text{-Cl})(\text{cod})]_2$

(M = Ir, Rh). Further reflux in the presence of acetic acid afforded the half-sandwich complexes with the chelating ligand in low to moderate yields (20-50%). The Rh(I) complex **15**, which is an intermediate in the synthesis of **14**, was isolated and characterised by NMR and MS.

Complex **11** was reacted with LiOAc affording the orthometalated complex **16**. Under similar reaction conditions, complex **10** did not react with LiOAc.

All complexes were characterised by analytical and spectroscopic methods. Suitable crystals for X-ray diffraction studies were obtained for complexes **10**, **12**, **13**, **14** and **16**.

Complexes **10** and **13** showed promising results in hydrogen borrowing reactions namely: transfer hydrogenation,  $\beta$ -alkylation of alcohols and N-alkylation of amines with primary alcohols.

The work described in this chapter was performed by the candidate. Dr. Mónica Viciano, a former PhD student in the group of Universitat Jaume I performed the catalytic studies of complex **10** in the  $\beta$ -alkylation of secondary alcohols. The X-ray diffraction studies were performed by Gabriel Peris and Dr. Mercedes Sanaú.

## 5.2. Introduction

The extensive work developed by Bergman and co-workers showed that "Cp\*Ir(PMe<sub>3</sub>)" complexes are very active in C-H activation processes.<sup>[1]</sup> The presence of a basic phosphine in the catalyst seems to be essential in the activity of the compound, since this type of complexes have shown activity towards H/D reactions (or other C-H activation processes) only when alkyl-phosphines such as PMe<sub>3</sub>, P(C<sub>6</sub>H<sub>11</sub>)<sub>3</sub> and P(CH<sub>2</sub>-*t*Bu)<sub>3</sub> are present.<sup>[2, 3]</sup>

N-heterocyclic carbenes (NHCs) are known to be better  $\sigma$ -donor ligands than even basic alkylphosphines, and some NHC complexes have shown improved activities towards C-H activation.<sup>[4-7]</sup> More recently, a series of complexes containing the fragment “Cp\*IrNHC” were prepared and used in several C-H activation catalytic processes.<sup>[8-16]</sup>

Although the first “Cp\*IrNHC” was published by Prinz and co-workers<sup>[4]</sup> in 2000, and showed good intramolecular C-H activation properties, it was only after 2005 that the catalytic properties of such type of species were extensively studied mainly by the groups of Fujita / Yamaguchi<sup>[6, 8-9, 11, 17]</sup> and Peris.<sup>[5, 7, 10, 12, 14, 16]</sup> So far, both groups have reported a large number of reactions catalysed by “Cp\*IrNHC”, such as: H/D exchange,<sup>[10]</sup> transfer hydrogenation of aldehydes, ketones and imines,<sup>[12]</sup> racemization of alcohols,<sup>[13, 14]</sup> diboration of olefins,<sup>[7]</sup> oxidation of alcohols,<sup>[8-9, 11, 14, 16]</sup> cross-coupling of alcohols and amines,<sup>[16]</sup>  $\beta$ -alkylation of alcohols<sup>[15]</sup> and N-alkylation of amines.<sup>[15]</sup>

One of the most versatile “Cp\*IrNHC” catalysts is complex **A** (Figure 5.1), which was used in a variety of catalytic reactions, often showing better results than other “Cp\*IrNHC” complexes.<sup>[10, 14, 16]</sup> With regard to the chiral versions of this type of complexes, the only enantiomerically pure species containing the “Cp\*IrNHC” fragment reported in the literature is complex **B** (Figure 5.1), which was used as catalyst for the diboration of olefins. However, the asymmetric induction observed was very low (~10% ee).<sup>[7]</sup>

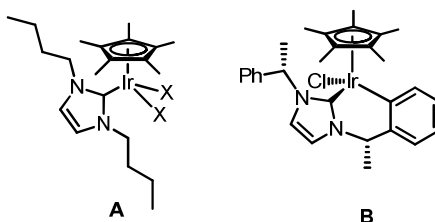
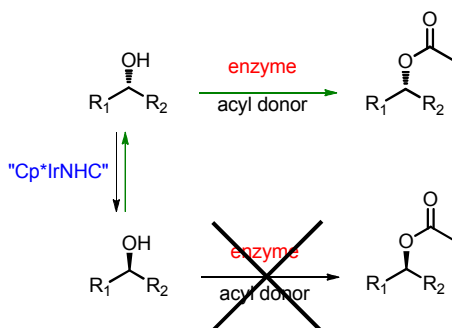


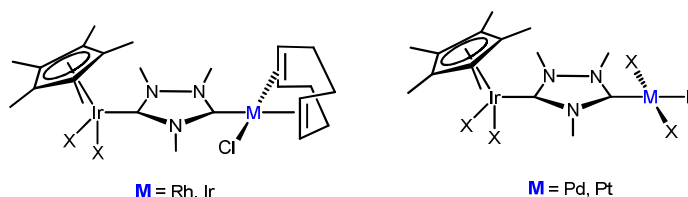
Figure 5.1. Examples of “Cp\*IrNHC” complexes.

Excellent asymmetric inductions were reported by Marr and co-workers<sup>[13]</sup> using a “Cp\*IrNHC” fragment in dynamic kinetic resolution of alcohols, represented in Figure 5.2. The strategy used was based on the enzyme catalysed acetylation that shifts the alcohol racemisation equilibrium. The ester products were obtained in good yields with high enantiomeric excesses.



**Figure 5.2.** Dynamic kinetic resolution of alcohols mediated by “Cp\*IrNHC” fragment.<sup>[13]</sup>

More recently, Peris and co-workers reported a series of bimetallic complexes containing the “Cp\*IrNHC” fragment (see some examples depicted in Figure 5.3). These complexes showed excellent catalytic properties in a variety of tandem multistep processes.<sup>[18-21]</sup>



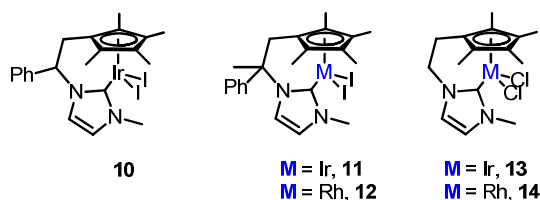
**Figure 5.3.** Examples of homo- and hetero-bimetallic complexes containing the “Cp\*IrNHC” fragment.<sup>[18-21]</sup>

## 5.3. Results and discussion

### 5.3.1. Coordination of Cp\*-NHC ligands to Rh and Ir

The Cp-functionalised imidazolium prolignands **1**, **2** and **5** were coordinated to Ir and Rh affording complexes **10-14**, Figure 5.4.

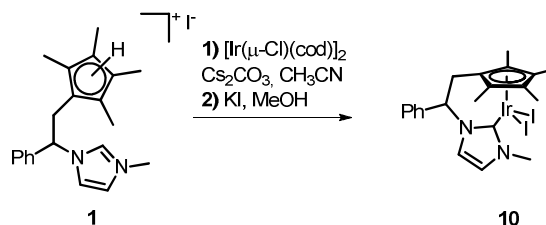




**Figure 5.4.** Cp\*-functionalised NHC complexes of Rh and Ir.

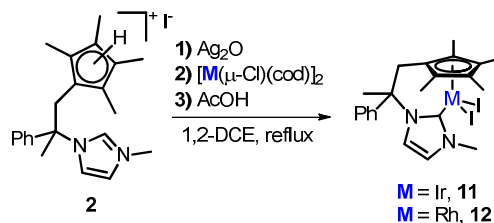
Two synthetic procedures were used for the coordination of the previously described proligands to the metallic fragments:

(i) The proligand **1** was coordinated to iridium by reaction with  $[\text{Ir}(\mu\text{-Cl})(\text{cod})]_2$  in the presence of  $\text{Cs}_2\text{CO}_3$  in acetonitrile (Scheme 5.2). Subsequent heating of the reaction mixture under reflux in methanol allowed for the preparation of the iridium complex **10** in good yields (65–70% based on iridium).



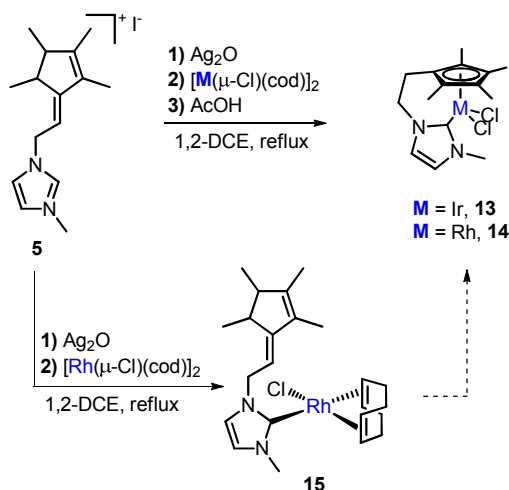
**Scheme 5.2.** Synthesis of complex **10**.

(ii) The proligands **2** and **5** were reacted with  $\text{Ag}_2\text{O}$  to form the corresponding silver-NHC which was subsequently transmetalated to  $[\text{M}(\mu\text{-Cl})(\text{cod})]_2$  ( $\text{M} = \text{Ir}, \text{Rh}$ ) and refluxed in acetic acid to promote the C–H activation of the cyclopentadienyl ring (Schemes 5.3 and 5.4). Complexes **11–14** were obtained in low to moderate yields (24 – 51% based on metal) using this procedure.



**Scheme 5.3.** Synthesis of complexes **11** and **12**.

The proligand **5** was isolated as the exocyclic isomer of the cyclopentadiene moiety. Therefore, it requires isomerisation of the double bond to the endocyclic isomer prior to coordination to the metal centre (Scheme 5.4). Our results suggest that this isomerisation step is catalysed by the metal centre and promoted by acidic media. In fact, complexes **13** and **14** could not be obtained by route i) which implies the use of  $\text{Cs}_2\text{CO}_3$ . The transmetalation of the carbene from the corresponding pre-formed silver-NHC, allowed the isolation of the intermediate **15**, which was characterised by NMR spectroscopy and mass spectrometry.



**Scheme 5.4.** Synthesis of complexes **13-15**.

Attempts to prepare the iridium complex **10** by direct reaction of the imidazolium proligand **1** with  $\text{IrCl}_3 \cdot n\text{H}_2\text{O}$  failed.

### 5.3.2. Characterisation of the metal complexes

Complexes **10-14** were characterised by analytical and spectroscopic methods. The NMR spectra of complexes **10-14** display analogue patterns. The selected chemical shifts are summarised in Table 5.1. For visual guidance the  $^1\text{H}$  NMR and  $\{^1\text{H}\} \text{ }^{13}\text{C}$  NMR spectra of complex **10** are depicted in Figure 5.5.

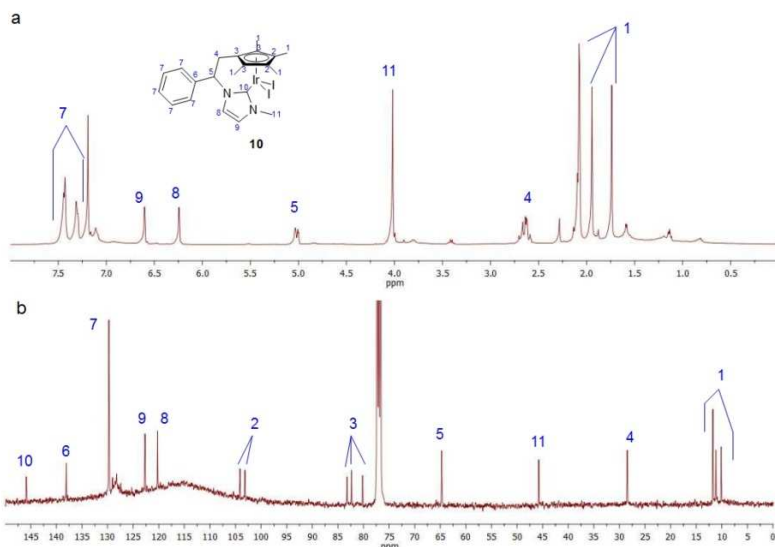
**Tabel 5.1.** Selected  $^1\text{H}$  and  $^{13}\text{C}$  NMR chemical shifts of complexes **10-14**.

|                                  |                              | <b>10</b> <sup>c</sup> | <b>11</b> <sup>c</sup> | <b>12</b> <sup>d</sup>                               | <b>13</b> <sup>c</sup> | <b>14</b> <sup>d</sup>                     |
|----------------------------------|------------------------------|------------------------|------------------------|--|------------------------|--|
| $^1\text{H}$ NMR <sup>a</sup>    | $\text{CH}_{\text{imid}}$    | 6.65 and 6.29          | 6.89 and 6.84          | 7.01 and 6.95  | 6.91 and 6.77          | 7.00 and 6.85                              |
|                                  | $\text{N-CH}_3$              | 4.07                   | 4.13                   | 4.14   | 4.08                   | 4.00                                       |
| $^{13}\text{C}$ NMR <sup>b</sup> | $\text{C}_{\text{NHC}}$      | 146                    | 148                    | 165 ( $^1J_{\text{Rh-C}} = 58.3$ Hz)                 | 150                    | 166 ( $^1J_{\text{Rh-C}} = 56$ Hz)         |
|                                  | $\text{Cp}^*_{\text{trans}}$ | 104 and 103            | 105.3, and 104.9       | 108.6 and 108.4 ( $^1J_{\text{Rh-C}} \sim 3$ Hz)     | 105                    | 110 ( $^1J_{\text{Rh-C}} = 4$ Hz)          |
|                                  | $\text{Cp}^*_{\text{cis}}$   | 84, 83 and 80          | 81.9, 81.7 and 79.9    | 89.9, 89.7 and 86.3 ( $^1J_{\text{Rh-C}} \sim 9$ Hz) | 84 and 77              | 91 and 87 ( $^1J_{\text{Rh-C}} \sim 9$ Hz) |

<sup>a</sup> in  $\text{CDCl}_3$ , 400 MHz, 300 K, chemical shifts reported in ppm. <sup>b</sup> in  $\text{CDCl}_3$ , 100 MHz, 300 K, chemical shifts reported in ppm. <sup>c</sup> comparable to other “ $\text{Cp}^*\text{Ir}^{\text{III}}\text{NHC}$ ” complexes.<sup>[5-12, 14-15, 17]</sup>

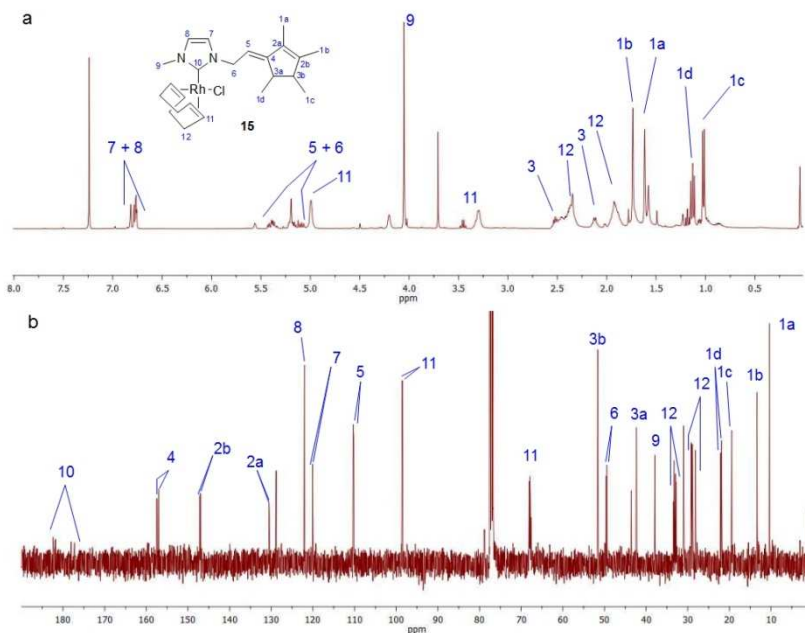
<sup>d</sup> comparable to other “ $\text{Cp}^*\text{Rh}^{\text{III}}\text{NHC}$ ”.<sup>[22-26]</sup>

The absence of the resonance of the acidic proton of the imidazolium salt (at  $\sim 10$  ppm), and the doublet at  $\sim 0.8$  ppm for the methyl protons of the cyclopentadienyl ring in the  $^1\text{H}$  NMR spectrum are two preliminary indications that the coordination of the cyclopentadienyl ring and the NHC has occurred. The imidazolylidene ring protons appear as two doublets (6 – 7 ppm) for all complexes. Complexes **10-12** display four resonances for the inequivalent methyl groups of the cyclopentadienyl ring (1.5 – 2.5 ppm), while complexes **13** and **14** show only two signals, each due to two methyl groups, as expected for the two-fold symmetry of the molecule. The  $\{^1\text{H}\}$   $^{13}\text{C}$  NMR spectra of complexes **10-14** unequivocally demonstrate that the coordination occurred by both the N-heterocyclic carbene and the cyclopentadienyl ring. The carbene carbon atom of the iridium complexes appears between 145-150 ppm, while the resonances of the  $\text{C}_{\text{carbene}}$  in the rhodium complexes are displayed at  $\sim 165$  ppm ( $^1J_{\text{Rh-C}} = 58$  Hz and  $^1J_{\text{Rh-C}} = 56$  Hz for complex **12** and **14** respectively), in agreement with previously reported “ $\text{Cp}^*\text{Ir}^{\text{III}}\text{NHC}$ ”<sup>[5-12, 14, 15, 17]</sup> and “ $\text{Cp}^*\text{Rh}^{\text{III}}\text{NHC}$ ”<sup>[22-26]</sup> complexes.



**Figure 5.5.** (a)  $^1\text{H}$  NMR (400 MHz,  $\text{CDCl}_3$ , 300K) and (b)  $\{^1\text{H}\}$   $^{13}\text{C}$  NMR (100 MHz,  $\text{CDCl}_3$ , 300K) spectra of complex **10**.

The Rh(I) complex **15**, which can be considered as an intermediate in the synthesis of **14**, was isolated as a mixture of two isomers. We have attributed these two isomers to the *E*-*Z* isomers at the exocyclic olefinic bond. The identity of complex **15** was established by  $^1\text{H}$  and  $\{^1\text{H}\}$   $^{13}\text{C}$  NMR spectroscopy and mass spectrometry. Details of the MS spectrum can be found in the experimental section. The  $^1\text{H}$  NMR and  $^{13}\text{C}$  NMR spectra of **15** are displayed in Figure 5.6. Because we could not separate the isomers, the NMR spectra correspond to their mixture. The two metallated carbene signals display a doublet at  $\sim 182$  ppm ( $^1J_{\text{Rh-C}} = 51$  Hz) in the  $^{13}\text{C}$  NMR spectrum, and are in the expected region for a 16-electron square-planar Rh(I)-NHC complex.<sup>[18]</sup> The  $^1\text{H}$  NMR spectrum gives a good evidence that neither double bond isomerisation to the thermodynamically more stable endocyclic isomer, nor C-H activation of Cp ring occurred, as the two methyl groups (1.15 and 1.04 ppm) still show the multiplicity caused by the coupling with the endocyclic protons. Moreover, the proton of the exocyclic double bond still displays a resonance at  $\sim 5$  ppm, typical for olefinic protons.

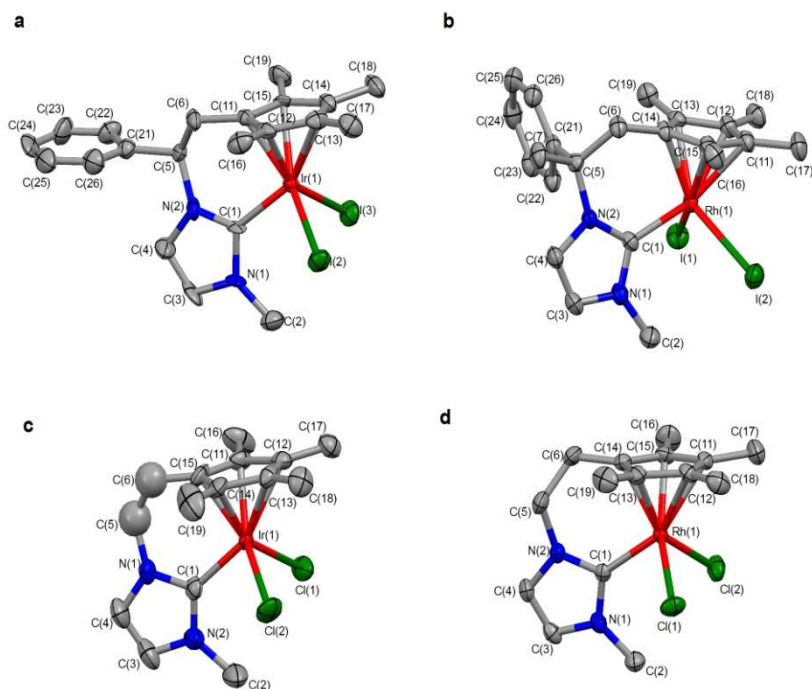


**Figure 5.6.** (a)  $^1\text{H}$  NMR (400 MHz,  $\text{CDCl}_3$ , 300K) and (b)  $\{^1\text{H}\}^{13}\text{C}$  NMR (100 MHz,  $\text{CDCl}_3$ , 300K) spectra of complex **15**.

Crystals suitable for X-ray diffraction studies were obtained for complexes **10**, **12**, **13** and **14** by slow diffusion of hexane into saturated chloroform solutions. The selected bond distances and angles are reported in Table 5.2, and the molecular diagrams are represented in Figure 5.7.

**Table 5.2.** Selected bond distances and angles of complexes **10**, **12**, **13** and **14**.<sup>a</sup>

|                 |                                | <b>10</b> <sup>b</sup> | <b>12</b> <sup>c</sup> | <b>13</b> <sup>b</sup> | <b>14</b> <sup>c</sup> |
|-----------------|--------------------------------|------------------------|------------------------|------------------------|------------------------|
| distances (Å)   | M-C <sub>NHC</sub>             | 2.044(11)              | 2.045(6)               | 2.041(12)              | 2.033(5)               |
|                 | M-C <sub>pcentroid</sub>       | 1.841                  | 1.825                  | 1.795                  | 1.796                  |
|                 | M-X<br>(average)               | 2.72                   | 2.71                   | 2.405                  | 2.44                   |
| Angles<br>(deg) | X <sub>1</sub> MX <sub>2</sub> | 94.7(4)                | 89.69(18)              | 92.3(3)                | 89.53(14)              |
|                 | X <sub>2</sub> MX <sub>1</sub> | 91.1(3)                | 97.5(2)                | 89.2(3)                | 95.18(16)              |
|                 | X <sub>1</sub> MX <sub>2</sub> | 96.13(3)               | 97.86(8)               | 91.82(16)              | 94.73(6)               |



**Figure 5.7.** Molecular diagrams of (a) complex **10**, (b) complex **12**, (c) complex **13**, (d) complex **14**.

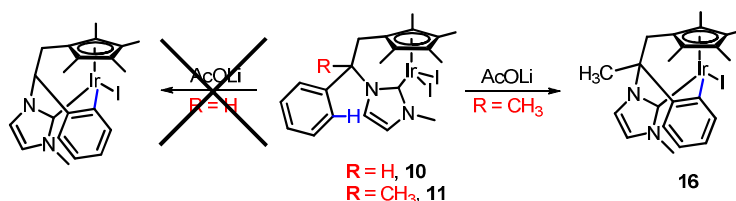
All molecular diagrams show similar half-sandwich structures. Apart from the chelating ligand, two halide ligands complete the coordination sphere about the metal centre. The M-C<sub>NHC</sub> distance is  $\sim 2.0$  Å, and lies in the expected range for both “Cp\*Ir<sup>III</sup>NHC” complexes<sup>[5-12, 14-15, 17]</sup> and “Cp\*Rh<sup>III</sup>NHC” complexes.<sup>[22-26]</sup> The distance between the metal and the cyclopentadienyl centroid is  $\sim 1.8$  Å, and also lies in the expected range for these types of complexes. The angles formed by the legs of the three legged piano-stools are in the interval of 90 – 98 °C and suggest a pseudo-octahedral geometry, as expected for d<sup>6</sup> complexes with a coordination number of 6.<sup>[27]</sup> Due to the *trans* influence of the strong  $\sigma$ -donor NHC ligand, the quaternary carbons of the cyclopentadienyl moiety that are *trans* to the NHC, present a slightly larger distance to the metal ( $\sim 2.3$  Å) than the carbons that are *cis* ( $\sim 2.1$  Å). This could account for the differences found in the chemical shift of the <sup>13</sup>C NMR signals of

each group, and also the different Rh-C coupling constants in complexes **12** and **14**. The carbons *trans* to the carbene are more distant to the rhodium centre, and therefore present a smaller coupling constant ( $^1J_{\text{Rh-C}} \sim 3$  Hz), in contrast the carbons *cis* are closer to the metal and have a larger coupling constant ( $^1J_{\text{Rh-C}} \sim 9$  Hz).

### 5.3.3. Intramolecular C-H activation studies

In previous works, the intramolecular C-H activation properties of “Cp\*Ir<sup>III</sup>NHC” complexes were studied, thus leading to the isolation of the corresponding chelate-metalated species.<sup>[5, 7, 10]</sup> The intramolecular aromatic C-H activation step that affords the mentioned complexes occurs under mild conditions and has the potential to become an easy and simple method for the preparation and isolation of enantiomerically pure chiral-at-metal complexes,<sup>[7]</sup> since it allows the metal to become a stereogenic centre.

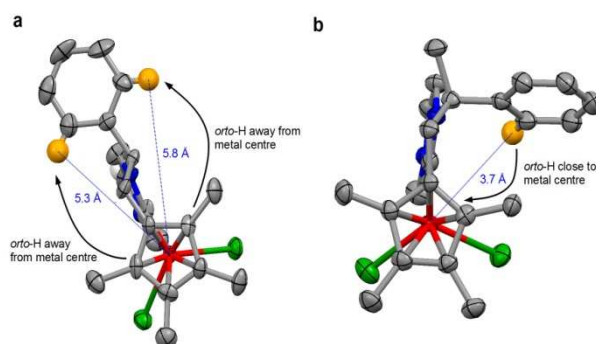
Based on these previous results, we performed a series of experiments in which the iridium complexes **10** and **11** were reacted with LiOAc, in order to check if the intramolecular C-H activation was possible. As can be seen in Scheme 5.5, the reaction of complex **11** in the presence of lithium acetate yielded **16** almost quantitatively. Compound **10** does not react under the same reaction conditions.



**Scheme 5.5.** Intramolecular C-H activation reactivity of complexes **10** and **11**.

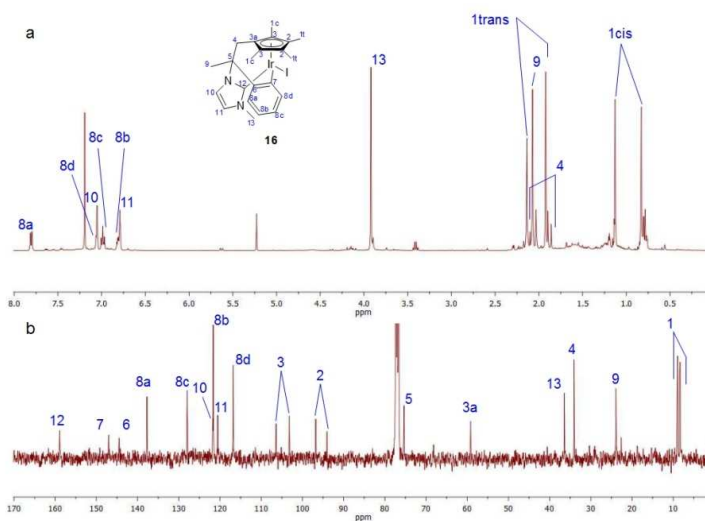
We attributed the different reactivity of these two complexes to the distinct substituents at the stereogenic carbon of the linker. In fact, the structural changes caused by the introduction of the methyl group at the

linker become evident when comparing the top view of the molecular diagrams of **10** and **12** (structurally analogue of **11**), shown in Figure 5.8. As can be observed in Figure 5.8.a, in complex **10** the phenyl group is pointing away from the molecule, and therefore is unable to intramolecular C-H activation. On the other hand, in complex **12** (and consequently in complex **11**) the phenyl group is pointing towards the metal, and therefore is prone to facilitate the intramolecular C-H activation step.



**Figure 5.8.** Top view of the molecular diagrams of complexes(a) **10** and (b) **12**, some atoms omitted for clarity.

The  $^1\text{H}$  NMR and  $^{13}\text{C}$  NMR spectra of **16** are displayed in Figure 5.9.

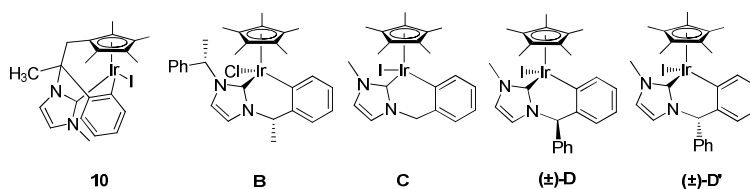


**Figure 5.9.** (a)  $^1\text{H}$  NMR (400 MHz,  $\text{CDCl}_3$ , 300K) and (b)  $\{^1\text{H}\}$   $^{13}\text{C}$  NMR (100 MHz,  $\text{CDCl}_3$ , 300K) spectra of complex **16**.



The evidence that *ortho*-metalation on complex **16** occurred is given by the presence of four resonances corresponding to the inequivalent protons of the phenyl ring in its  $^1\text{H}$  NMR spectrum (Figure 5.10.a). The  $\{^1\text{H}\}^{13}\text{C}$  NMR spectrum (Figure 5.10.b) shows that the resonance of the carbene carbon appears at  $\delta$  159 (**16**) (compare to  $\delta$  145 in **11**), and the resonance due to the metaled carbon of the phenyl ring is seen at 147 ppm, confirming that *ortho*-metalation has occurred. These chemical shifts are in agreement with the ones found in previously isolated *ortho*-metalated “Cp\*Ir<sup>III</sup>NHC” complexes, whose data are shown in Table 5.3.<sup>[5, 7, 10]</sup>

**Table 5.3.** Selected  $^{13}\text{C}$  NMR chemical shifts of complex **16** and analogs.

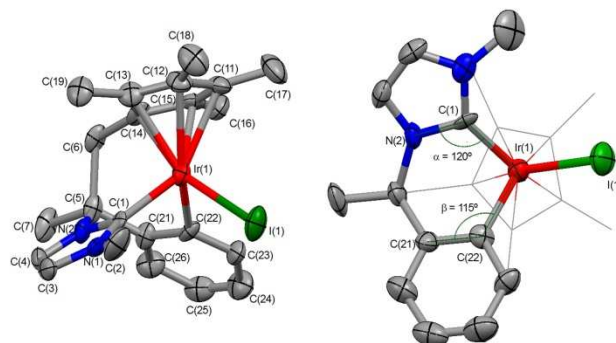


|                     |                     | <b>10</b>        | <b>B</b>         | <b>C</b>         | <b>D</b>         | <b>D'</b>        |
|---------------------|---------------------|------------------|------------------|------------------|------------------|------------------|
| $^{13}\text{C}$ NMR | C <sub>NHC</sub>    | 159 <sup>a</sup> | 159 <sup>b</sup> | 155 <sup>b</sup> | 154 <sup>b</sup> | 155 <sup>b</sup> |
|                     | C <sub>Phenyl</sub> | 147 <sup>a</sup> | 144 <sup>b</sup> | 141 <sup>b</sup> | 145 <sup>b</sup> | 142 <sup>b</sup> |
| Reference           |                     | this work        | [7]              | [10]             | [5]              | [5]              |

<sup>a</sup> in CDCl<sub>3</sub>, 100 MHz, 300 K, chemical shifts reported in ppm. <sup>b</sup> in CDCl<sub>3</sub>, 75 MHz, 300 K, chemical shifts reported in ppm.

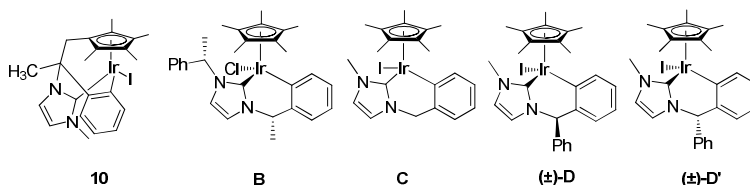
Figure 5.11 shows two views of the molecular diagram of complex **16**. The distance between the Cp\*<sup>\*</sup>-centroid and the metal centre is  $\sim 1.8$  Å and lies in the same region as the distances found in the crystal structures of compounds **10** and **13**. The Ir-C<sub>carbene</sub> bond distance is 1.950 Å, slightly shorter than in complexes **10** and **13** ( $\sim 2.04$  Å), but similar to other Cp\*IrNHC complexes with chelating NHC ligands.<sup>[5, 7, 10]</sup> The chelating bicyclic ligand formed upon *ortho*-metallation in complex **16** presents high ring tension as can be noticed by comparing the

endocyclic angles of the imidazolylidene ( $\alpha = \text{M}^{\wedge}\text{C}_{\text{NHC}}^{\wedge}\text{N} = 120.5^\circ$ ) and phenyl ring ( $\beta = \text{M}^{\wedge}\text{C}_{\text{Ph}}^{\wedge}\text{C} = 115.4^\circ$ ), with other known *ortho*-metalated complexes, as can be observed by comparing the data shown in Table 5.4.



**Figure 5.10.** Two perspectives of the molecular diagram of **16**.

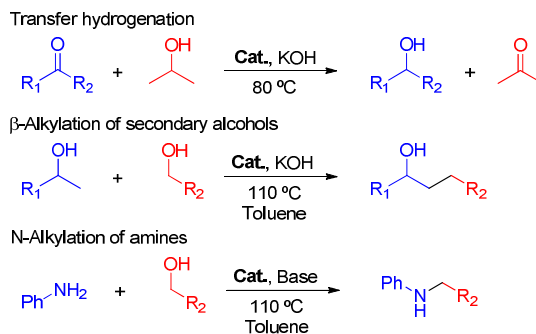
**Table 5.4.** Selected bond length and angles of complex **16** and analogs.



|               | <b>16</b>  | <b>B</b>   | <b>C</b> | <b>D</b>  | <b>D'</b> |           |
|---------------|--|------------|----------|-----------|-----------|-----------|
| distances (Å) | Ir-C <sub>NHC</sub>                              | 1.951(17)  | 1.99(1)  | 2.014(7)  | 2.019(9)  | 2.001(4)  |
|               | Ir-C <sub>centroid</sub>                         | 1.84       | 1.85     | 1.85      | 1.88      | 1.87      |
|               | Ir-C <sub>Phenyl</sub>                           | 2.074(18)  | 2.04(1)  | 2.068(8)  | 2.078(8)  | 2.051(4)  |
|               | Ir-X   | 2.6985(17) | 2.412(3) | 2.7078(7) | 2.7240(8) | 2.7047(4) |
| Angles (deg)  | X <sup>∧</sup> Ir <sup>∧</sup> C <sub>NHC</sub>  | 102.8(6)   | 89.4(3)  | 90.4(2)   | 88.7(2)   | 91.8(1)   |
|               | Ph <sup>∧</sup> Ir <sup>∧</sup> C <sub>NHC</sub> | 83.2(7)    | 83.9(4)  | 85.7(3)   | 85.8(3)   | 85.8(1)   |
|               | X <sup>∧</sup> Ir <sup>∧</sup> C <sub>Ph</sub>   | 96.2(5)    | 87.7(3)  | 88.4(2)   | 86.3(2)   | 87.8(1)   |
|               | Ir <sup>∧</sup> C <sub>NHC</sub> <sup>∧</sup> N  | 120(1)     | 124.0(9) | 124.2(5)  | 127.1(6)  | 126.2(3)  |
|               | Ir <sup>∧</sup> C <sub>Ph</sub> <sup>∧</sup> C   | 115(1)     | 124.5(8) | 123.9(6)  | 125.4(5)  | 125.6(3)  |
| Reference     | this work  | [7]        | [10]     | [5]       | [5]       |           |

### 5.3.4. Catalysis

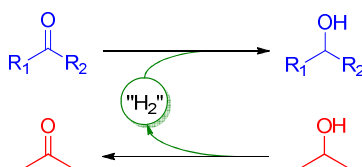
As we have mentioned before, previous studies by the groups of Fujita<sup>[6, 8, 9, 11]</sup> and Peris,<sup>[5, 10, 12, 14]</sup> showed that Cp\*IrNHC complexes are very active in hydrogen borrowing processes, especially those involving the transformations of primary and secondary alcohols. With this in mind, we decided to study the transfer hydrogenation between ketones and alcohols, and some other reactions involving a borrowing-hydrogen methodology,<sup>[28]</sup> such as the alkylation of secondary alcohols and amines with primary alcohols (Scheme 5.6). These types of catalytic reactions have important beneficial implications from an environmental perspective, as they use alcohols as alkylating agents, avoiding the use of alkyl halides and multistep approaches.<sup>[29]</sup>



**Scheme 5.6.** Catalytic reactions studied.

#### 5.3.4.1. Transfer hydrogenation

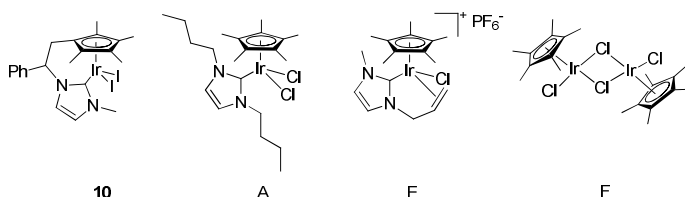
In the catalytic transfer hydrogenation reaction depicted in Scheme 5.7, the catalyst oxidizes an alcohol with a ketone, which is reduced. This reaction is a dynamic equilibrium that depends on the relative concentration of the substrates.



**Scheme 5.7.** Transfer hydrogenation.

Preliminary studies on the catalytic transfer hydrogenation were performed using catalyst **10** (0.1 or 0.01 mol%) in refluxing *iso*-propanol, and acetophenone, cyclohexanone or benzophenone as substrates. The progress of the reaction was monitored by  $^1\text{H}$  NMR spectroscopy. Table 5.5 summarises the results obtained when using complexes **10**, **A**, **E** and **F** as catalysts.

**Table 5.5.** Catalytic transfer hydrogenation.



| entry | catalyst               | substrate     | % cat | t (h) | TON  | % yield | Ref       |
|-------|------------------------|---------------|-------|-------|------|---------|-----------|
| 1     | <b>10</b> <sup>a</sup> | acetophenone  | 0.1   | 5.5   | 990  | >99     | this work |
| 2     | <b>10</b> <sup>a</sup> | cyclohexanone | 0.1   | 2.5   | 870  | 87      | this work |
| 3     | <b>10</b> <sup>a</sup> | cyclohexanone | 0.1   | 4.5   | 990  | >99     | this work |
| 4     | <b>10</b> <sup>a</sup> | cyclohexanone | 0.01  | 20    | 9900 | >99     | this work |
| 5     | <b>10</b> <sup>a</sup> | benzophenone  | 0.1   | 2     | 130  | 13      | this work |
| 6     | <b>10</b> <sup>a</sup> | benzophenone  | 0.1   | 8     | 990  | >99     | this work |
| 7     | <b>A</b> <sup>b</sup>  | cyclohexanone | 0.1   | 8     | 990  | 99      | [14]      |
| 8     | <b>A</b> <sup>b</sup>  | cyclohexanone | 0.01  | 17    | 2900 | 29      | [14]      |
| 9     | <b>A</b> <sup>b</sup>  | acetophenone  | 0.1   | 8     | 500  | 50      | [14]      |
| 10    | <b>A</b> <sup>b</sup>  | benzophenone  | 0.1   | 8     | 500  | 50      | [14]      |
| 11    | <b>E</b> <sup>c</sup>  | cyclohexanone | 0.1   | 5     | 990  | >99     | [12]      |
| 12    | <b>E</b> <sup>c</sup>  | acetophenone  | 0.1   | 19    | 700  | 70      | [12]      |
| 13    | <b>F</b> <sup>a</sup>  | cyclohexanone | 0.1   | 2.5   | 50   | 5       | this work |
| 14    | <b>F</b> <sup>a</sup>  | cyclohexanone | 0.1   | 17    | 970  | 97      | this work |
| 15    | <b>F</b> <sup>a</sup>  | benzophenone  | 0.1   | 2.5   | 30   | 3       | this work |
| 16    | <b>F</b> <sup>a</sup>  | benzophenone  | 0.1   | 17    | 270  | 27      | this work |

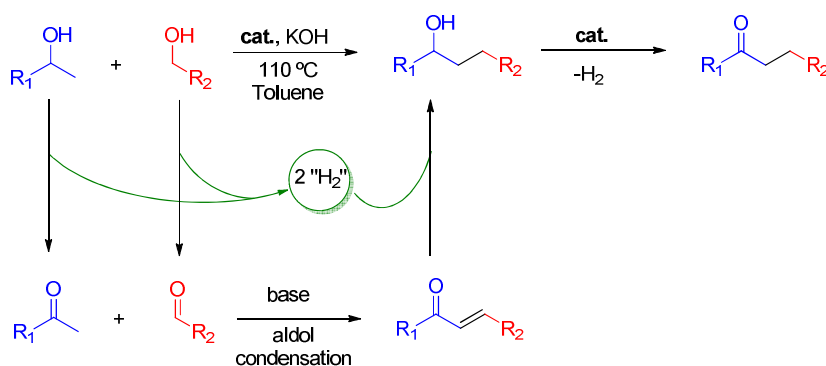
<sup>a</sup> 2 mmol of ketone, KOH (10 mL, 0.2M in *i*-PrOH), T = 80 °C. <sup>b</sup> 0.45 M substrate in *i*-PrOH at room temperature. Cat/AgOTf 1:3. <sup>c</sup> 1 mmol of ketone, KOH (10 mL, 0.05M in *i*-PrOH), reflux. Yields determined by  $^1\text{H}$  NMR spectroscopy.

As observed, complex **10** is able to catalytically reduce both aliphatic and aromatic ketones even at low catalyst loadings. The introduction of the NHC ligand has a very positive effect on the enhancement of the catalytic activities of the catalyst compared to the activities shown by  $[\text{Cp}^*\text{IrCl}_2]_2$  (compare entries 1–6 with 13–16, Table 1). Catalyst loadings of 0.1 mol% afforded full conversions to the corresponding alcohols in times ranging from 3 to 5 h. A catalyst loading as low as  $10^{-2}$  mol % was used in the reduction of cyclohexanone, achieving full conversions, despite longer reaction times being needed (20 h). The high turnover numbers (TONs) obtained indicate that the catalyst is stable under the reaction conditions used. Some other previously reported  $\text{Cp}^*\text{IrNHC}$  complexes were previously reported to catalyse the same reaction. Complex **A**, and some analogues, were reported to perform this reaction at room temperature with addition of a catalytic amount of  $\text{AgOTf}$  instead of using a base.<sup>[14]</sup> The alkene functionalised complex **E** was reported to catalyse transfer hydrogen in similar reaction conditions.<sup>[12]</sup> Although all these complexes reduced cyclohexanone at similar rates, complex **10** preformed the reduction of aromatic ketones (acetophenone and benzophenone) at much higher reactions rates. As Peris group previously reported,<sup>[5]</sup> the fact that **10** shows high catalytic activity in the transfer hydrogenation of ketones contrasts with the negligible performances shown by other bis-chelating  $\text{Cp}^*\text{Ir(III)(NHC)}$  complexes, thus implying that the blocking of the two coordination vacant sites by the chelating ligand prevents any catalytic activity.

#### 5.3.4.2. $\beta$ -Akylation of secondary alcohols with primary alcohols

The mechanism of the  $\beta$ -alkylation of alcohols implies the oxidation of alcohols to ketone and aldehyde as the first step. Aldol condensation

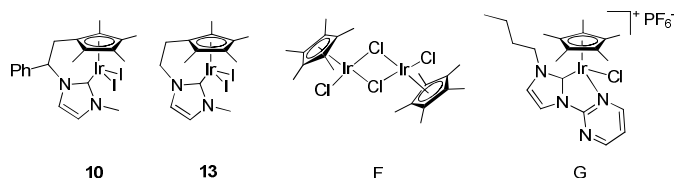
produces an  $\alpha$ - $\beta$  insaturated ketone, which is then reduced to form the final secondary alcohol, as shown in Scheme 5.8.



**Scheme 5.8.**  $\beta$ -alkylation of alcohols.

The catalytic activities of complexes **10** and **13** were checked. The results are summarised in Table 5.6, including those reported afterwards for complex **G**.

The reactions were carried out with a fixed catalyst loading of 1 mol % in the presence of KOH in toluene at  $110^\circ C$ . Again, the results show an improvement compared to the results obtained when using  $[Cp^*IrCl_2]_2$ . As can be observed in Table 5.6, both **10** and **13** are active at low catalyst loadings (1 mol%). Aromatic primary alcohols gave better selectivities than aliphatic alcohols to the desired alcohols, and also needed shorter reaction times to achieve full conversions. The selectivity of the process is highly dependent on the reaction times, because dehydrogenation of the resulting alcohol to the corresponding ketone is observed when the catalytic reaction is kept for long reaction times (see entries 5, 6 and 7, 8). This dehydrogenation process is not so strange if we take into account the previous work by Fujita, Yamaguchi, and Peris in which a  $Cp^*Ir$  complexes are used for the dehydrogenation of alcohols in an "oxidant-free" environments.<sup>[8-9, 11, 16, 30]</sup>

**Table 5.6.**  $\beta$ -alkylation of secondary alcohols with primary alcohols<sup>a</sup>

| entry | catalyst               | R <sub>1</sub> | R <sub>2</sub>                       | t (h) | % conv | % alcohol | % ketone | Ref       |
|-------|------------------------|----------------|--------------------------------------|-------|--------|-----------|----------|-----------|
| 1     | <b>10</b> <sup>a</sup> | Ph             | Ph                                   | 3     | 70     | 100       | 0        | this work |
| 2     | <b>10</b> <sup>a</sup> | Ph             | Ph                                   | 6     | 90     | 100       | 0        | this work |
| 3     | <b>10</b> <sup>a</sup> | Ph             | Ph                                   | 9     | >95    | 100       | 0        | this work |
| 4     | <b>10</b> <sup>a</sup> | Ph             | Ph                                   | 24    | >99    | 100       | 0        | this work |
| 5     | <b>10</b> <sup>a</sup> | Ph             | 4-Cl(C <sub>6</sub> H <sub>4</sub> ) | 6     | 87     | 100       | 0        | this work |
| 6     | <b>10</b> <sup>a</sup> | Ph             | 4-Cl(C <sub>6</sub> H <sub>4</sub> ) | 9     | 100    | 50        | 50       | this work |
| 7     | <b>10</b> <sup>a</sup> | Ph             | Pr                                   | 3     | 100    | 80        | 20       | this work |
| 8     | <b>10</b> <sup>a</sup> | Ph             | Pr                                   | 6     | 100    | 50        | 50       | this work |
| 9     | <b>13</b> <sup>a</sup> | Ph             | Ph                                   | 3     | 70     | 100       | 0        | this work |
| 10    | <b>13</b> <sup>a</sup> | Ph             | Ph                                   | 6     | 80     | 100       | 0        | this work |
| 11    | <b>13</b> <sup>a</sup> | Ph             | Ph                                   | 24    | >99    | 100       | 0        | this work |
| 12    | <b>F</b> <sup>a</sup>  | Ph             | Ph                                   | 9     | 68     | 100       | 0        | this work |
| 13    | <b>F</b> <sup>a</sup>  | Ph             | Pr                                   | 3     | 89     | 64        | 36       | this work |
| 14    | <b>F</b> <sup>a</sup>  | Ph             | Pr                                   | 6     | 93     | 54        | 46       | this work |
| 15    | <b>G</b> <sup>b</sup>  | Ph             | Ph                                   | 3     | 93     | 100       | 0        | [15]      |
| 16    | <b>G</b> <sup>b</sup>  | Ph             | 4-Cl(C <sub>6</sub> H <sub>4</sub> ) | 3     | 96     | 100       | 0        | [15]      |
| 17    | <b>G</b> <sup>b</sup>  | Ph             | 4-Cl(C <sub>6</sub> H <sub>4</sub> ) | 6     | 100    | 80        | 20       | [15]      |
| 18    | <b>G</b> <sup>b</sup>  | Ph             | Pr                                   | 5     | 82     | 60        | 22       | [15]      |

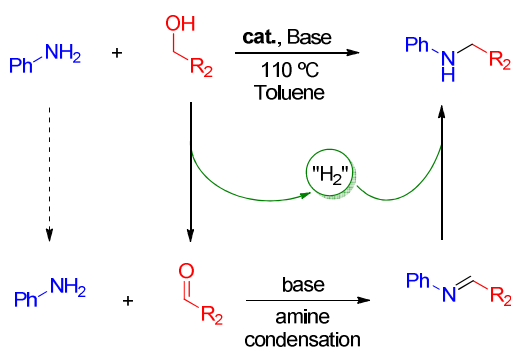
<sup>a</sup> 1 mmol of primary and secondary alcohol, 1 mmol (100 mol%) of KOH, 0.3 mL of toluene, 1 mol % cat., T = 110 °C. <sup>b</sup> 2 mmol of primary and secondary alcohol, 2 mmol (100 mol%) of KOH, 0.5 mL of toluene, 1 mol % cat., T = 110 °C. Conversions and yields determined by <sup>1</sup>H NMR spectroscopy.

To the best of our knowledge, complexes **10** and **13** were the first “Cp\*IrNHC” complexes to be reported as active in the catalytic  $\beta$ -alkylation of secondary alcohols, considering the short reaction times needed for completion of the process and the low catalyst loadings used.

Recently, but after our work was done and published, Crabtree and co-workers<sup>[15]</sup> reported similar activities when using a pyrimidine functionalised “Cp\*IrNHC” complex **G**.

#### 5.3.4.3. N-Alkylation of amines with primary alcohols

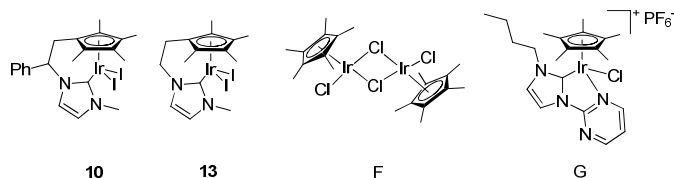
The alkylation of amines by primary alcohols with loss of water is a thermodynamically favoured process, Scheme 5.9.<sup>[31]</sup> Typically, the reaction consists of the coupling of a primary or secondary amine with a primary alcohol to provide the corresponding final alkylated amine. For this reaction, only a few examples describing Ru<sup>[32-33]</sup> and Ir<sup>[34-35]</sup> catalysts have been reported. The synthetic scope of these reactions span the range from simple amines to quinolines, indoles, and other heterocycles with more complex products being generated through tandem multistep sequences.<sup>[36-37]</sup> As shown in Scheme 5.9, the first step is the oxidation of the alcohol followed by imine condensation, and subsequent reduction to the corresponding amine.



**Scheme 5.9.** N-alkylation of amines.

The results on the N-alkylation of aniline with primary alcohols using the chelating “Cp\*-NHClr” complexes **10** and **13** are depicted in Table 5.7, including those reported afterwards for complex **G**.



**Table 5.7.** N-Alkylation of aniline with primary alcohols

| entry | catalyst               | alcohol        | base               | t (h) | % yield | Ref       |
|-------|------------------------|----------------|--------------------|-------|---------|-----------|
| 1     | <b>10</b> <sup>a</sup> | benzyl alcohol | KOH                | 9     | 54      | this work |
| 2     | <b>10</b> <sup>b</sup> | benzyl alcohol | KOH                | 25    | 67      | this work |
| 3     | <b>10</b> <sup>b</sup> | benzyl alcohol | KOH                | 45    | 76      | this work |
| 4     | <b>10</b> <sup>b</sup> | benzyl alcohol | KO <sup>t</sup> Bu | 16    | 85      | this work |
| 5     | <b>10</b> <sup>b</sup> | 1-butanol      | KO <sup>t</sup> Bu | 16    | 47      | this work |
| 6     | <b>10</b> <sup>b</sup> | 1-butanol      | KO <sup>t</sup> Bu | 24    | 55      | this work |
| 7     | <b>13</b> <sup>b</sup> | benzyl alcohol | KO <sup>t</sup> Bu | 17    | 93      | this work |
| 8     | <b>F</b> <sup>b</sup>  | benzyl alcohol | KOH                | 13    | 36      | this work |
| 9     | <b>F</b> <sup>b</sup>  | benzyl alcohol | KO <sup>t</sup> Bu | 16    | 60      | this work |
| 10    | <b>F</b> <sup>b</sup>  | 1-butanol      | KO <sup>t</sup> Bu | 16    | 29      | this work |
| 11    | <b>G</b> <sup>c</sup>  | benzyl alcohol | NaHCO <sub>3</sub> | 45    | 98      | [15]      |
| 12    | <b>G</b> <sup>c</sup>  | 1-butanol      | NaHCO <sub>3</sub> | 45    | 43      | [15]      |

<sup>a</sup> 2 mmol of aniline and alcohol, 0.5 mmol (50 mol %) of base, 0.3 mL of toluene, 2.5 mol % cat., T = 110 °C. <sup>b</sup> 2 mmol of aniline and alcohol, 2 mmol (100 mol %) of base, 0.3 mL of toluene, 0.75 mol % cat., T = 110 °C. <sup>c</sup> 1 mmol of aniline and alcohol, 0.5 mmol (50 mol %) of base, 0.7 mL of toluene, 1 mol % cat., T = 110 °C, and 4 Å molecular sieves. Yields determined by <sup>1</sup>H NMR.

As shown in Table 5.7, complex **10** was able to facilitate the alkylation of aniline with aliphatic and aromatic primary alcohols in moderate to good yields. Complex **13** was tested for the alkylation of aniline with benzyl alcohol showing slightly better yield in lower reaction time than complex **10**. The conversions were only moderate, but comparable to the results provided by [Cp\*IrCl<sub>2</sub>]<sub>2</sub> catalysts.<sup>[34-35]</sup> However, under the same reaction conditions both **10** and **13** achieved higher conversions than [Cp\*IrCl<sub>2</sub>]<sub>2</sub>

(compare entries 4 and 7 with 9 and 5 with 10). After our work was published, Crabtree and co-workers<sup>[15]</sup> reported complex **G** showed similar yields even with when using a weak base (NaHCO<sub>3</sub>) in less than stoichiometric amount (50 mol%), probably due to the increased driving force caused by removing water with molecular sieves.

## 5.4. Conclusions

In this chapter we described the easy coordination of Cp\*-functionalised imidazolium proligands to Rh and Ir by transmetallation from the corresponding preformed Ag-NHC complex. Additionally, the coordination of Cp\*-functionalised imidazolium proligands to Ir by *in situ* deprotonation with a weak base is also described. Both metallation methodologies to the (Cp\*-NHC)M complexes constitute valuable protocols that can be extended to the preparation of complexes with other transition metals.

The preliminary studies on the catalytic activity of the Ir complex **10**, show that it displays excellent activity in a wide set of borrowing-hydrogen processes, including the transfer hydrogenation,  $\beta$ -alkylation of secondary alcohols with primary alcohols, and amination of primary alcohols. In this regard, the iridium complex **10** is a very versatile catalyst in a variety of organic transformations.

## 5.5. Experimental procedures

### 5.5.1. Materials and methods

All reactions were carried out under inert atmosphere. When required, solvents were dried via standard techniques. NMR spectra were recorded on a Bruker Avance III 400 MHz and a Varian Innova 500 MHz spectrometers with CDCl<sub>3</sub> (Cambridge Isotope Laboratories, Inc.) as solvent. Elemental analyses were performed in our laboratories at ITQB.

Electrospray mass spectra (ESI-MS) were recorded on a Micromass Quattro LC instrument. Data for structural characterisation was collected in a Siemens Smart CCD.  $[\text{Ir}(\mu\text{-Cl})(\text{cod})]_2$ <sup>[38]</sup> and  $[\text{Rh}(\mu\text{-Cl})(\text{cod})]_2$ <sup>[39]</sup> were synthesized according to literature procedures. All other reagents are commercially available and were used as received.

### 5.5.2. Synthesis and characterization

#### Coordination route i) – general procedure

A mixture of  $\text{Cs}_2\text{CO}_3$  (10 eq),  $[\text{Ir}(\mu\text{-Cl})(\text{cod})]_2$  (0.5 eq) and **1** (1 eq) in acetonitrile was heated to 50°C for 4 hours. After cooling to room temperature, the reaction mixture was filtered, the filtrate was evaporated to dryness and KI (5 eq) and methanol were added to the residue. After being refluxed overnight, the reaction mixture was allowed to cool to room temperature and the solvent was removed under vacuum, and the remaining solid was purified by flash chromatography ( $\text{CH}_2\text{Cl}_2$ ).

#### Coordination route ii) – general procedure

A mixture of  $\text{Ag}_2\text{O}$  (1.2 eq) and the corresponding imidazolium salt (1 eq) were refluxed in 1,2-dichloroethane for 1h. Then,  $[\text{M}(\mu\text{-Cl})(\text{cod})]_2$  (0.5 eq, M = Ir and Rh) was added and the mixture was refluxed for 30 min, followed by addition of glacial acetic acid. After refluxing overnight, the suspension was filtered through Celite, the filtrate evaporated to dryness and KI (5 eq) and methanol were added to the remaining residue. The mixture was then refluxed for a further 1 h. After cooling, the solvent was removed in vacuum and the crude solid was purified by flash chromatography ( $\text{CH}_2\text{Cl}_2$ / acetone).

#### Complex 10

Yield: 68%. <sup>1</sup>H NMR (400MHz,  $\text{CDCl}_3$ ):  $\delta$  7.49 (m, 3H, PhH), 7.36(m, 2H, PhH), 6.65 (d, 1H, <sup>3</sup>J<sub>H-H</sub> = 1.6 Hz, CH<sub>imid</sub>), 6.29 (d, 1H, <sup>3</sup>J<sub>H-H</sub> =1.6 Hz,

$CH_{\text{Imid}}$ ), 5.07 (dd, 1H,  $^3J_{\text{H-H}} = 3.2$  Hz,  $^3J_{\text{H-H}} = 11.4$  Hz,  $CH_{\text{Linker}}$ ), 4.07 (s, 3H, N- $CH_3$ ), 2.68 (m, 2H,  $CH_2(\text{Linker})$ ), 2.13 (s, 3H,  $CH_3(\text{Cp}^*)$ ), 2.12 (s, 3H,  $CH_3(\text{Cp}^*)$ ), 1.99 (s, 3H,  $CH_3(\text{Cp}^*)$ ), 1.79 (s, 3H,  $CH_3(\text{Cp}^*)$ ).  $\{^1\text{H}\}^{13}\text{C}$  NMR (100MHz,  $\text{CDCl}_3$ ):  $\delta$  146 ( $C_{\text{NHC-Ir}}$ ), 138 ( $C_{\text{Ph}}$ ), 130 ( $C_{\text{Ph}}$ ), 123 ( $CH_{\text{Imid}}$ ), 120 ( $CH_{\text{Imid}}$ ), 104 ( $C_{\text{Cp}^*}$ ), 103 ( $C_{\text{Cp}^*}$ ), 84 ( $C_{\text{Cp}^*}$ ), 83 ( $C_{\text{Cp}^*}$ ), 80 ( $C_{\text{Cp}^*}$ ), 65 ( $CH_{\text{Linker}}$ ), 46 (N- $CH_3$ ), 29 ( $CH_2(\text{Linker})$ ), 12 ( $CH_3(\text{Cp}^*)$ ), 11 ( $CH_3(\text{Cp}^*)$ ), 10 ( $CH_3(\text{Cp}^*)$ ). Anal. Calc for  $\text{C}_{21}\text{H}_{27}\text{I}_2\text{N}_2\text{Ir}$ : C, 33.57; H, 3.35; N 3.73. Found: C, 33.28; H, 3.28; N, 3.22.

### Complex 11

Yield: 24%.  $^1\text{H}$  NMR (400MHz,  $\text{CDCl}_3$ ,  $\delta$ ): 7.27-7.20 (m, 5H, PhH), 6.89 (d, 1H,  $^3J_{\text{H-H}} = 2.16$  Hz,  $CH_{\text{Imid}}$ ), 6.84 (d, 1H,  $^3J_{\text{H-H}} = 2.16$  Hz,  $CH_{\text{Imid}}$ ), 4.13 (s, 3H, N- $CH_3$ ), 2.98 (d, 1H,  $^2J_{\text{H-H}} = 15.3$  Hz,  $CH_2(\text{linker})$ ), 2.66 (d, 1H,  $^2J_{\text{H-H}} = 15.3$  Hz,  $CH_2(\text{linker})$ ), 2.02 (s, 3H,  $CH_3(\text{linker})$ ), 1.96 (s, 3H,  $CH_3(\text{Cp}^*)$ ), 1.92 (s, 3H,  $CH_3(\text{Cp}^*)$ ), 1.73 (s, 3H,  $CH_3(\text{Cp}^*)$ ), 0.82 (s, 3H,  $CH_3(\text{Cp}^*)$ ).  $\{^1\text{H}\}^{13}\text{C}$  NMR (100MHz,  $\text{CDCl}_3$ ):  $\delta$  148.3 ( $C_{\text{NHC-Ir}}$ ), 145.4 ( $C_{\text{Ph}}$ ), 129.2 ( $CH_{\text{Ph}}$ ), 128.1 ( $CH_{\text{Ph}}$ ), 126.3 ( $CH_{\text{Ph}}$ ), 124.1 ( $CH_{\text{Imid}}$ ), 119.9 ( $CH_{\text{Imid}}$ ), 105.3 ( $C_{\text{Cp}^*}$ ), 104.9 ( $C_{\text{Cp}^*}$ ), 81.9 ( $C_{\text{Cp}^*}$ ), 81.5 ( $C_{\text{Cp}^*}$ ), 69.3 ( $C_{\text{linker}}$ ), 47.1 (N- $CH_3$ ), 34.3 ( $CH_2(\text{linker})$ ), 33.8 ( $CH_3(\text{linker})$ ), 11.9 ( $CH_3(\text{Cp}^*)$ ), 11.6 ( $CH_3(\text{Cp}^*)$ ), 10.5 ( $CH_3(\text{Cp}^*)$ ), 9.0 ( $CH_3(\text{Cp}^*)$ ). MS (ESI, 25 V):  $m/z$  [ $M - I$ ] $^+$  calc for  $\text{C}_{22}\text{H}_{27}\text{IN}_2\text{Ir}$ , 639.1; found, 639.3.

### Complex 12

Yield: 51%.  $^1\text{H}$  NMR (400MHz,  $\text{CDCl}_3$ ):  $\delta$  7.35-7.22 (m, 5H, PhH), 7.01 (d, 1H,  $^3J_{\text{H-H}} = 2.0$  Hz,  $CH_{\text{Imid}}$ ), 6.95 (d, 1H,  $^3J_{\text{H-H}} = 2.0$  Hz,  $CH_{\text{Imid}}$ ), 4.14 (s, 3H, N- $CH_3$ ), 3.05 (d, 1H,  $^2J_{\text{H-H}} = 15.3$  Hz,  $CH_2(\text{linker})$ ), 2.77 (d, 1H,  $^2J_{\text{H-H}} = 15.3$  Hz,  $CH_2(\text{linker})$ ), 2.09 (s, 3H,  $CH_3(\text{linker})$ ), 1.71 (s, 3H,  $CH_3(\text{Cp}^*)$ ), 1.63 (s, 3H,  $CH_3(\text{Cp}^*)$ ), 1.42 (s, 3H,  $CH_3(\text{Cp}^*)$ ), 0.51 (s, 3H,  $CH_3(\text{Cp}^*)$ ).  $\{^1\text{H}\}^{13}\text{C}$  NMR (100MHz,  $\text{CDCl}_3$ ):  $\delta$  166.8 (d,  $C_{\text{NHC-Rh}}$ ,  $^1J_{\text{C-Rh}} = 59.0$  Hz), 145.6 ( $C_{\text{Ph}}$ ), 129.4 ( $CH_{\text{Ph}}$ ), 128.3 ( $CH_{\text{Ph}}$ ), 126.4 ( $CH_{\text{Ph}}$ ), 124.9 ( $CH_{\text{Imid}}$ ), 121.5 ( $CH_{\text{Imid}}$ ),

109.6 (m,  $C_{(Cp^*)}$ ), 90.9 (m,  $C_{(Cp^*)}$ ), 87.4 (d,  $^1J_{C-Rh} = 8$  Hz,  $C_{(Cp^*)}$ ), 70.4 ( $C_{(linker)}$ ), 48.1 (N-CH<sub>3</sub>), 35.1 (CH<sub>2(linker)</sub>), 33.9 (CH<sub>3(linker)</sub>), 12.7 (CH<sub>3(Cp^\*)</sub>), 12.4 (CH<sub>3(Cp^\*)</sub>), 11.4 (CH<sub>3(Cp^\*)</sub>), 9.9 (CH<sub>3(Cp^\*)</sub>). MS (ESI, 5 V):  $m/z$  [M - I]<sup>+</sup> calc for C<sub>22</sub>H<sub>27</sub>IN<sub>2</sub>Rh, 549.0; found, 549.1.

### Complex 13

Yield: 24%. <sup>1</sup>H NMR (500MHz, CDCl<sub>3</sub>): δ 6.91 (br, 1H, CH<sub>Imid</sub>), 6.77 (br, 1H, CH<sub>Imid</sub>), 4.13 (m, 2H, CH<sub>2(linker)</sub>), 4.08 (s, 3H, NCH<sub>3</sub>), 2.51 (m, 2H, CH<sub>2(linker)</sub>), 1.7 (br, 6H, CH<sub>3(Cp^\*)</sub>), 1.6 (br, 6H, CH<sub>3(Cp^\*)</sub>). {<sup>1</sup>H}<sup>13</sup>C NMR (125 MHz, CDCl<sub>3</sub>): δ 150.3 (C<sub>NHC-Ir</sub>), 124.1 (CH<sub>Imid</sub>), 121.3 (CH<sub>Imid</sub>), 105.1 (C<sub>Cp^\*</sub>), 83.8 (C<sub>Cp^\*</sub>), 77.5 (C<sub>Cp^\*</sub>), 77.2 (C<sub>Cp^\*</sub>), 50.6 (CH<sub>2(linker)</sub>), 39.8 (NCH<sub>3</sub>), 29.9 (CH<sub>2(linker)</sub>), 21.2 (CH<sub>3(Cp^\*)</sub>), 9.88 (CH<sub>3(Cp^\*)</sub>), 8.7 (CH<sub>3(Cp^\*)</sub>). MS (ESI, 15 V):  $m/z$  [M - Cl]<sup>+</sup> calc for C<sub>15</sub>H<sub>21</sub>ClIrN<sub>2</sub>, 457.1; found, 457.2.

### Complex 12

Yield: 37%. <sup>1</sup>H NMR (500MHz, CDCl<sub>3</sub>): δ 7.00 (d, 1H, <sup>3</sup>J<sub>H-H</sub> = 2 Hz, CH<sub>Imid</sub>), 6.85 (d, 1H, <sup>3</sup>J<sub>H-H</sub> = 2 Hz, CH<sub>Imid</sub>), 4.30 (m, 2H, CH<sub>2(linker)</sub>), 4.00 (s, 3H, NCH<sub>3</sub>), 2.55 (m, 2H, CH<sub>2(linker)</sub>), 1.77 (br, 6H, CH<sub>3(Cp^\*)</sub>), 1.48 (br, 6H, CH<sub>3(Cp^\*)</sub>). {<sup>1</sup>H}<sup>13</sup>C NMR (125MHz, CDCl<sub>3</sub>): δ 166.2 (d, C<sub>NHC-Rh</sub>, <sup>1</sup>J<sub>C-Rh</sub> = 55.7 Hz), 124.7 (CH<sub>Imid</sub>), 121.6 (CH<sub>Imid</sub>), 110.0 (d, C<sub>Cp^\*</sub>, <sup>1</sup>J<sub>C-Rh</sub> = 4.0 Hz), 91.0 (d, C<sub>Cp^\*</sub>, <sup>1</sup>J<sub>C-Rh</sub> = 8.0 Hz), 86.7 (d, C<sub>Cp^\*</sub>, <sup>1</sup>J<sub>C-Rh</sub> = 9.6Hz), 50.6 (CH<sub>2(linker)</sub>), 40.4 (NCH<sub>3</sub>), 29.9 (CH<sub>2(linker)</sub>), 21.4 (CH<sub>3(Cp^\*)</sub>), 9.8 (CH<sub>3(Cp^\*)</sub>), 9.4 (CH<sub>3(Cp^\*)</sub>). MS (ESI, 25 V):  $m/z$  [M - Cl]<sup>+</sup> calc for C<sub>15</sub>H<sub>21</sub>ClRhN<sub>2</sub>, 367.0; found, 366.8.

### Complex 15

To a solution of **5** (100 mg, 0.28 mmol) in 1,2-dichloroethane (10 mL), Ag<sub>2</sub>O (180 mg, 0.78 mmol) was added at room temperature. After refluxing for 1h, [Rh(μ-Cl)(cod)]<sub>2</sub> (70 mg, 0.14 mmol) was added. The reaction mixture was refluxed for half an hour, then filtered over celite

and evaporated to dryness. The remaining solid was washed with ether yielding **15** as a yellow solid. Yield: 55 mg, 41%.  $^1\text{H}$  NMR (400MHz,  $\text{CDCl}_3$ ):  $\delta$  6.84-6.78 (m, 2H,  $\text{CH}_{\text{Imid}}$ ), 5.41 (m, 1H,  $\text{CH}_{2(\text{linker})}$ ), 5.2 (m, 1H,  $\text{CH}_{\text{linker}}$ ), 5.14 (m, 1H,  $\text{CH}_{2(\text{linker})}$ ), 5.01 (br, 2H,  $\text{CH}_{\text{cod}}$ ), 4.07 (s, 3H, N- $\text{CH}_3$ ), 3.32 (br, 2H,  $\text{CH}_{\text{cod}}$ ), 2.55 (m, 1H,  $\text{CH}_{(\text{Cp}^*)}$ ), 2.37 (m, 4H,  $\text{CH}_{2(\text{cod})}$ ), 2.14 (q, 1H,  $^3J_{\text{H-H}} = 7.0$  Hz,  $\text{CH}_{(\text{Cp}^*)}$ ), 1.92 (m, 4H,  $\text{CH}_{2(\text{cod})}$ ), 1.76 (s, 3H,  $\text{CH}_{3(\text{Cp}^*)}$ ), 1.63 (s, 3H,  $\text{CH}_{3(\text{Cp}^*)}$ ), 1.15 (two d, 3H,  $^3J_{\text{H-H}} = 7.2$  Hz,  $\text{CH}_3_{\text{Cp}^*}$ ), 1.04 (d, 3H,  $^3J_{\text{H-H}} = 7.0$  Hz,  $\text{CH}_{3(\text{Cp}^*)}$ ).  $\{^1\text{H}\}^{13}\text{C}$  NMR (100MHz,  $\text{CDCl}_3$ )  $\delta$  181.7 (two d,  $\text{C}_{\text{NHC-Rh}}$ ,  $^1J_{\text{C-Rh}} = 51$  Hz), 157.5 + 157.0 ( $\text{C}_{\text{Cp}^*}$ ), 147.1 + 147 ( $\text{C}_{\text{Cp}^*}$ ), 130.53 + 130.46 ( $\text{C}_{\text{Cp}^*}$ ), 122.0 ( $\text{CH}_{\text{Imid}}$ ), 120.1 ( $\text{CH}_{\text{Imid}}$ ), 110.3 + 110.2 ( $\text{CH}_{\text{linker}}$ ), 98.6 (d,  $\text{CH}_{\text{cod}}$ ,  $^1J_{\text{C-Rh}} = 7.0$  Hz), 68.7-67.9 (m,  $\text{CH}_{\text{cod}}$ ), 51.6 ( $\text{CH}_{\text{Cp}^*}$ ), 49.6 + 49.4 ( $\text{CH}_{2(\text{linker})}$ ), 42.4 + 42.3 ( $\text{CH}_{\text{Cp}^*}$ ), 37.9 (N- $\text{CH}_3$ ), 33.4-32.9 + 29.2-28.9 ( $\text{CH}_{2(\text{cod})}$ ), 22.1 + 21.9 ( $\text{CH}_{3(\text{Cp}^*)}$ ), 19.5 + 19.4 ( $\text{CH}_{3(\text{Cp}^*)}$ ), 13.4 ( $\text{CH}_{3(\text{Cp}^*)}$ ), 10.4 ( $\text{CH}_{3(\text{Cp}^*)}$ ). MS (ESI):  $m/z$   $[\text{M} - \text{I}]^+$  calc for  $\text{C}_{23}\text{H}_{34}\text{N}_2\text{Rh}$  441.2; found, 441.2.

### Complex 16

In a J. Young NMR tube equipped with a Teflon screw cap, a solution of **10** (20 mg, 0.026 mmol) in deuterated methanol (0.5 mL) was treated with lithium acetate (20 mg, 0.3 mmol) and heated at 60 °C for 16 h. Compound **16** was obtained as an orange solid in quantitative yield.  $^1\text{H}$  NMR (400MHz,  $\text{CDCl}_3$ ):  $\delta$  7.85 (dd, 1H,  $^3J_{\text{H-H}} = 7.5$  Hz,  $^4J_{\text{H-H}} = 1.3$  Hz, PhH), 7.11 (m, 1H, PhH), 7.10 (d, 1H,  $^3J_{\text{H-H}} = 2.2$  Hz,  $\text{CH}_{\text{Imid}}$ ), 7.03 (t, 1H,  $^3J_{\text{H-H}} = 7.5$  Hz, PhH), 6.86 (m, 1H, PhH), 6.84 (d, 1H,  $^3J_{\text{H-H}} = 2.2$  Hz,  $\text{CH}_{\text{Imid}}$ ), 3.97 (s, 3H, N $\text{CH}_3$ ), 2.18 (s, 3H,  $\text{CH}_{2(\text{linker})}$ ), 2.18 (s, 3H,  $\text{CH}_{3(\text{Cp}^*)}$ ), 2.12 (s, 3H,  $\text{CH}_{3(\text{Cp}^*)}$ ), 1.92 (d, 1H,  $^2J_{\text{H-H}} = 14.9$  Hz,  $\text{CH}_{2(\text{linker})}$ ), 1.18 (s, 3H,  $\text{CH}_{3(\text{Cp}^*)}$ ), 0.88 (s, 3H,  $\text{CH}_{3(\text{Cp}^*)}$ ).  $\{^1\text{H}\}^{13}\text{C}$  NMR (100MHz,  $\text{CDCl}_3$ ):  $\delta$  159.1 ( $\text{C}_{\text{NHC-Ir}}$ ), 147.2 ( $\text{C}_{\text{Ph-Ir}}$ ), 144.7 ( $\text{C}_{\text{Ph}}$ ), 137.9 ( $\text{CH}_{\text{Ph}}$ ), 128.1 ( $\text{CH}_{\text{Ph}}$ ), 121.9 ( $\text{CH}_{\text{Ph}}$ ), 121.8 ( $\text{CH}_{\text{Imid}}$ ), 120.7 ( $\text{CH}_{\text{Ph}}$ ), 117.0 ( $\text{CH}_{\text{Imid}}$ ), 106.6 ( $\text{C}_{\text{Cp}^*}$ ), 103.3

---

(C<sub>Cp\*</sub>), 96.9 (C<sub>Cp\*</sub>), 94.2 (C<sub>Cp\*</sub>), 75.4 (C<sub>linker</sub>), 59.4 (C<sub>Cp\*</sub>), 36.6 (NCH<sub>3</sub>), 34.5 (CH<sub>2(linker)</sub>), 24.1 (CH<sub>3(linker)</sub>), 9.2 (CH<sub>3(Cp\*)</sub>), 9.1 (CH<sub>3(Cp\*)</sub>), 8.6 (CH<sub>3(Cp\*)</sub>), 8.4 (CH<sub>3(Cp\*)</sub>).

### 5.5.3. Catalysis - standard procedures

#### Hydrogen Transfer:

A mixture of the ketone (2 mmol), KOH (10 mL, 0.2 M in *i*-PrOH), and catalyst (1 mL, 0.002 M in CH<sub>2</sub>Cl<sub>2</sub>) was refluxed. The reaction was monitored by <sup>1</sup>H NMR spectroscopy by introducing aliquots of the reacting solution in an NMR tube with 0.5 mL of CDCl<sub>3</sub>.

#### β-Alkylation of Secondary Alcohols with Primary Alcohols:

The reaction was carried out with a mixture of a secondary alcohol (1 mmol), a primary alcohol (1 mmol), 1 mol % of catalyst, and a base, KOH (1 mmol) in toluene (0.3 mL) at 110 °C. The reaction was monitored by <sup>1</sup>H NMR spectroscopy by introducing aliquots of the reacting solution inside an NMR tube with 0.5 mL of CDCl<sub>3</sub>.

#### N-Alkylation of Amines with Alcohols:

A mixture of the amine (2.0 mmol), alcohol (2.0 mmol), catalyst (0.75 mol %), toluene (0.3 mL), and KO<sup>t</sup>Bu (2.0 mmol) was placed in a Schlenk with a Teflon screw tap and the mixture was stirred and heated to 110 °C. The reaction was monitored by <sup>1</sup>H NMR spectroscopy by introducing aliquots of the reacting solution inside an NMR tube with 0.5 mL of CDCl<sub>3</sub>.

### 5.5.4. X-Ray diffraction studies

Single crystals of **10**, **12**, **13**, **14**, and **16** were mounted on a glass fiber in a random orientation. Data collection was performed at room temperature on a Siemens Smart CCD diffractometer using graphite monochromated Mo K $\alpha$  radiation ( $\lambda = 0.71073$  Å) with a nominal crystal to

detector distance of 4.0 cm. Space group assignment was based on systematic absences, E statistics and successful refinement of the structures. The structure was solved by direct methods with the aid of successive difference Fourier maps and were refined using the SHELXTL 6.1 software package.<sup>[40]</sup> All non-hydrogen were refined anisotropically, except C(5) and C(6) in compound **7**, that were refined isotropically. These two atoms are probably disordered and cause several problems in the refinement, like the fact that the distances around them, C(5)-C(6) and C(6)-C(15) are shorter than expected. Hydrogen atoms were assigned to ideal positions and refined using a riding model. The diffraction frames were integrated using the SAINT package.<sup>[41]</sup> Crystals from compound **16** diffracted very poorly. During the integration process, reflections showing negative intensities were omitted. Because of this, some reflections were missed and the completeness was lower than usual.

## 5.6. Acknowledgements

We wish to acknowledge M. C. Almeida and Dr. A. Coelho for providing data from the Elemental Analysis Services at ITQB. Dr. Cristian Vicent is acknowledge for providing data from Mass Spectrometry. The Bruker Avance III 400 MHz spectrometer is part of the National NMR Network and was purchased in the framework of the National Program for Scientific Re-equipment, contract REDE/1517/RMN/2005, with funds from POCI 2010 (FEDER) and Fundação para a Ciência e a Tecnologia (FCT).

## 5.7. References

- [1] An extensive work that start with this seminal communication: A. H. Janowicz, R. G. Bergman, *J. Am. Chem. Soc.* **1982**, *104*, 352.
- [2] R. G. Bergman, *Science* **1984**, *223*, 902.



- 
- [3] B. A. Arndtsen, R. G. Bergman, *Science* **1995**, *270*, 1970.
- [4] M. Prinz, M. Grosche, E. Herdtweck, W. A. Herrmann, *Organometallics* **2000**, *19*, 1692.
- [5] R. Corberán, M. Sanaú, E. Peris, *Organometallics* **2006**, *25*, 4002.
- [6] F. Hanasaka, Y. Tanabe, K. Fujita, R. Yamaguchi, *Organometallics* **2006**, *25*, 826.
- [7] R. Corberán, V. Lillo, J. A. Mata, E. Fernandez, E. Peris, *Organometallics* **2007**, *26*, 4350.
- [8] F. Hanasaka, K. I. Fujita, R. Yamaguchi, *Organometallics* **2004**, *23*, 1490.
- [9] F. Hanasaka, K. Fujita, R. Yamaguchi, *Organometallics* **2005**, *24*, 3422.
- [10] R. Corberán, M. Sanaú, E. Peris, *J. Am. Chem. Soc.* **2006**, *128*, 3974.
- [11] F. Hanasaka, K. Fujita, R. Yamaguchi, *Organometallics* **2006**, *25*, 4643.
- [12] R. Corberán, M. Sanaú, E. Peris, *Organometallics* **2007**, *26*, 3492.
- [13] A. C. Marr, C. L. Pollock, G. C. Saunders, *Organometallics* **2007**, *26*, 3283.
- [14] R. Corberán, E. Peris, *Organometallics* **2008**, *27*, 1954.
- [15] D. Gnanamgari, E. L. O. Sauer, N. D. Schley, C. Butler, C. D. Incarvito, R. H. Crabtree, *Organometallics* **2009**, *28*, 321.
- [16] A. Prades, R. Corberán, M. Poyatos, E. Peris, *Chem.-Eur. J.* **2008**, *14*, 11474.
- [17] Y. Tanabe, F. Hanasaka, K. Fujita, R. Yamaguchi, *Organometallics* **2007**, *26*, 4618.
- [18] A. Zanardi, R. Corberán, J. A. Mata, E. Peris, *Organometallics* **2008**, *27*, 3570.
- [19] A. Zanardi, J. A. Mata, E. Peris, *J. Am. Chem. Soc.* **2009**, *131*, 14531.
- [20] A. Zanardi, J. A. Mata, E. Peris, *Chem.-Eur. J.* **2010**, *16*, 10502.
- [21] A. Zanardi, J. A. Mata, E. Peris, *Chem.-Eur. J.* **2010**, *16*, 13109.
-

- [22] S. McGrandle, G. C. Saunders, *J. Fluorine Chem.* **2005**, *126*, 451.
- [23] X. Wang, S. Liu, L. H. Weng, G. X. Jin, *Chem.-Eur. J.* **2007**, *13*, 188.
- [24] X. Q. Xiao, G. X. Jin, *J. Organomet. Chem.* **2008**, *693*, 316.
- [25] X. Q. Xiao, Y. J. Lin, G. X. Jin, *Dalton Trans.* **2008**, 2615.
- [26] S. P. Downing, P. J. Pogorzelec, A. A. Danopoulos, D. J. Cole-Hamilton, *Eur. J. Inorg. Chem.* **2009**, 1816.
- [27] R. H. Crabtree, *The Organometallic Chemistry of the Transition Metals*, 5th ed., John Wiley & Sons, Inc, **2009**.
- [28] T. D. Nixon, M. K. Whittlesey, J. M. J. Williams, *Dalton Trans.* **2009**, 753.
- [29] G. Guillena, D. J. Ramon, M. Yus, *Angew. Chem. Int. Ed.* **2007**, *46*, 2358.
- [30] K. Fujita, C. Asai, T. Yamaguchi, F. Hanasaka, R. Yamaguchi, *Org. Lett.* **2005**, *7*, 4017.
- [31] G. Guillena, D. J. Ramon, M. Yus, *Chem. Rev.* **2010**, *110*, 1611.
- [32] A. Tillack, D. Hollmann, D. Michalik, M. Beller, *Tetrahedron Lett.* **2006**, *47*, 8881.
- [33] M. H. S. A. Hamid, J. M. J. Williams, *Chem. Commun.* **2007**, 725.
- [34] K. Fujita, Z. Z. Li, N. Ozeki, R. Yamaguchi, *Tetrahedron Lett.* **2003**, *44*, 2687.
- [35] K. I. Fujita, T. Fujii, R. Yamaguchi, *Org. Lett.* **2004**, *6*, 3525.
- [36] G. E. Dobereiner, R. H. Crabtree, *Chem. Rev.* **2010**, *110*, 681.
- [37] R. Yamaguchi, K. Fujita, M. W. Zhu, *Heterocycles* **2010**, *81*, 1093.
- [38] Y. Lin, K. Nomiya, R. G. Finke, *Inorg. Chem.* **1993**, *32*, 6040.
- [39] G. Giordano, R. H. Crabtree, *Inorg. Syn.* **1990**, *28*, 88.
- [40] G. M. Sheldrick, SHELXTL, version 6.1, Bruker AXS, Inc., Madison, WI, 2000.
- [41] SAINT, Bruker Analytical X-ray System, version 5.0, Madison, WI, 1998.

## 5.8. Supporting Information

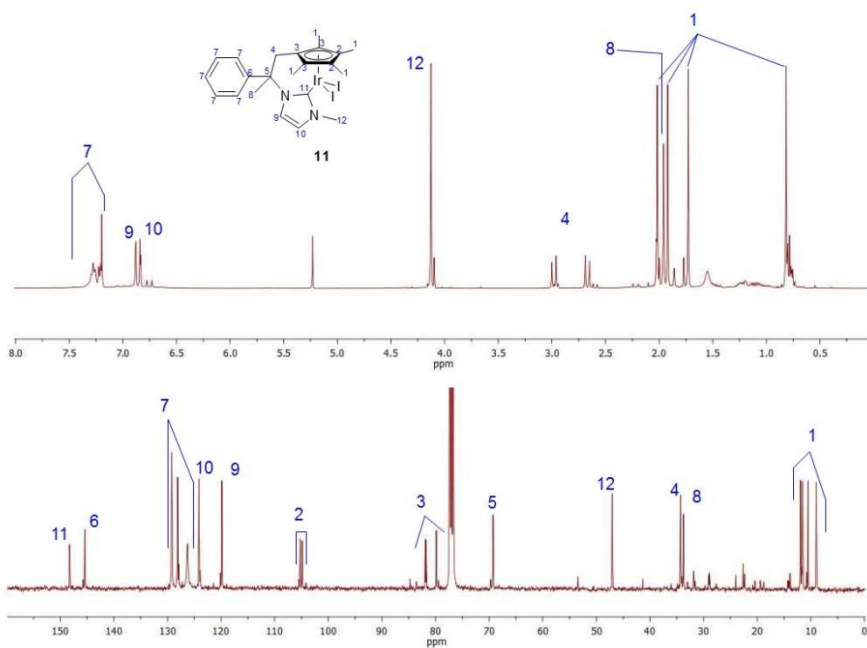


Figure 5.11.  $^1\text{H}$  NMR and  $\{^1\text{H}\}^{13}\text{C}$  NMR spectra of complex 11 (400 MHz,  $\text{CDCl}_3$ , 300K).

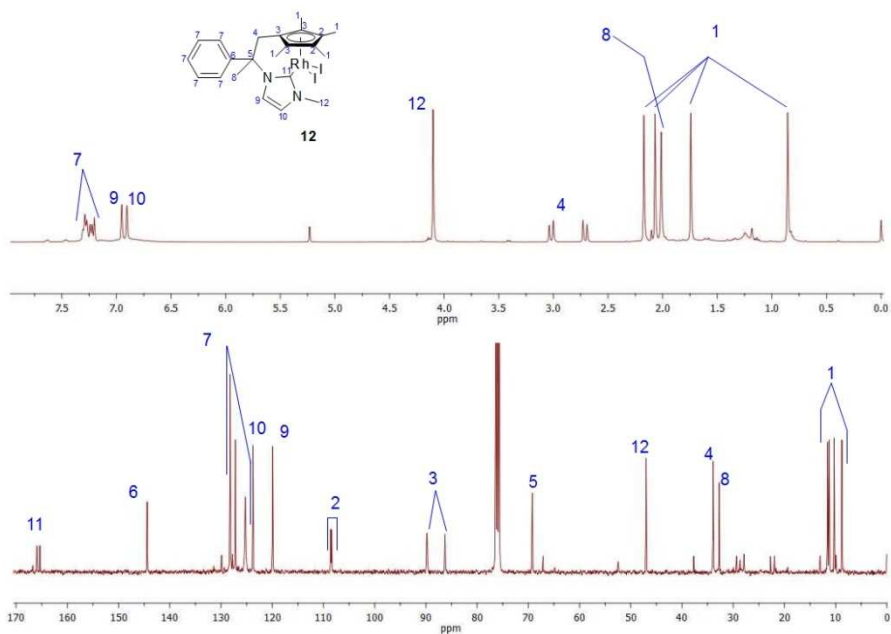
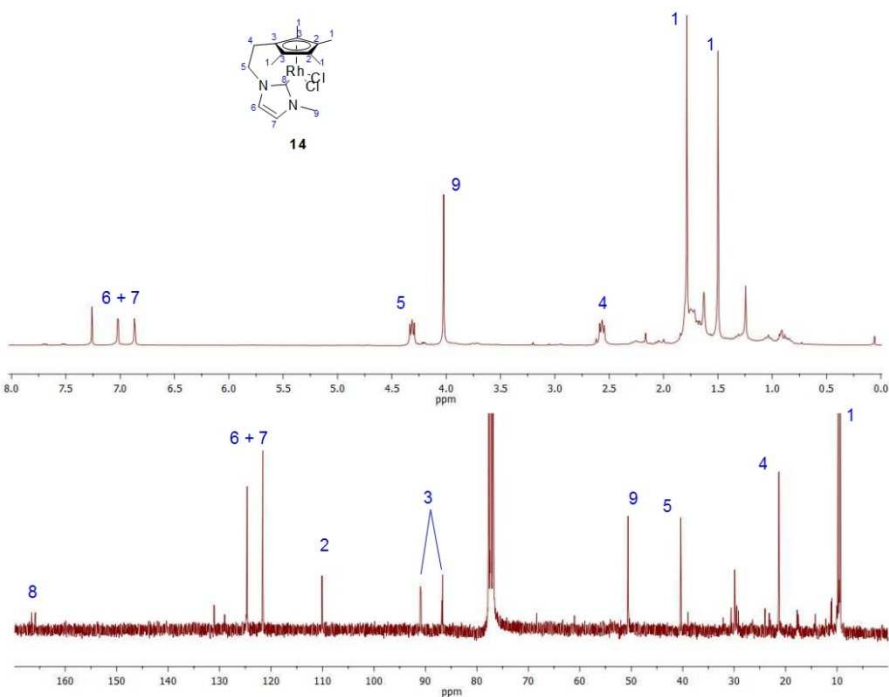
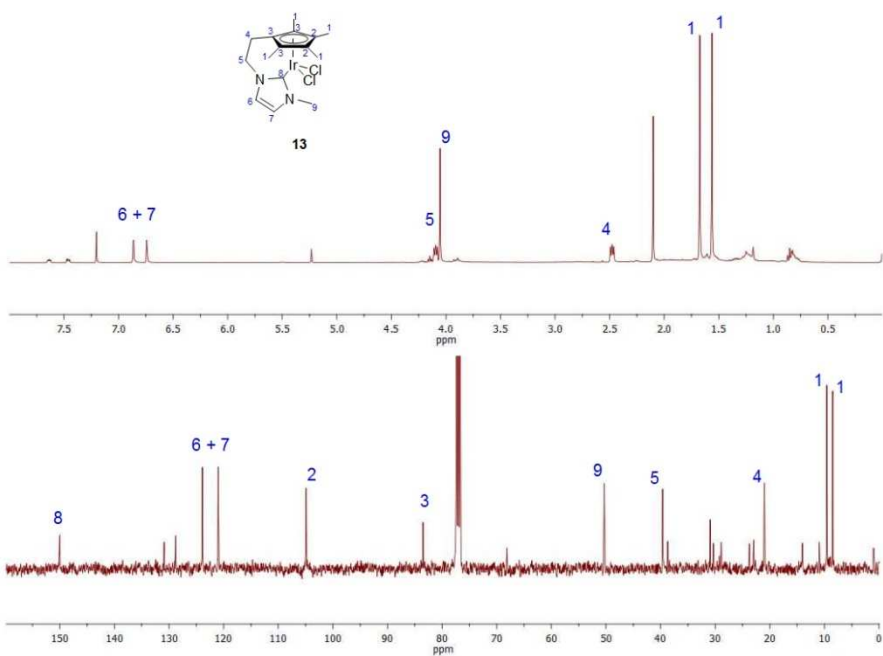


Figure 5.12.  $^1\text{H}$  NMR and  $\{^1\text{H}\}^{13}\text{C}$  NMR spectra of complex 12 (400 MHz,  $\text{CDCl}_3$ , 300K).

Cyclopentadienyl-Functionalised N-Heterocyclic Carbenes:  
Synthesis, Coordination to Mo, Ru, Rh and Ir and Catalytic Applications.



---

# 6. COORDINATION TO Ru, RESOLUTION OF CHIRAL-AT-METAL COMPLEXES AND ISOMERISATION OF ALLYLIC ALCOHOLS

---

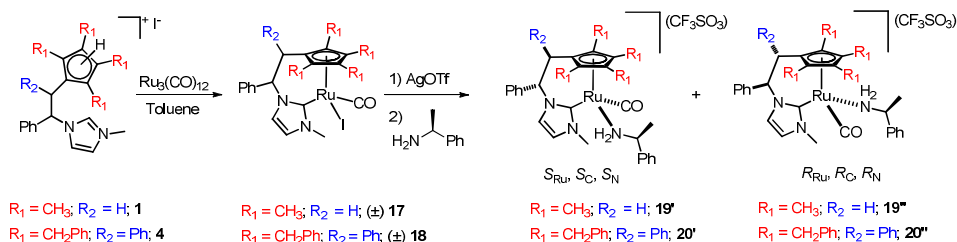
|      |  |     |
|------|--|-----|
| 6.1. | Abstract   | 95  |
| 6.2. | Introduction   | 96  |
| 6.3. | Results and discussion                                       | 97  |
|      | 6.3.1. Synthesis of ruthenium complexes,                     | 97  |
|      | 6.3.2. Characterisation of <b>17</b> and <b>18</b> ,         | 98  |
|      | 6.3.3. Enantiomeric resolution of chiral-at-metal complexes, | 102 |
|      | 6.3.4. Catalysis,  | 104 |
| 6.4. | Conclusions  | 107 |
| 6.5. | Experimental procedures                                      | 108 |
|      | 6.5.1. Materials and methods,                                | 108 |
|      | 6.5.2. Synthesis and characterisation,                       | 109 |
|      | 6.5.3. X-Ray diffraction studies,                            | 113 |
| 6.6. | Acknowledgments  | 113 |
| 6.7. | References   | 113 |
| 6.8. | Supporting information                                       | 115 |

Cyclopentadienyl-Functionalised N-Heterocyclic Carbenes:  
Synthesis, Coordination to Mo, Ru, Rh and Ir and Catalytic Applications.

---

## 6.1. Abstract

This chapter describes the diastereoselective synthesis of  $(\text{Cp}^*\text{-NHC})\text{Ru}(\text{CO})\text{I}$  (**17**) and  $(\text{Cp}^{\text{Bz}}\text{-NHC})\text{Ru}(\text{CO})\text{I}$  (**18**). The resolution of the enantiomers is achieved by derivatization with (*S*)-1-phenylethylamine, as depicted in Scheme 6.1.



**Scheme 6.1.** Synthesis of  $(\text{Cp}^{\text{X}}\text{-NHC})\text{Ru}(\text{CO})\text{I}$  and  $[(\text{Cp}^{\text{X}}\text{-NHC})\text{Ru}(\text{CO})(\text{S}-\text{PhCH}(\text{NH}_2)\text{CH}_3)]\text{OTf}$  complexes.

The ruthenium complexes **17** and **18** were prepared by direct reaction of the pro-ligands  $[\text{Cp}^{\text{X}}\text{-NHC}]\text{I}$  **1** and **4** with  $\text{Ru}_3(\text{CO})_{12}$  in refluxing toluene. Both complexes were fully characterised by NMR and IR spectroscopy, HR-MS spectrometry and X-ray diffraction studies.

The reaction of a racemic mixture of  $(\text{Cp}^{\text{X}}\text{-NHC})\text{Ru}(\text{CO})\text{I}$  (**17** or **18**) with silver triflate and (*S*)-1-phenylethylamine yielded two diastereoisomers that were separated by preparative thin layer chromatography in low yields (**19'** + **19''** ~32% and **20'** + **20''** ~25%). The cationic complexes were characterised by NMR and IR spectroscopy and HR-MS spectrometry, although we were unable to determine the absolute configuration of each of the isolated complexes.

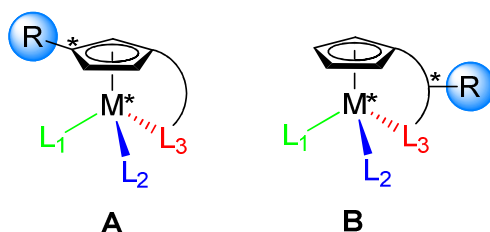
Preliminary studies showed that  $(\text{Cp}^*\text{-NHC})\text{Ru}(\text{CO})\text{I}$  (**17**) is an efficient catalyst in the isomerisation of allylic alcohols to ketones, both in water and in THF.

The work in this chapter was entirely performed by the candidate except for the X-ray diffraction studies, which were carried out by Gabriel Peris and Dr. José A. Mata.

## 6.2. Introduction

Some of the reasons that may justify the rich chemistry of ruthenium are its ability to afford a wide range of stable oxidation states and coordination geometries, and also to provide electronically unsaturated species. These properties have turned this metal into one of the richest sources of catalysts for a wide variety of organic transformations.<sup>[1-3]</sup> Among Ru-complexes those containing the cyclopentadienyl-type ligands have constituted an interesting class of complexes because they can provide 16-electron species that can have important catalytic applications.

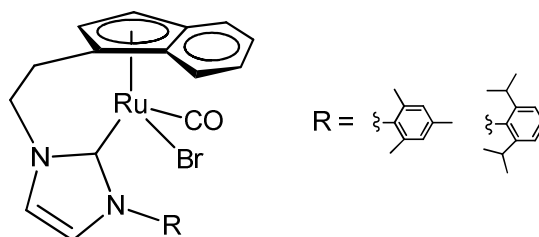
We were very interested in obtaining a family of Ru-chiral catalysts that were applicable to asymmetric catalysis. Half sandwich complexes offer a very good opportunity to design chiral-at-metal compounds of this metal.<sup>[4-6]</sup> In fact, many chiral-at-metal species are based on half-sandwich metal complexes.<sup>[7-9]</sup> Particularly, the use of chiral Cp ligands with tethered phosphines has proven to be a successful approach for controlling the metal configuration.<sup>[8]</sup> The configurational stability resulting from the introduction of the anchoring functionality, allows for the preparation of diastereomeric species, as shown in Figure 6.1. The punctual chirality at the metal centre can be controlled by introduction of a planar chiral Cp ring (**A** in Figure 6.1) or by introduction of an additional chiral centre at the bridge (**B** in Figure 6.1).



**Figure 6.1.** Possible topologies for diastereomeric half-sandwich complexes.



While half-sandwich Ru(II) complexes with tethered phosphines are quite well studied,<sup>[8]</sup> their NHC analogs are almost unexplored. In fact, only two examples of complexes containing the fragment “(Cp'-NHC)Ru” have been reported in the literature (Figure 6.2). The indenyl-functionalised NHC complexes were obtained in residual yield by reaction of the corresponding imidazolium salt with Ru<sub>3</sub>(CO)<sub>12</sub> in refluxing toluene. However, the chelating ligands used were achiral and no studies were made concerning the formation of diastomeric complexes or isolation of enantiomerically pure chiral-at-metal complexes.<sup>[10]</sup>



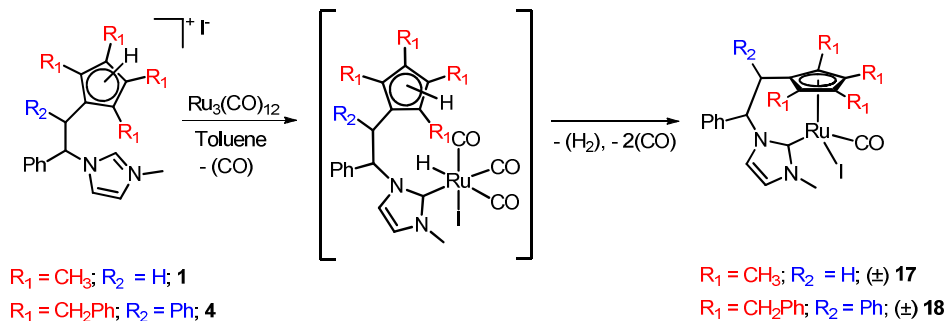
**Figure 6.2.** “(Ind-NHC)Ru” complexes reported in the literature.<sup>[10]</sup>

Half-sandwich complexes containing the fragment “Cp’Ru(NHC)” are scarce, with only an handful of examples reported<sup>[11-18]</sup> despite their catalytic efficiency in alkyne dimerisation,<sup>[11]</sup> racemisation of alcohols,<sup>[14-15]</sup> hydrogenation of ketones, esters, epoxides and imines,<sup>[17]</sup> and transfer hydrogenation of ketones.<sup>[18]</sup>

## 6.3. Results and discussion

### 6.3.1. Synthesis of ruthenium complexes

The direct reaction of the (Cp\*-NHC)I and (Cp<sup>Bz</sup>-NHC)I imidazolium proligands **1** and **4** with Ru<sub>3</sub>(CO)<sub>12</sub> in refluxing toluene, afforded the corresponding ruthenium complexes **17** and **18**, respectively, in good yields (65-70%), as depicted in Scheme 6.2.



**Scheme 6.2.** Synthesis of  $(\text{Cp}^x\text{-NHC})\text{Ru}(\text{CO})\text{I}$  complexes **17** and **18**.

The coordination of the ligand may be a consequence of the oxidative addition of the C-H bond of the imidazolium to the Ru(0), followed by reductive elimination of hydrogen from the Ru-H and a proton from the cyclopentadiene group, that coordinates to the metal as a cyclopentadienyl. This mechanism was previously suggested by Wang and co-workers for the coordination of an indenyl-functionalized NHC,<sup>[10]</sup> but in that case the yields of the reaction products were very low.

The presence of the stereogenic center at the aliphatic linker between the NHC and Cp ring and at the metal centre, suggested that four stereoisomers (two diastereomers) should be expected. However, the NMR characterisation of the products revealed that only one diastereomer had been formed as a racemic mixture of the two possible enantiomers.

### 6.3.2. Characterisation of **17** and **18**

Complexes **17** and **18** were characterised by IR, <sup>1</sup>H and <sup>13</sup>C NMR spectroscopy, MS spectrometry and X-ray diffraction studies. The selected spectroscopy data is depicted in Table 6.1.

The IR spectra of **17** and **18** show the CO stretching bands at 1910 (**17**) and 1923  $\text{cm}^{-1}$  (**18**), which suggest the higher electron-donating character of the  $\text{Cp}^x\text{-NHC}$  ligand compared to the  $\text{Cp}^{\text{Bz}}\text{-NHC}$

one. The same trend was found for the related molybdenum<sup>[19]</sup> (discussed in chapter 3) and iron<sup>[20]</sup> complexes.

**Table 6.1.** Selected IR frequencies, <sup>1</sup>H and <sup>13</sup>C NMR chemical shifts of complexes **17** and **18**.

|           | IR <sup>a</sup>                       | <sup>1</sup> H NMR <sup>b</sup> | <sup>13</sup> C NMR <sup>c</sup> |     |
|-----------|---------------------------------------|---------------------------------|----------------------------------|-----|
|           | $\nu_{\text{CO}}$ (cm <sup>-1</sup> ) | N-CH <sub>3</sub>               | C <sub>NHC</sub>                 | CO  |
| <b>17</b> | 1910                                  | 3.75                            | 184                              | 209 |
| <b>18</b> | 1923                                  | 3.83                            | 182                              | 208 |

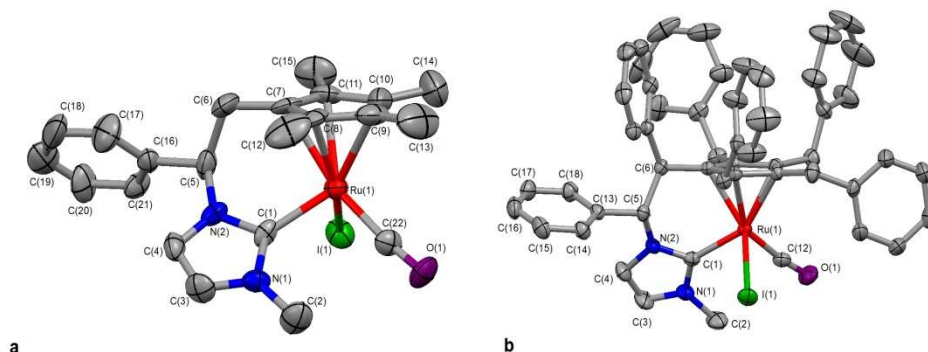
<sup>a</sup> in KBr pellets. <sup>b</sup> in CDCl<sub>3</sub>, 300 MHz, 300 K. <sup>c</sup> in CDCl<sub>3</sub>, 125 MHz, 300 K. All chemical shifts reported in ppm.

NMR spectroscopy allows the confirmation that both reactions leading to **17** and **18** are diastereoselective. In order to confirm that only one of the diastereomers was formed, we performed the NMR spectrum of the species in different solvents, and VT NMR experiments were, so that we could discard the existence of a dynamic equilibrium for the interconversion of the two possible diastereomers.<sup>[21]</sup> The <sup>1</sup>H NMR spectrum of **17** shows two doublets at 6.68 and 6.25 ppm, due to the protons of the imidazolylidene ring. The four methyl groups of the cyclopentadienyl ring display four signals at 2.29, 2.02, 1.96 and 1.47 ppm, as a consequence of the asymmetry of the molecule. The <sup>13</sup>C NMR confirms the coordination of both the Cp\* and NHC fragments of the ligand, with a signal at 184.1 ppm attributed to the Ru-C<sub>carbene</sub> and five distinctive signals due to the Cp ring. The <sup>1</sup>H NMR spectrum of **18** shows the signals due to the protons of the imidazolylidene ring at 6.63 and 5.90 ppm. The two protons at the aliphatic C<sub>2</sub> linker between the Cp and NHC rings appear as two doublets at 3.56 and 3.40 ppm, with the characteristic  $J_{\text{H-H}}$  value of a relative *anti* disposition (16 Hz). The <sup>13</sup>C NMR spectrum shows the signal due to the Ru-C<sub>carbene</sub> carbon at 182.2 ppm.

The molecular structure of complexes **17** and **18** were confirmed by means of X-ray diffraction studies. Table 6.2 shows the selected bond distances and angles, and the molecular diagrams of the ruthenium complexes are depicted in Figure 6.3. The crystals of both compounds contained a racemic mixture of the two enantiomers.

**Table 6.2.** Selected distances and angles of complexes **17** and **18**.

|               | <b>17</b>                | <b>18</b>  |
|---------------|--------------------------|------------|
| distances (Å) | M-C <sub>NHC</sub>       | 2.05(12)   |
|               | M-Cp <sub>centroid</sub> | 1.877      |
|               | M-I                      | 2.7377(13) |
|               | M-CO                     | 1.863(13)  |
| Angles (deg)  | C <sub>NHC</sub> ^M^I    | 92.2(3)    |
|               | I^M^CO                   | 90.0(4)    |
|               | CO^M^C <sub>NHC</sub>    | 99.8(5)    |



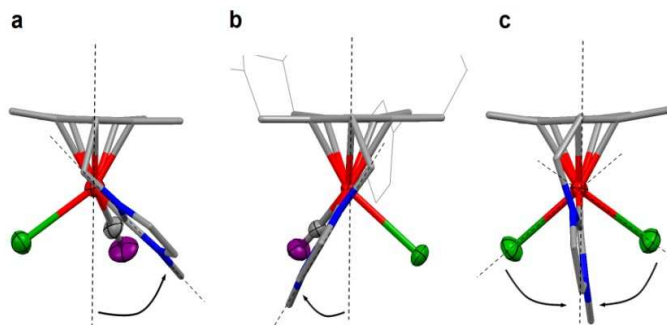
**Figure 6.3.** Molecular diagrams of complexes **17** and **18**.

The molecular diagrams of **17** and **18** show similar half-sandwich structures. Apart from the chelating ligand, one iodide, and one CO ligand complete the coordination sphere about the metal centre. The M-C<sub>NHC</sub> (~2.05 Å for both complexes) and M-Cp<sub>centroid</sub> (1.877 for **17** and 1.858 for **18**) distances are in the expected range for half-sandwich ruthenium complexes and compare well with the distances reported for

$\text{Cp}^*\text{Ru}(\text{NHC})(\text{CO})\text{Cl}$  (NHC = 1,3-dicyclohexylimidazolylidene).<sup>[22]</sup> The angles between the legs of the piano stools suggest a pseudo-octahedral geometry.

The molecular structures of these two molecules provide a suitable explanation for the diastereoselectivity of the reactions. Figure 6.4 shows a schematic view of complexes **17** and **18**.

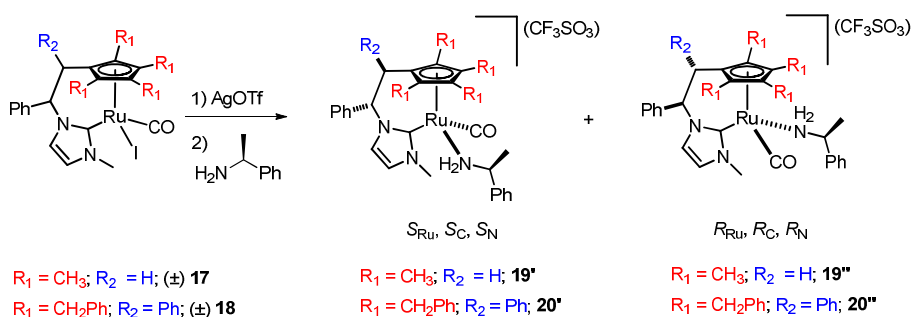
As seen in Figure 6.4, in complexes **17** and **18** the CO ligand and azole ring are on the same side of the molecule adopting an eclipsed conformation. The deviation from an ideal parallel alignment of the azole plane and the vertical axis is forced by the asymmetry of the ethylene linker between the azole and the cyclopentadienyl functionalities. As can be seen, this deviation locates the N-methyl groups of both **17** and **18** close to the carbonyl groups, avoiding the more bulky iodide ligand. The other diastereomers (not observed and not depicted in Figure 6.3) would consist of the reverse situation in which the N-methyl group is close to the iodine, affording a sterically strained situation. This is a result of the higher steric hindering caused by the iodide ligand compared to the CO. In other complexes not showing a chiral-at-metal situation (for example complex **10**), the NHC ligand adopts a staggered conformation closely parallel to the  $\text{M}-\text{Cp}_{\text{centroid}}$  axis, as a result of the similar steric hindering by the iodide ligands.



**Figure 6.4.** Deviation from an ideal parallel alignment of the azole plane and the vertical axis in complexes (a) **17** and (b) **18** compared to (c) complex **10**. Some atoms were removed for clarity.

### 6.3.3. Enantiomeric resolution of chiral-at-metal complexes

We envisioned that the coordination of a enantiomerically pure chiral amine to the ruthenium complexes **17** and **18** should allow the formation of the corresponding two separable diastereoisomers. The reaction proceeded as shown in Scheme 6.3, with the addition of  $\text{Ag}(\text{O}_3\text{SCF}_3)$  for the removal of the iodide prior to the addition of the (*S*)-1-phenylethylamine.



**Scheme 6.3.** Preparation of organometallic salts **19** and **20**.

For each complex (**17** and **18**) the reaction afforded a mixture of four diastereoisomers at room temperature, which converted to only two diastereoisomers after heating at 70°C (0.5 – 1h). The diastereoisomers of **19** and **20** were successfully separated by preparative thin-layer chromatography. Although analysis of the crude product by NMR suggested quantitative yield, low yields were isolated after chromatography. Unfortunately, we were unable to obtain crystals suitable for X-ray diffraction studies, thus the determination of the absolute configuration of each complex was not possible. However, it is reasonable to assume that the (*S*)-1-phenylethylamine ligand occupies the least hindered coordination vacant in the organometallic complex. Since we were unable to assign the absolute configuration, the isolated complexes will be referred as **19A**, **19B**, **20A** and **20B**. Therefore **19A**

and **19B** correspond to either **19**-( $R_{Ru}, R_C, S_N$ ) or **19**-( $S_{Ru}, S_C, S_N$ ), and **20A** and **20B** correspond to either **20**-( $R_{Ru}, R_C, S_N$ ) or **20**-( $S_{Ru}, S_C, S_N$ ).

The enantiomerically pure complexes **19A**, **19B**, **20A** and **20B** were characterised by means of IR, NMR and ESI-MS. The selected spectroscopic data is summarised in Table 6.3.

**Table 6.3.** Selected IR frequencies,  $^1\text{H}$  and  $^{13}\text{C}$  NMR chemical shifts of complexes **19** and **20**.

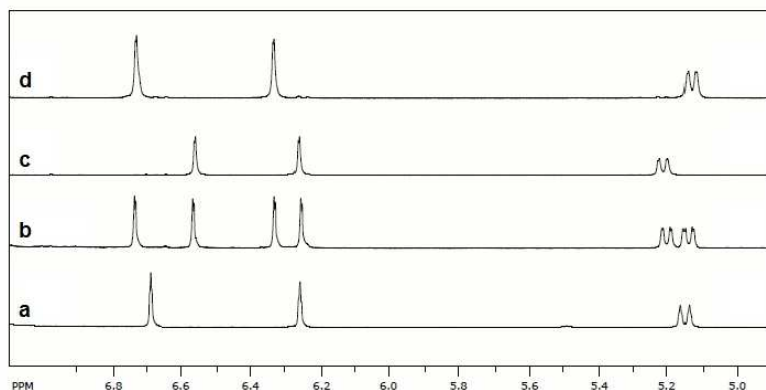
|             | IR <sup>a</sup>                        | $^1\text{H}$ NMR <sup>b</sup> | $^{13}\text{C}$ NMR <sup>c</sup> |     |
|-------------|--|-------------------------------|----------------------------------|-----|
|             | $\nu_{\text{CO}}$ ( $\text{cm}^{-1}$ ) | N-CH <sub>3</sub>             | C <sub>NHC</sub>                 | CO  |
| <b>19 A</b> | 1918                                   | 3.20                          | 180                              | 208 |
| <b>19 B</b> | 1919                                   | 3.63                          | 180                              | 210 |
| <b>20 A</b> | 1925                                   | 3.04                          | 180                              | 210 |
| <b>20 B</b> | 1924                                   | 3.75                          | 181                              | 210 |

<sup>a</sup> in KBr pellets. <sup>b</sup> in  $\text{CDCl}_3$ , 500 MHz, 300 K. <sup>c</sup> in  $\text{CDCl}_3$ , 125 MHz, 300 K. All chemical shifts reported in ppm.

Following the same trend as the neutral complexes **17** and **18**, the IR spectra of the cationic complexes **19** and **20** suggest a higher electron-donor character of the Cp\* ring than the Cp<sup>Bz</sup>, as shown by the IR stretching frequencies of the carbonyl ligands at 1918 (**19A**), 1919 (**19B**), 1925 (**20A**) and 1924 (**20B**)  $\text{cm}^{-1}$ .

Figure 6.5 shows the region of the imidazolyliene and the CHPh protons of  $^1\text{H}$  NMR spectra of compound **17** before (**a**) and after (**b**) addition of the chiral amine, and after purification of both enantiomers (**c** and **d**). We characterised both species by NMR spectroscopy and mass spectrometry. The  $^1\text{H}$  NMR spectrum of **19A** show the signals due to the protons of the imidazolyliene at 6.52 and 6.26 ppm (6.73 and 6.33 ppm in **19B**). The characteristic doublet of doublets assigned to the CHPh proton of the Cp\*-NHC linker appears at 5.21 ppm (5.13 ppm in **19B**). The  $^{13}\text{C}$  NMR spectrum of **19A** shows the characteristic signals due to

the carbonyl group at 208.2 ppm (209.7 ppm in **19B**) and to the Ru- $C_{\text{carbene}}$  at 179.5 ppm (180.3 ppm in **19B**).



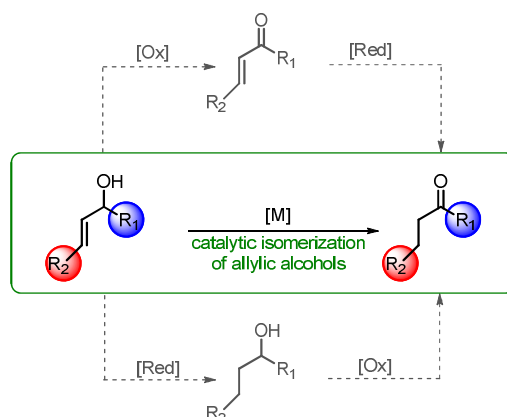
**Figure 6.5.** Region of the imidazolyliene and  $CHPh$  protons of the  $^1H$  NMR spectra of: a) **17**, b) **19A** and **19B**, and c) **19A**, d) **19B**. The definitive assignment has not been made, therefore **19A** and **19B** correspond to either **19**-( $R_{Ru}, R_C, S_N$ ) or **19**-( $S_{Ru}, S_C, S_N$ ).

The  $^1H$  NMR spectra of **20A** and **20B** show the signals due to the N-methyl groups at the imidazole rings at 3.04 (**20A**) and 3.75 ppm (**20B**). The signals due to the imidazolyliene protons appear at 6.67 and 6.42 ppm (**20A**) and 6.51 and 6.38 ppm (**20B**). Each isomer displays eight distinctive doublets attributed to the diastereotopic methylene protons at the four benzyl groups, between 4.2 and 3.1 ppm. The  $^{13}C$  NMR spectra show the signals due to the carbonyl groups at 209.7 (**20A**) and 209.6 ppm (**20B**), and to the metalated Ru- $C_{\text{carbene}}$  carbons at 180.2 (**6A**) and 181.2 ppm (**20B**).

#### 6.3.4. Catalysis

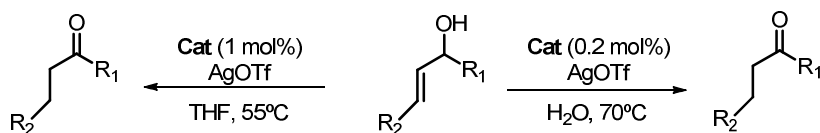
The catalytic isomerisation of allylic alcohols allows the direct preparation of the corresponding carbonyl compounds, thus simplifying the conventional two-step organic procedures (Scheme 6.4).





**Scheme 6.4.** Catalytic isomerisation of allylic alcohols *versus* conventional two-step organic procedures.

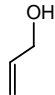
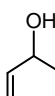

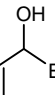
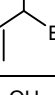
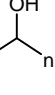
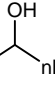
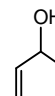
We thought that **17** and **18** may possess the structural and electronic requirements to be efficient catalysts for this reaction. The reactions were carried out using a catalyst loading of 1 or 0.2 mol %. Prior to the addition of the substrates, compounds **17** and **18** were dissolved in the reaction solvent (THF or H<sub>2</sub>O) together with 3 equiv of AgOTf as halide abstractor, in order to activate the catalysts (Scheme 6.5). Also, it is noteworthy that the addition of AgOTf facilitates the solubility of the two compounds in H<sub>2</sub>O, probably via the formation of the corresponding [(Cp'-NHC)Ru(CO)(H<sub>2</sub>O)](OTf) species.



**Scheme 6.5.** Catalytic isomerisation of allylic alcohols, Cat = **17** or **18**.

As seen in Table 6.1, complex **17** is far more active than complex **18**. This fact might be a consequence of the more electron rich character of the cyclopentadienyl ring and less sterically hindered environment surrounding the metal centre in complex **17** when compared to complex **18**.

**Table 6.4.** Catalytic isomerisation of allylic alcohols.<sup>a</sup>

| Entry | Substrat  | Cat. <sup>b</sup> | Cat. Load (mol%) | Solv             | T (°C) | t (h) | Yield (%) <sup>c</sup> |
|-------|---|-------------------|------------------|------------------|--------|-------|------------------------|
| 1     |    | <b>17</b>         | 1                | THF              | 55     | 1     | 99                     |
| 2     |   | <b>17</b>         | 0.2              | H <sub>2</sub> O | 75     | 2     | 99                     |
| 3     |    | <b>17</b>         | 1                | THF              | rt     | 6     | 99                     |
| 4     |   | <b>17</b>         | 1                | THF              | 55     | 3     | 99                     |
| 5     |    | <b>17</b>         | 1                | THF              | 75     | 0.33  | 99                     |
| 6     |   | <b>18</b>         | 1                | THF              | 55     | 24    | 20                     |
| 7     |    | <b>17</b>         | 0.2              | H <sub>2</sub> O | 75     | 4     | 99                     |
| 8     |    | <b>17</b>         | 1                | THF              | 55     | 3     | 99                     |
| 9     |   | <b>18</b>         | 1                | THF              | 55     | 24    | 25                     |
| 10    |    | <b>17</b>         | 0.2              | H <sub>2</sub> O | 75     | 4     | 99                     |
| 11    |   | <b>17</b>         | 0.2              | H <sub>2</sub> O | 75     | 4     | 99                     |
| 12    |   | <b>17</b>         | 0.2              | H <sub>2</sub> O | 75     | 24    | 20                     |
| 13    |  | <b>17</b>         | 1                | THF              | 55     | 24    | 60                     |

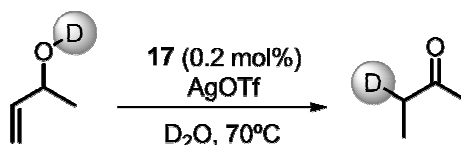
<sup>a</sup> Reactions carried out with 0.4 mmol of substrate in 0.5 mL of THF or 4 mL H<sub>2</sub>O. <sup>b</sup> Activated by Ag(O<sub>3</sub>SCF<sub>3</sub>), 10 min at rt. <sup>c</sup> Yield determined by <sup>1</sup>H NMR.

Remarkably, in contrast with other known ruthenium catalysts,<sup>[23-25]</sup> **17** does not need the addition of base in order to perform good activities, thus simplifying the reaction procedure and widening its scope to aldehydes and base-sensitive ketones. The activity of the catalyst in H<sub>2</sub>O was high, although we needed to increase the temperature to 75°C (reactions in THF are performed at 55°C), for which full conversions were achieved even with catalyst loadings as low as 0.2 mol % (entries 2, 7, 10, 11 and 12). Changes in the alkyl chain of the alcohol functionality do

not influence the overall performance of the catalyst (compare entries 4, 8, 7 and 10, 11). However, terminal allyl groups react much faster than internal groups, (entries 2, 12, and 4 and 13).

In a parallel experiment, the catalytic isomerisation of 3-buten-2-ol was performed in deuterated water. Under these reaction conditions, the acidic OH functionality immediately exchanges to OD.

The monitoring of the reaction of isomerisation of 1-buten-3-ol in  $D_2O$  and  $H_2O$ , shows that both reactions occur at the same reaction rates, which indicates that the isotopic effect is negligible ( $k_D/k_H \approx 1$ ). This observation is also supporting the idea that the activation of the OH bond does not play a role in the catalytic cycle, thus strengthening the idea of the out-of-cycle tautomerisation. Moreover, this experiment allowed for the preparation of the quantitatively mono-deuterated ketone, 2-butanone-3-*d* (Scheme 6.6).



**Scheme 6.6.** Catalytic isomerisation of 3-buten-2-ol in  $D_2O$ .

## 6.4. Conclusions

In this chapter we have described the convenient synthesis of two ruthenium complexes with Cp-functionalised N-heterocyclic carbenes. The synthetic procedure consists of the direct reaction of the corresponding imidazolium Cp-NHC proligands, and  $[Ru_3(CO)_{12}]$ , which affords the diastereoselective formation of the reaction products in high yield. The coordination of the ligand may be a consequence of the oxidative addition of the C-H bond of the imidazolium to the  $Ru(0)$ , followed by reductive elimination of hydrogen from the  $Ru-H$  and a proton

from the cyclopentadiene group, that coordinates to the metal as a cyclopentadienyl.

The two compounds obtained have been fully characterised, both by spectroscopic techniques and by X-ray diffraction. Interestingly, both species present stereogenic centres at the metal and at the linker between the azole and the cyclopentadienyl rings. The diastereomeric resolution of the two enantiomers has been performed by addition of an enantiomerically pure chiral amine, thus allowing the NMR detection of the mixture of the two enantiomers. The separation of the enantiomers has been made by preparative thin-layer chromatography, allowing the spectroscopic characterisation of each enantiomerically pure chiral complex.

Compounds **17** and **18** have been tested in the catalytic isomerisation of allylic alcohols. The more sterically crowded complex, **18**, shows very low activity, while **17** is very active in THF and H<sub>2</sub>O. The isomerisation of a O-deuterated allylic alcohol, provides the corresponding ketone with the deuterium at the  $\alpha$ -carbon, supporting the idea that the reaction proceeds by an intramolecular mechanism. The negligible isotopic effect ( $k_D/k_H \approx 1$ ) is in accordance with the previously reported mechanistic studies that suggest that the reaction proceeds through the catalytic isomerisation of the allylic alcohol to an enol, followed by an out-of-cycle tautomerisation to the ketone. Although we did not explore this any further, this might be an easy method for the preparation of ketones mono-deuterated in the  $\alpha$  position.

## 6.5. Experimental procedures

### 6.5.1. Materials and methods

All reactions were carried out under inert atmosphere. When required, solvents were dried via standard techniques. The ligands were

synthesised as previously mentioned in chapter 3. All other reagents are commercially available and were used as received. NMR spectra were recorded on Varian Innova 300 MHz and 500 MHz spectrometers with  $\text{CDCl}_3$  (Cambridge Isotope Laboratories, Inc.) as solvent. Electrospray mass spectra (ESI-MS) were recorded on a Micromass Quattro LC instrument. A QTOF I (quadrupole-hexapole-TOF) mass spectrometer with an orthogonal Z-spray-electrospray interface (Micromass, Manchester, UK) was used for high resolution mass spectrometry (HRMS). The drying gas as well as nebulising gas was nitrogen at a flow of 400L/h and 80 L/h respectively.

### 6.5.2. Synthesis and characterisation

#### Synthesis of ruthenium complexes—general procedure

A suspension of the imidazolium salt (3 equivalents) and  $\text{Ru}_3(\text{CO})_{12}$  (1 equivalent) was refluxed in toluene overnight. The resulting red suspension was evaporated to dryness and purified by column chromatography ( $\text{CH}_2\text{Cl}_2/\text{Acetone}$ ) yielding the desired ruthenium(II) complex.

#### Complex 17

Yield: 57%.  $^1\text{H}$  NMR (500 MHz,  $\text{CDCl}_3$ ):  $\delta$  7.46 (m, 5H), 6.68 (d,  $J=2.1\text{Hz}$ , 1H), 6.25 (d,  $J=2.1\text{Hz}$ , 1H), 5.15 (dd,  $J=2.7\text{Hz}$   $J=11.4\text{Hz}$ , 1H), 3.75 (s, 3H), 2.76 (m, 2H), 2.29 (s, 3H), 2.02 (s, 3H), 1.96 (s, 3H), 1.47 (s, 3H).  $\{^1\text{H}\}$   $^{13}\text{C}$  NMR ( $\text{CDCl}_3$ , 125 MHz):  $\delta$  209.1, 184.1, 137.8, 129.4, 129.0, 121.6, 119.6, 104.4, 99.1, 95.1, 89.8, 83.2, 67.7, 39.8, 29.1, 11.9, 11.1, 10.97, 10.52. MS (ESI):  $m/z$ :  $[M-I]^+$  calcd for  $\text{C}_{22}\text{H}_{25}\text{N}_2\text{ORu}$ : 435.1, found: 435.0,  $[M+\text{Na}]^+$  calcd for  $\text{C}_{22}\text{H}_{25}\text{N}_2\text{NaORu}$ : 585.0, found: 484.9. HRMS (ESI-TOF):  $m/z$ :  $[M]^+$  calcd for  $\text{C}_{22}\text{H}_{25}\text{N}_2\text{ORu}$ : 435.1017, found: 435.1017. IR (KBr):  $\nu$  (CO)=1910  $\text{cm}^{-1}$ .

### Complex 18

Yield: 55%.  $^1\text{H}$  NMR (300 MHz,  $\text{CDCl}_3$ ):  $\delta$  7.17-6.30 (m, 30H), 6.63 (m, 1H), 5.94 (m, 1H), 5.90 (d,  $J=11.1\text{Hz}$ , 1H), 4.39 (d,  $J=17.4\text{Hz}$ , 1H), 4.36 (d,  $J=11.1\text{Hz}$ , 1H), 4.08 (d,  $J=17.1\text{Hz}$ , 1H), 3.56 (d,  $J=15.9\text{Hz}$ , 1H), 3.40 (d,  $J=16.8\text{Hz}$ , 1H), 3.34 (d,  $J=17.7\text{Hz}$ , 1H), 3.17 (d,  $J=16.8\text{Hz}$ , 1H), 3.11 (d,  $J=15.9\text{Hz}$ , 1H), 2.86 (d,  $J=16.2\text{Hz}$ , 1H).  $\{^1\text{H}\}$   $^{13}\text{C}$  NMR ( $\text{CDCl}_3$ , 75 MHz):  $\delta$  208.0, 182.2, 140.0, 139.7, 139.2, 138.9, 138.2, 137.0, 130.6, 129.6, 129.0-127.4, 126.4-126.2, 125.7, 125.3, 121.7, 121.3, 107.5, 102.5, 99.2, 96.2, 89.1, 70.6, 44.4, 40.2, 34.4, 31.9, 31.5, 31.25. MS (ESI):  $m/z$ :  $[M-I]^+$  calcd for  $\text{C}_{52}\text{H}_{45}\text{N}_2\text{ORu}$ : 815.26, found: 815.2,  $[M-I+\text{CH}_3\text{CN}]^+$  calcd for  $\text{C}_{54}\text{H}_{48}\text{N}_3\text{ORu}$ : 856.28, found: 856.2.  $[M+\text{Na}]^+$  calcd for  $\text{C}_{52}\text{H}_{45}\text{IN}_2\text{NaORu}$ : 965.15, found: 965.1. HRMS (ESI-TOF):  $m/z$ :  $[M]^+$  calcd for  $\text{C}_{52}\text{H}_{45}\text{N}_2\text{ORu}$ : 815.2590, found: 815.2590. IR (KBr):  $\nu$  (CO)=1923  $\text{cm}^{-1}$ .

### Preparation of diastereomers and resolution of complexes 19 and 20

A solution of the appropriate complex ( **17** or **18**) and  $\text{Ag}(\text{O}_3\text{SCF}_3)$  (1.2 equivalents) in dichloroethane was stirred at room temperature (10-15 min). Then 1-(*S*)-phenylethylamine (1.2 eq) was added and the reaction mixture heated to 70  $^\circ\text{C}$  (0.5-1 h). The remaining yellow solution was filtered through celite, and the volatiles removed under vacuum. The solid was redissolved in the minimum amount of  $\text{CH}_2\text{Cl}_2$  and applied in a preparative TLC. The chromatographic plate was eluted several times until clear resolution of two yellow bands. Eluent phase: diethyl ether/hexane (8/2) for **19** and diethyl ether for **20**.

### Complex 19A

Yield: 16%.  $^1\text{H}$  NMR (500 MHz,  $\text{CDCl}_3$ ):  $\delta$  7.60 (d,  $J=7\text{Hz}$ , 2H), 7.44-7.36 (m, 3H), 7.24-7.18 (m, 5H), 6.52 (s, 1H), 6.26 (s, 1H), 5.21 (dd,  $J=12.5\text{Hz}$

$J=2\text{Hz}$ , 1H), 3.62 (m, 1H), 3.42 (m, 2H), 3.20 (s, 3H), 2.78-2.63 (m, 2H), 1.97 (s, 3H), 1.95 (s, 3H), 1.77 (s, 3H), 1.51 (d,  $J=6.8\text{Hz}$ , 3H), 1.16 (s, 3H).  $\{^1\text{H}\} \text{ }^{13}\text{C}$  NMR ( $\text{CDCl}_3$ , 125 MHz):  $\delta$  208.2, 179.5, 142.2, 136.4, 129.0, 128.9, 128.5, 127.6, 126.2, 121.7, 120.6, 103.4, 99.8, 96.5, 89.0, 80.4, 66.7, 66.2, 38.5, 28.3, 26.4, 10.2, 9.7, 9.6, 8.9. HRMS (ESI-TOF):  $m/z$   $[M]^+$  calcd for  $\text{C}_{30}\text{H}_{36}\text{N}_3\text{ORu}$ : 556.1910, found: 556.1910. IR (KBr):  $\nu$  (CO)=1919  $\text{cm}^{-1}$ .

### Complex 19B

Yield 16%.  $^1\text{H}$  NMR (500 MHz,  $\text{CDCl}_3$ ):  $\delta$  7.60 (d,  $J=7.2\text{Hz}$ , 2H), 7.44-7.36 (m, 5H), 7.30 (t,  $J=7.5\text{Hz}$ , 2H), 7.20 (d,  $J=7\text{Hz}$ , 1H), 6.73 (br, 1H), 6.33 (s, 1H), 5.13 (dd,  $J=12.2\text{Hz}$   $J=2.2\text{Hz}$ , 1H), 3.74 (br, 2H), 3.63 (s, 3H), 2.76-2.64 (m, 3H), 1.81 (s, 3H), 1.72 (s, 3H), 1.46 (d,  $J=6.5\text{Hz}$ , 3H), 1.41 (s, 3H), 1.16 (s, 3H).  $\{^1\text{H}\} \text{ }^{13}\text{C}$  NMR ( $\text{CDCl}_3$ , 125 MHz):  $\delta$  209.7, 180.3, 143.3, 136.8, 129.7, 129.5, 129.3, 129.2, 128.2, 127.1, 122.7, 121.3, 104.5, 99.9, 96.6, 90.4, 81.4, 67.7, 62.7, 39.5, 28.7, 24.2, 10.7, 10.3, 9.6, 9.2. HRMS (ESI-TOF):  $m/z$   $[M]^+$  calcd for  $\text{C}_{30}\text{H}_{36}\text{N}_3\text{ORu}$ : 556.1910, found: 556.1904. IR (KBr):  $\nu$  (CO)=1918  $\text{cm}^{-1}$ .

### Complex 20A

Yield: 12.5%).  $^1\text{H}$  NMR (500 MHz,  $\text{CDCl}_3$ ):  $\delta$  8.07 (d,  $J=7\text{Hz}$ , 1H), 7.42 (t,  $J=7.5\text{Hz}$ , 3H), 7.31-6.92 (m, 23H), 6.67 (d,  $J=8\text{Hz}$ , 1H), 6.63 (br, 2H), 6.42 (d,  $J=7.5\text{Hz}$ , 2H), 6.32 (m, 3H), 6.26 (t,  $J=7.5\text{Hz}$ , 1H), 6.16 (d,  $J=11\text{Hz}$ , 1H), 6.10 (br, 2H), 6.03 (br, 1H), 4.32 (d,  $J=18\text{Hz}$ , 1H), 4.29 (t,  $J=6.5\text{Hz}$ , 1H), 4.20 (d,  $J=16.5\text{Hz}$ , 1H), 4.05 (d,  $J=11\text{Hz}$ , 1H), 3.53 (d,  $J=16.5\text{Hz}$ , 1H), 4.45 (d,  $J=14.5\text{Hz}$ , 1H), 4.41 (d,  $J=18.5\text{Hz}$ , 1H), 3.04 (s, 3H), 1.99 (d,  $J=15.5\text{Hz}$ , 1H), 1.14 (d, 6.5 Hz, 3H).  $^{13}\text{C}\{^1\text{H}\}$  NMR ( $\text{CDCl}_3$ , 125 MHz):  $\delta$  209.7, 180.2, 142.3, 142.1, 138.5, 138.4, 136.4, 136.0, 135.3, 132.9, 130.0-125.3, 122.5, 121.3, 113.0, 102.3, 100.5, 95.7, 87.1,

70.0, 62.3, 44.4, 39.2, 32.0, 31.7, 30.11, 29.8, 29.7, 28.4. MS (ESI-TOF):  $m/z$ :  $[M]^+$  calcd for  $C_{60}H_{56}N_3ORu$ : 936.3484, found: 936.3507. IR (KBr):  $\nu$  (CO)=1925  $cm^{-1}$ .

### **Complex 20B**

Yield: 12.5%.  $^1H$  NMR (500 MHz,  $CDCl_3$ ):  $\delta$  7.91 (d,  $J=8Hz$ , 1H), 7.39-7.25 (m, 5H), 7.19-7.13 (m, 8H), 7.10-6.97 (m, 8H), 7.0-6.77 (m, 6H), 6.58 (br, 2H), 6.51 (d,  $J=8Hz$ , 2H), 6.38 (t,  $J=7.5Hz$ , 2H), 6.31 (t,  $J=6.5Hz$ , 1H), 6.25-6.20 (m, 3H), 4.29 (d,  $J=14.5Hz$ , 1H), 4.25 (d,  $J=11.5Hz$ , 1H), 4.13 (d,  $J=16.5Hz$ , 1H), 3.80 (m, 1H), 3.75 (s, 3H), 3.58 (d,  $J=16.5Hz$ , 1H), 3.35-3.20 (m, 3H), 3.08 (d,  $J=14.5Hz$ , 1H), 3.39 (d,  $J=16Hz$ , 1H), 2.39 (d,  $J=16.5Hz$ , 1H), 0.94 (d,  $J=6.5Hz$ , 1H).  $\{^1H\}$   $^{13}C$  NMR ( $CDCl_3$ , 125 MHz):  $\delta$  209.6, 181.2, 144.1, 141.4, 138.8, 138.5, 136.6, 136.0, 133.0, 130-126.9, 122.75, 112.5, 101.4, 96.2, 87.0, 71.1 63.8, 44.8, 40.0, 32.2, 30.3, 22.3. HRMS (ESI-TOF):  $m/z$ :  $[M]^+$  calcd for  $C_{60}H_{56}N_3ORu$ : 936.3484, found: 936.3518. IR (KBr):  $\nu$  (CO)=1924  $cm^{-1}$ .

### **Catalytic experiments – general procedure**

*In THF*: A solution of catalyst (1 mol%) in 0.5 mL of THF was treated with AgOTf (1-2 mol%) and stirred at room temperature for 10 min. Then, 0,8 mmol of substrate was added and the reaction heated to 55°C and monitored by  $^1H$  NMR.

*In H<sub>2</sub>O*: A solution of catalyst (0.2 mol%) in 4 mL of H<sub>2</sub>O was treated with AgOTf (0.2 mol%) and stirred at room temperature for 10 min. Then, 0,4 mmol of substrate was added and the reaction heated to 75°C and monitored by  $^1H$  NMR.

*Kinetic isotopic effect*: A solution of **17** (0.9 mg, 0.2 mol%) in 4 mL of H<sub>2</sub>O/D<sub>2</sub>O was treated with AgOTf (0.3 mg, 0.2 mol%) and stirred at room



temperature for 10 min. Then, 1-buten-3-ol (43  $\mu\text{L}$ , 0.4 mmol) was added and the reaction heated to 75°C, aliquots (50  $\mu\text{L}$ ) were taken, dissolved in  $\text{D}_2\text{O}$  and the  $^1\text{H}$  NMR spectra recorded.

### 6.5.3. X-Ray diffraction studies

Single crystals of **17** and **18** were mounted on a glass fiber in a random orientation. Data collection was performed at room temperature on a Siemens Smart CCD diffractometer using graphite monochromated  $\text{Mo-K}\alpha$  radiation ( $\lambda=0.71073 \text{ \AA}$ ) with a nominal crystal to detector distance of 4.0 cm. Space group assignment was based on systematic absences, E statistics and successful refinement of the structures. The structure was solved by direct methods with the aid of successive difference Fourier maps and were refined using the SHELXTL 6.1 software package.<sup>[26]</sup> All non-hydrogen were refined anisotropically. Hydrogen atoms were assigned to ideal positions and refined using a riding model. The diffraction frames were integrated using the SAINT package.<sup>[27]</sup>

## 6.6. Acknowledgements

Dr. Cristian Vicent is acknowledged for providing data from Mass Spectrometry.

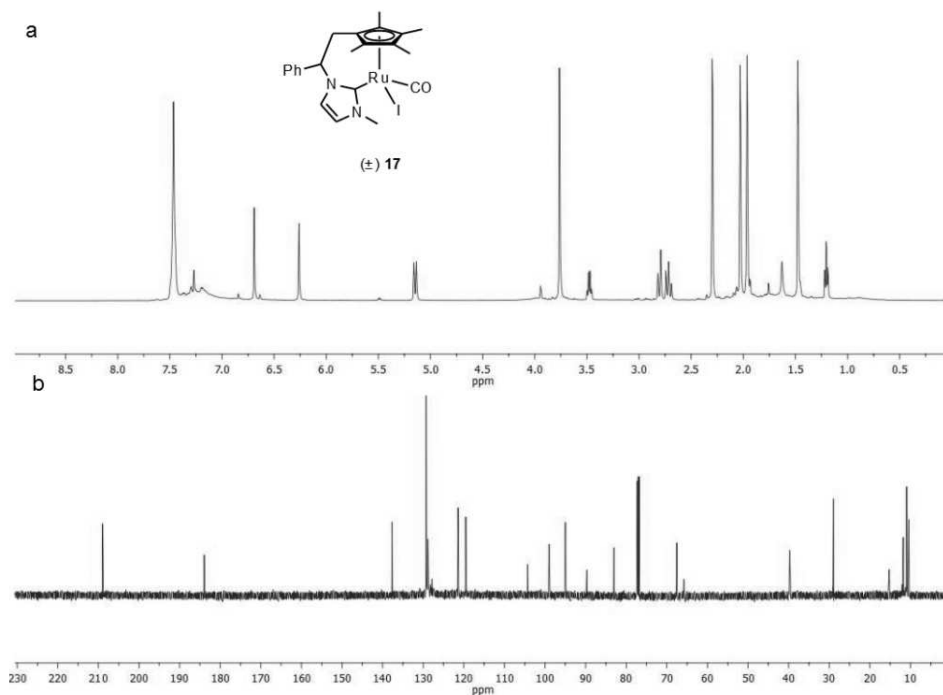
## 6.7. References

- [1] B. M. Trost, M. U. Frederiksen, M. T. Rudd, *Angew. Chem. Int. Ed.* **2005**, *44*, 6630.
- [2] E. Colacino, J. Martinez, F. Lamaty, *Coord. Chem. Rev.* **2007**, *251*, 726.
- [3] V. Dragutan, I. Dragutan, L. Delaude, A. Demonceau, *Coord. Chem. Rev.* **2007**, *251*, 765.
- [4] M. Prinz, M. Grosche, E. Herdtweck, W. A. Herrmann, *Organometallics* **2000**, *19*, 1692.

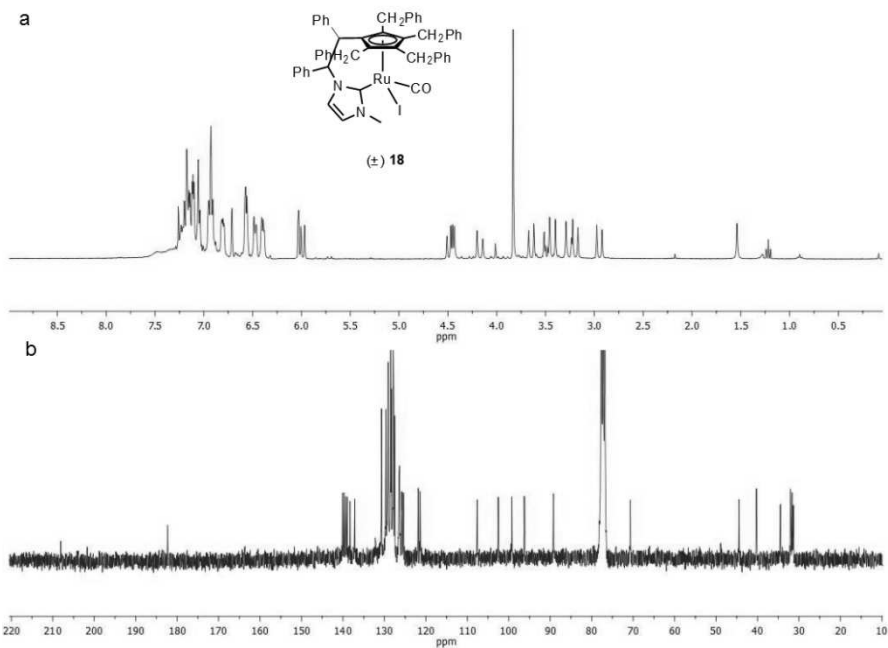
- [5] R. Corberán, M. Sanaú, E. Peris, *Organometallics* **2006**, *25*, 4002.
- [6] R. Corberán, V. Lillo, J. A. Mata, E. Fernandez, E. Peris, *Organometallics* **2007**, *26*, 4350.
- [7] H. Brunner, *Angew. Chem. Int. Ed.* **1999**, *38*, 1195.
- [8] C. Ganter, *Chem. Soc. Rev.* **2003**, *32*, 130.
- [9] J. K. Liu, X. F. Wu, J. A. Iggo, J. L. Xiao, *Coord. Chem. Rev.* **2008**, *252*, 782.
- [10] C. Y. Zhang, F. Luo, B. Cheng, B. Li, H. B. Song, S. S. Xu, B. Q. Wang, *Dalton Trans.* **2009**, 7230.
- [11] W. Baratta, W. A. Herrmann, P. Rigo, J. Schwarz, *J. Organomet. Chem.* **2000**, *593-594*, 489.
- [12] L. Jafarpour, E. D. Stevens, S. P. Nolan, *J. Organomet. Chem.* **2000**, *606*, 49.
- [13] W. Baratta, E. Herdtweck, W. A. Herrmann, P. Rigo, J. Schwarz, *Organometallics* **2002**, *21*, 2101.
- [14] J. Bosson, S. P. Nolan, *J. Org. Chem.* **2010**, *75*, 2039.
- [15] J. Bosson, A. Poater, L. Cavallo, S. P. Nolan, *J. Am. Chem. Soc.* **2010**, *132*, 13146.
- [16] F. E. Hahn, A. R. Naziruddin, A. Hepp, T. Pape, *Organometallics* **2010**, *29*, 5283.
- [17] W. W. N. O, A. J. Lough, R. H. Morris, *Chem. Commun.* **2010**, *46*, 8240.
- [18] V. Miranda-Soto, D. B. Grotjahn, A. L. Cooksy, J. A. Golen, C. E. Moore, A. L. Rheingold, *Angew. Chem. Int. Ed.* **2011**, *50*, 631.
- [19] V. V. K. M. Kandepi, A. P. da Costa, E. Peris, B. Royo, *Organometallics* **2009**, *28*, 4544.
- [20] V. V. K. M. Kandepi, J. M. S. Cardoso, E. Peris, B. Royo, *Organometallics* **2010**, *29*, 2777.
- [21] J. W. Faller, J. Parr, A. R. Lavoie, *New J. Chem.* **2003**, *27*, 899.
- [22] W. Baratta, E. Herdtweck, W. A. Herrmann, P. Rigo, J. D. Schwarz, *Organometallics* **2002**, *21*, 2101.
- [23] P. Crochet, J. Diez, M. A. Fernandez-Zumel, J. Gimeno, *Adv. Synth. Catal.* **2006**, *348*, 93.

- [24] A. E. Diaz-Alvarez, P. Crochet, M. Zablocka, C. Duhayon, V. Cadierno, J. Gimeno, J. P. Majoral, *Adv. Synth. Catal.* **2006**, *348*, 1671.
- [25] P. Crochet, M. A. Fernandez-Zumel, J. Gimeno, M. Scheele, *Organometallics* **2006**, *25*, 4846.
- [26] G. M. Sheldrick, *SHELXTL, version 6.1, Bruker AXS, Inc, Madison, WI, 2000.*
- [27] *SAINT, Bruker Analytical X-ray System, version 5.0, Madison, WI, 1998.*

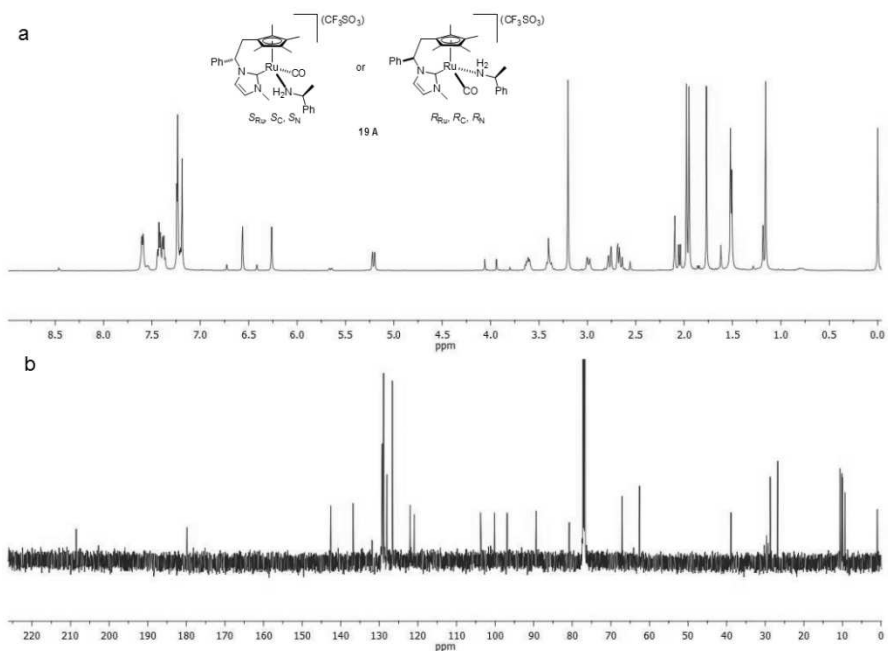
## 6.8. Supporting information



**Figure 6.6.** (a)  $^1\text{H}$  NMR (500 MHz,  $\text{CDCl}_3$ , 300K) and (b)  $\{^1\text{H}\}^{13}\text{C}$  NMR (125 MHz,  $\text{CDCl}_3$ , 300K) spectra of complex **17**.

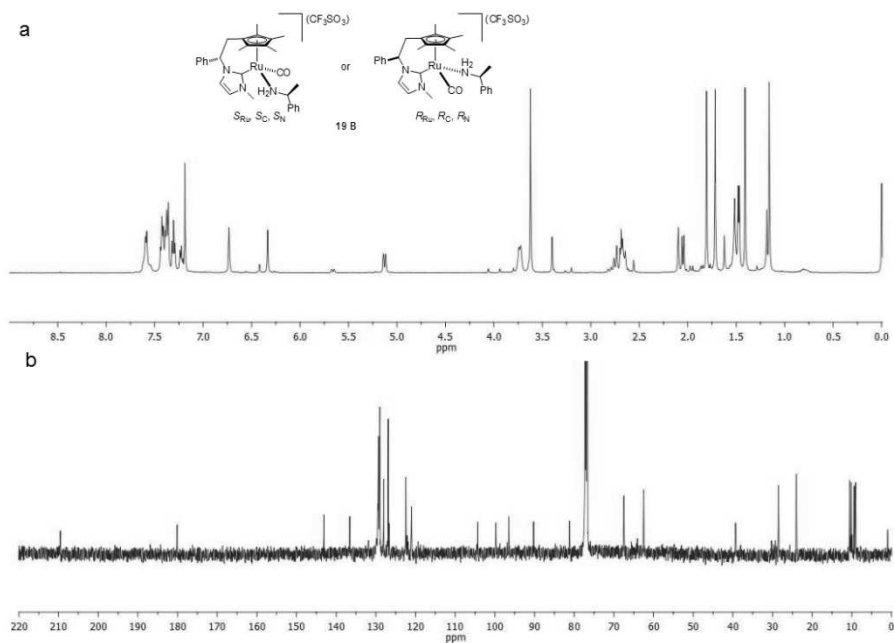


**Figure 6.7.** (a)  $^1\text{H}$  NMR (300 MHz,  $\text{CDCl}_3$ , 300K) and (b)  $\{^1\text{H}\}^{13}\text{C}$  NMR (75 MHz,  $\text{CDCl}_3$ , 300K) spectra of complex **18**.

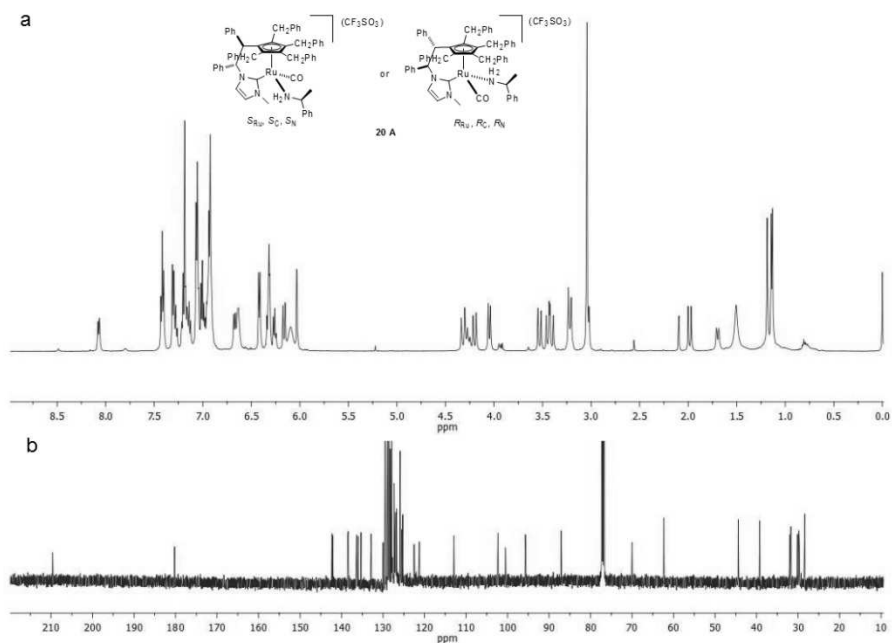


**Figure 6.8.** (a)  $^1\text{H}$  NMR (500 MHz,  $\text{CDCl}_3$ , 300K) and (b)  $\{^1\text{H}\}^{13}\text{C}$  NMR (125 MHz,  $\text{CDCl}_3$ , 300K) spectra of complex **19A**.

6. Coordination to Ru, resolution of chiral-at-metal complexes and isomerisation of allylic alcohols

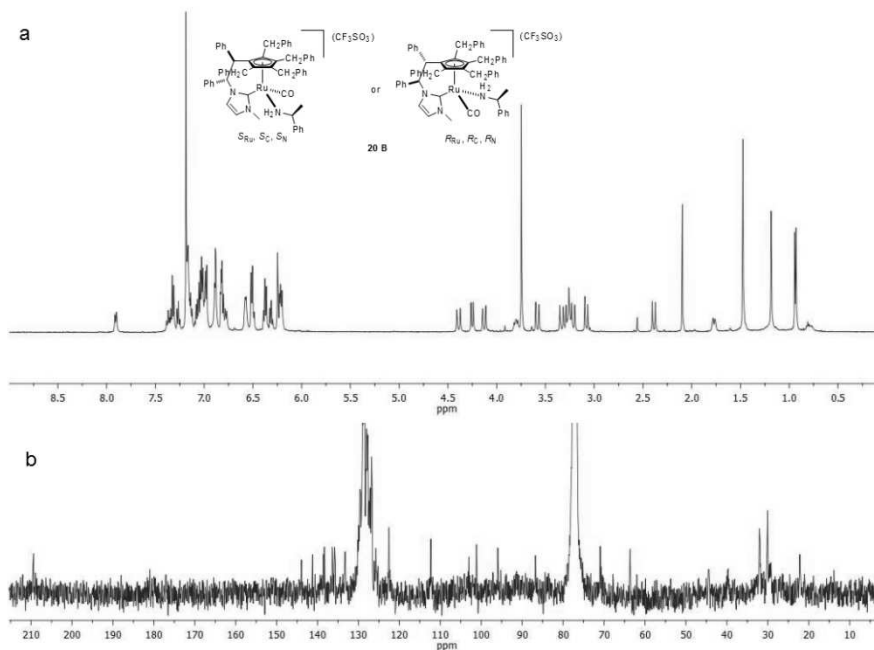


**Figure 6.9.** (a)  $^1\text{H}$  NMR (500 MHz,  $\text{CDCl}_3$ , 300K) and (b)  $\{^1\text{H}\}^{13}\text{C}$  NMR (125 MHz,  $\text{CDCl}_3$ , 300K) spectra of complex **19B**.



**Figure 6.10.** (a)  $^1\text{H}$  NMR (500 MHz,  $\text{CDCl}_3$ , 300K) and (b)  $\{^1\text{H}\}^{13}\text{C}$  NMR (125 MHz,  $\text{CDCl}_3$ , 300K) spectra of complex **20A**.

Cyclopentadienyl-Functionalised N-Heterocyclic Carbenes:  
Synthesis, Coordination to Mo, Ru, Rh and Ir and Catalytic Applications.



---

# 7.

## ENANTIOMERICALLY PURE CP-FUNCTIONALISED NHC LIGAND: SYNTHESIS AND COORDINATION TO Rh AND Ir

---

|      |   |     |
|------|---|-----|
| 7.1. | Abstract  | 121 |
| 7.2. | Introduction  | 122 |
| 7.3. | Results and discussion  | 123 |
|      | 7.3.1. Synthesis and characterisation of an enantiomerically pure Cp-imidazolium salt, 123                |     |
|      | 7.3.2. Synthesis and characterisation of Rh and Ir complexes containing the Cp-NHC ligand <b>21</b> , 124 |     |
| 7.4. | Conclusions   | 128 |
| 7.5. | Experimental procedures   | 129 |
|      | 7.5.1. Materials and methods, 129   |     |
|      | 7.5.2. Synthesis and characterisation, 129  |     |
| 7.6. | Acknowledgments   | 131 |
| 7.7. | References  | 132 |
| 7.8. | Supporting Information  | 132 |

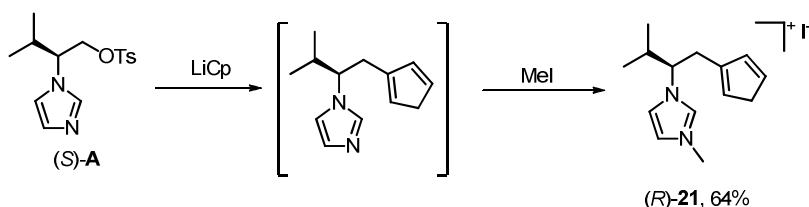
Cyclopentadienyl-Functionalised N-Heterocyclic Carbenes:  
Synthesis, Coordination to Mo, Ru, Rh and Ir and Catalytic Applications.

---



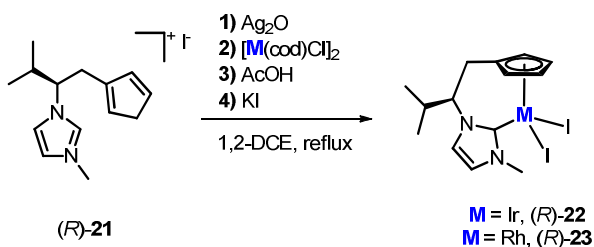
## 7.1. Abstract

This chapter describes the synthesis of the first enantiomerically pure Cp-functionalised NHC ligand. The ligand precursor (*R*)-**21** was synthesised as depicted in Scheme 7.1 by reaction of lithium cyclopentadienyl with the imidazole tosylate (*S*)-**A** and subsequent treatment with iodomethane.



**Scheme 7.1.** Synthesis of enantiomerically pure Cp-functionalised imidazolium salt.

Compound (*R*)-**21** was successfully coordinated to iridium and rhodium by transmetalation from the corresponding pre-formed Ag-Cp-NHC complex to  $[M(\mu\text{-Cl})(\text{cod})]_2$  ( $M = \text{Ir}, \text{Rh}$ ), and subsequent reflux in the presence of acetic acid, as shown in Scheme 7.2.



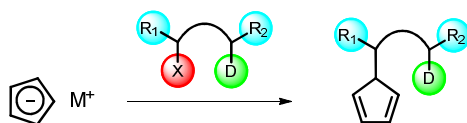
**Scheme 7.2.** Synthesis of enantiomerically pure Ir and Rh complexes **22** and **23**.

All compounds were characterised by NMR spectroscopy and MS spectrometry. Crystals suitable for X-ray diffraction studies were obtained for complex **22**.

The work described in this chapter was entirely performed by the candidate except for the X-ray diffraction studies, which were performed by Dr. Gabriel Peris and Dr. José A. Mata, at the Universitat Jaume I.

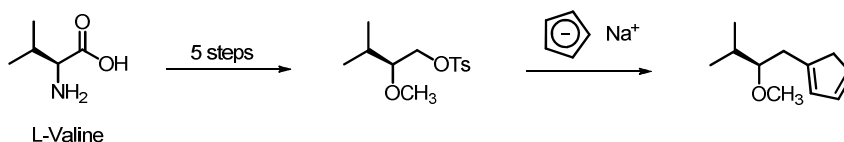
## 7.2. Introduction

The direct alkylation of cyclopentadienyl salts of alkaline metals, depicted in Scheme 7.3, has been extensively used to prepare functionalised cyclopentadienyl ligands.<sup>[1, 2]</sup>



**Scheme 7.3.** Direct alkylation of Cp anions (M = Li or Na; X = Cl, Br, I, OTs, OMs).

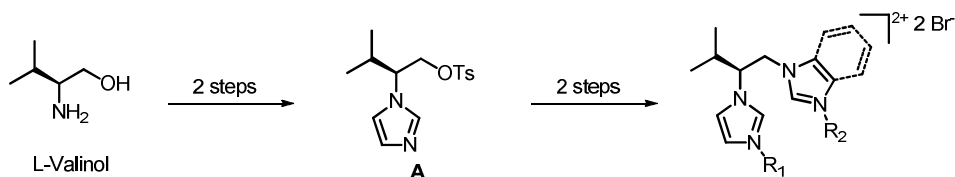
In 1987, Huang and Qian<sup>[3]</sup> reported the synthesis of the first examples of chiral donor-functionalised cyclopentadienyl ligands. The Cp-functionalised ethers were prepared by direct alkylation of NaCp with a chiral tosylate, derived from  $\alpha$ -hydroxy and  $\alpha$ -amino carboxylic acids (Scheme 7.4).



**Scheme 7.4.** Synthesis of enantiomerically pure donor-functionalised Cp ligands.<sup>[3]</sup>

More recently, Diez and Nagel<sup>[4, 5]</sup> reported a very similar synthetic approach towards the synthesis of chiral bis-carbenes, Scheme 7.5.

We envisioned that a similar approach could be used in the synthesis of enantiomerically pure Cp-functionalised NHCs.

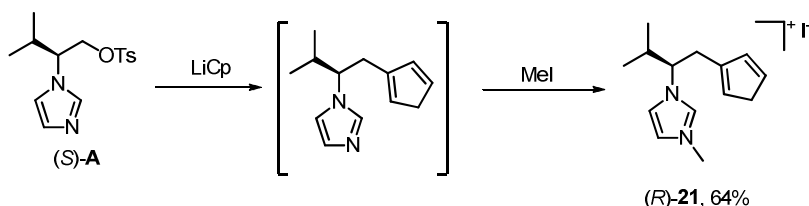


**Scheme 7.5.** Synthesis of enantiomerically pure bis-NHC ligands.<sup>[4, 5]</sup>

## 7.3. Results and discussion

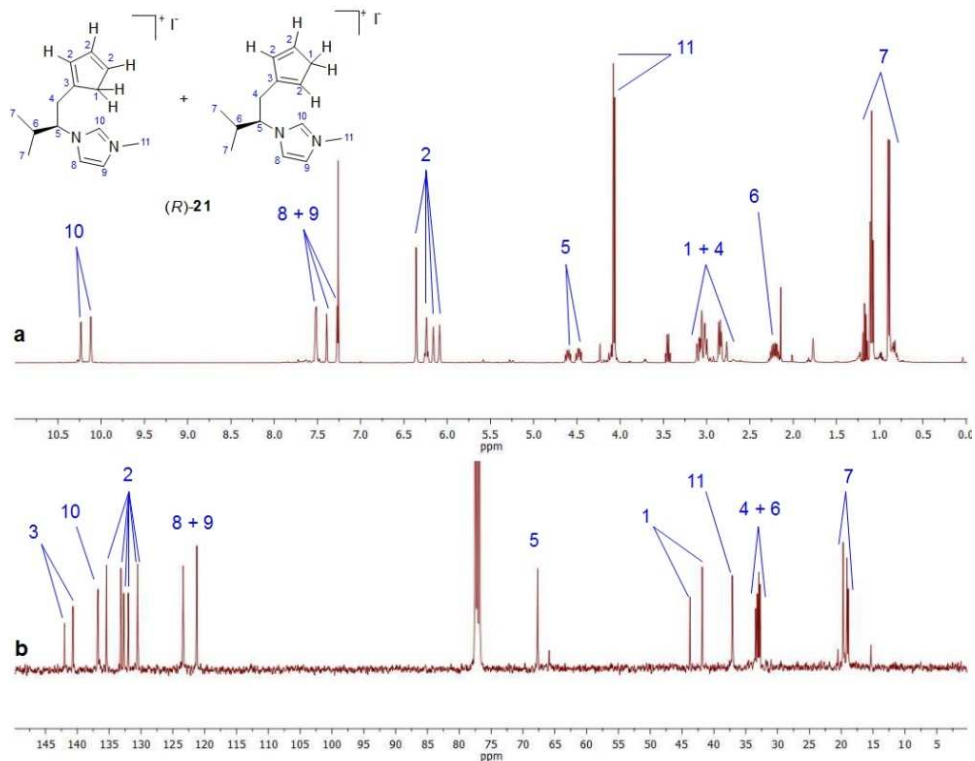
### 7.3.1. Synthesis and characterisation of an enantiomerically pure Cp-imidazolium salt

The enantiomerically pure Cp-imidazolium iodide (*R*)-**21** was prepared following the synthetic pathway depicted in Scheme 7.6. The imidazole tosylate (*S*)-**A** was prepared following the procedure reported by Nagel and co-workers.<sup>[4, 5]</sup> The reaction of **A** with LiCp followed by treatment with MeI, afforded pure (*R*)-**21** in good yield.



**Scheme 7.6.** Synthesis of enantiomerically pure Cp-functionalised NHC ligand **21**.

The imidazolium salt (*R*)-**21** was characterised by  $^1\text{H}$  and  $^{13}\text{C}$  NMR spectrometry and MS spectroscopy. The  $^1\text{H}$  and  $^{13}\text{C}$  NMR spectra are shown in Figure 7.1. Its NMR spectra showed the presence of two isomers resulting from the different position of the double bond in the cyclopentadienyl ring. Therefore, a double set of signals with ~1:1 ratio were observed in both  $^1\text{H}$  and  $^{13}\text{C}$  NMR spectra. The  $^1\text{H}$  NMR spectra showed the typical signals for the imidazolium salts: at 10.24 and 10.12 ppm for the NCHN proton, at 7.52, 7.39 and 7.27 ppm for the olefinic protons and at 4.08 and 4.06 ppm for the methyl protons. The protons of the cyclopentadienyl ring resonance at 6.36, 6.14, 6.09 ppm for the olefinic protons and ~3 ppm for the two non-olefinic protons. The  $^{13}\text{C}$  NMR spectra shows the characteristic resonances for the NCHN carbon at 136.7 ppm, and at 37.1 ppm for the methyl group of the imidazolium ring.

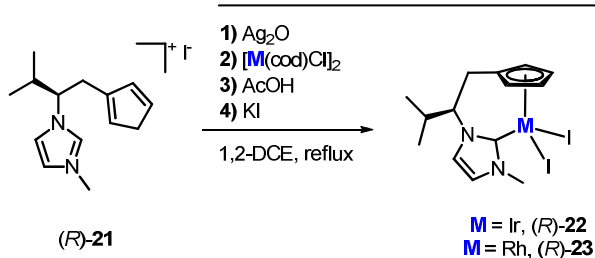


**Figure 7.1.** (a)  $^1\text{H}$  NMR (400 MHz,  $\text{CDCl}_3$ , 300K) spectrum of (*R*)-**21** (b)  $\{^1\text{H}\}$   $^{13}\text{C}$  NMR (100 MHz,  $\text{CDCl}_3$ , 300K) spectrum of (*R*)-**21**.

### 7.3.2. Synthesis and characterisation of Rh and Ir complexes containing the Cp-NHC ligand **21**

The imidazolium salt (*R*)-**21** was coordinated to rhodium and iridium following the method previously described by us.<sup>[6]</sup> The pro-ligand **21** was reacted with  $\text{Ag}_2\text{O}$  and the resulting Ag-NHC transmetalated the carbene to the metal precursor  $[\text{M}(\mu\text{-Cl})(\text{cod})]_2$  ( $\text{M} = \text{Ir}, \text{Rh}$ ). Refluxing the reaction mixture in the presence of acetic acid afforded complexes **22** and **23**, as shown in Scheme 7.7.

The iridium and rhodium complexes were purified by column chromatography and isolated as red crystalline solids.



**Scheme 7.7.** Synthesis of enantiomerically pure Ir and Rh complexes **22** and **23**.

Both complexes were characterised by  $^1\text{H}$  and  $^{13}\text{C}$  NMR spectroscopy and MS spectrometry. Additionally, the molecular structure of **22** was determined by X-ray diffraction studies. The selected spectroscopy data of complexes **22** and **23** are summarised in Table 7.1. Figure 7.2 shows the  $^1\text{H}$  and  $^{13}\text{C}$  NMR spectra of (*R*)-**22**.

**Table 7.1.** Selected  $^1\text{H}$  and  $^{13}\text{C}$  NMR chemical shifts of iridium and rhodium complexes (*R*)-**22** and (*R*)-**23**.

|                         | $^1\text{H}$ NMR <sup>a</sup> |                   |   | $^{13}\text{C}$ NMR <sup>b</sup> |  |
|-------------------------|-------------------------------|-------------------|---|----------------------------------|--|
|                         | $\text{CH}_{\text{imid}}$     | N-CH <sub>3</sub> | C <sub>NHC</sub>                          | Cp* <sub>trans</sub>             | Cp* <sub>cis</sub>   |
| ( <i>R</i> )- <b>22</b> | 6.87 and 6.79                 | 4.05              | 137.9                                     | 92.2 and 90.1                    | 87.5, 73.3 and 72.8  |
| ( <i>R</i> )- <b>23</b> | 6.99 and 6.85                 | 3.99              | 156.1<br>( $^1J_{\text{Rh-C}} = 54.8$ Hz) | 96.0 and 94.04                   | 95.6, 81.4 ( $^1J_{\text{Rh-C}} = 6.6$ Hz) and 80.8<br>( $^1J_{\text{Rh-C}} = 6.4$ Hz) |

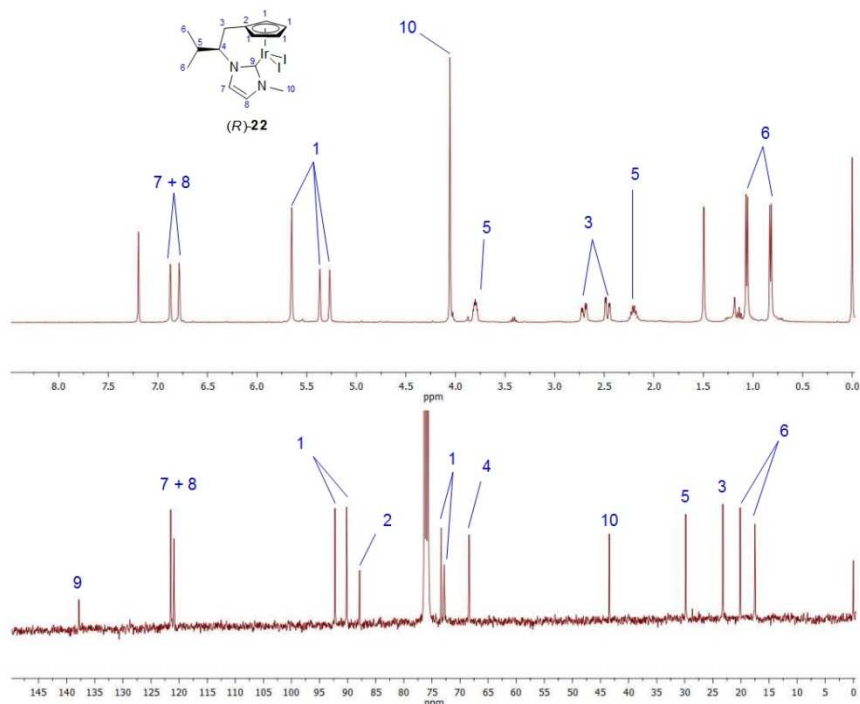
<sup>a</sup> in CDCl<sub>3</sub>, 400 MHz, 300 K, chemical shifts in ppm. <sup>b</sup> in CDCl<sub>3</sub>, 100 MHz, 300 K, chemical shifts in ppm.

As shown in Figure 7.2, the  $^1\text{H}$  NMR of complex **22** displays the signals corresponding to the CH protons at the imidazole ring at 6.87 and 6.79 ppm. The signal due to the N-CH<sub>3</sub> protons appear at 4.05 ppm. Due to the asymmetry of the molecule the protons of the Cp ring are inequivalent, and display three resonances at 5.65, 5.37 and 5.27 ppm. The methylene protons of the linker are diastereotopic, exhibiting two double doublets at 2.70 and 2.47 ppm.

The  $^{13}\text{C}$  NMR of complex **22** confirms the asymmetry of the molecule, as seen by the five resonances at 92.2, 90.1, 87.5, 73.3 and 72.8 ppm for

the carbons of the Cp ring. The characteristic signal due to the metallated carbene-carbon appears at 137.9 ppm.

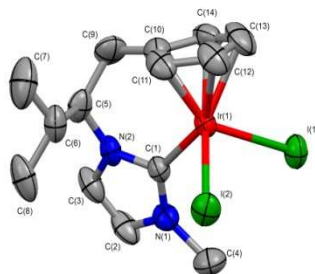
The NMR spectra of the rhodium complex **23** are very similar to the iridium ones. The  $^{13}\text{C}$  NMR spectrum displays the signal assigned to the metallated carbene-carbon at 156 ppm, with a typical Rh-C coupling constant of 54.8 Hz.



**Figure 7.2.** (a)  $^1\text{H}$  NMR (400 MHz,  $\text{CDCl}_3$ , 300K) and (b)  $\{^1\text{H}\}^{13}\text{C}$  NMR (100 MHz,  $\text{CDCl}_3$ , 300K) spectra of complex (R)-**22** (400 MHz,  $\text{CDCl}_3$ , 300K).

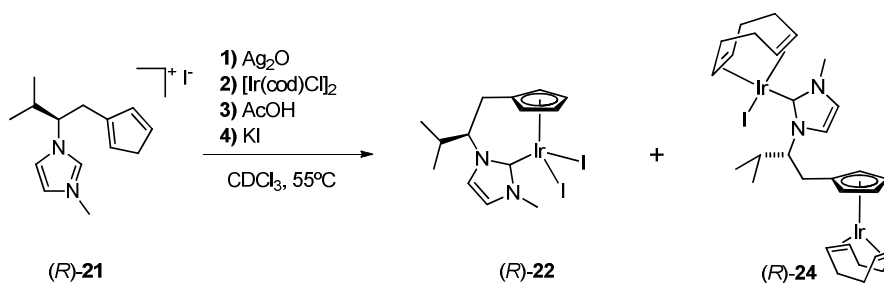
Crystals suitable for X-ray diffraction studies were obtained for complex **22**. The molecular diagram of the half-sandwich complex **22** is depicted in Figure 7.3. Apart from the chelating ligand, two iodide ligands complete the coordination sphere around the metal centre. The  $\text{M}-\text{C}_{\text{NHC}}$  distance is 2.04 Å and the distance between the metal and the cyclopentadienyl centroid is  $\sim 1.8$  Å, both in the range of previously reported “Cp\*-NHC” $\text{IrX}_2$  complexes.<sup>[6, 7]</sup> The angles of the three legged

piano stools are in the range of 90-97 °C, in agreement with a pseudo-octahedral geometry.

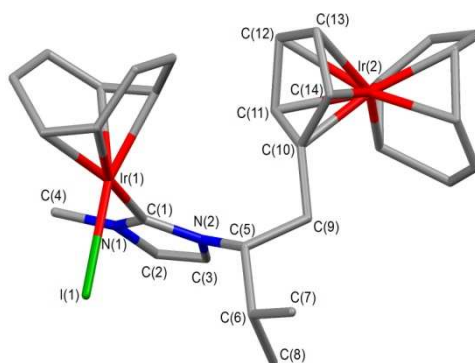


**Figure 7.3.** Molecular diagram of (*R*)-**22**. Selected bond distances (Å) and angles (deg) are: Ir(1)-C(1) 2.041(7), Ir(1)-I(1) 2.7402(6), Ir(1)-I(2) 2.7050(7), Ir(1)-Cp(centroid) 1.839, C(1)-Ir(1)-I(1) 95.8(2), C(1)-Ir(1)-I(2) 90.6(2), I(1)-Ir(1)-I(2) 96.67(2).

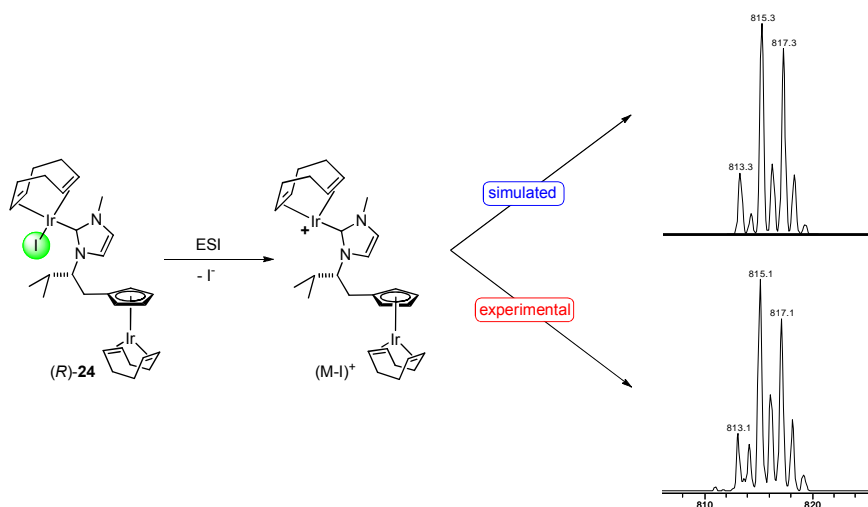
As shown in Scheme 7.8, the reaction between  $[\text{Ir}(\mu\text{-Cl})(\text{cod})]_2$ ,  $\text{Ag}_2\text{O}$  and (*R*)-**21**, allowed the detection of the dimetallic species (*R*)-**24**, along with compound (*R*)-**22**. Complex (*R*)-**24** was purified by column chromatography, and crystallised from  $\text{CDCl}_3$  solution. Although these crystals were not of enough quality for resolving the structure by X-ray diffraction studies with an adequate refinement, it allowed us to confirm the proposed structure. The molecular diagram is shown in Figure 7.4. The dimetallic compound **24** was also characterised by mass spectrometry ( $[\text{M-I}]^+ = 815.1$  m/z, Figure 7.5). Similar Rh dimetallic species, in which two “Rh(cod)” fragments are linked through an indenyl-functionalised NHC ligand have been recently reported by Cole-Hamilton and co-workers.<sup>[8]</sup>



**Scheme 7.8.** Synthesis of monometallic and bimetallic iridium complexes **22** and **24**, respectively.



**Figure 7.4.** Molecular diagram of (*R*)-**24**. Selected bond distances (Å) and angles (deg) are: Ir(1)-C(1) 2.0201(1), Ir(1)-I(1) 2.6531(2), Ir(2)-Cp(centroid) 1.917, C(1)-Ir(1)-I(1) 91.82.



**Figure 7.5.** (a) Simulated and (b) experimental MS spectra of  $[M-I]^+$  ion corresponding to the ionization of complex (*R*)-**24**.

## 7.4. Conclusions

In this chapter we have described a new synthetic approach to enantiomerically pure Cp-functionalised NHCs. The synthesis relies on the direct reaction of lithium cyclopentadienyl with a chiral imidazole tosylate.

The enantiomerically pure ligand Cp-NHC was coordinated to iridium and rhodium by transmetalation of the in situ pre-formed silver



carbene to  $[M(\mu\text{-Cl})(\text{cod})]_2$  ( $M = \text{Ir}, \text{Rh}$ ), and subsequent C-H activation of the cyclopentadiene affording chelating (Cp-NHC) $M$ I<sub>2</sub> ( $M = \text{Ir}, \text{Rh}$ ) complexes.

The molecular structure of (Cp-NHC)IrI<sub>2</sub> (**22**) complex showed the cyclopentadienyl-NHC ligand chelating the iridium centre in a three-legged piano-stool geometry.

Further studies to explore the asymmetric catalytic behaviour of the enantiomerically pure metal complexes are underway.

## 7.5. Experimental procedures

### 7.5.1. Materials and methods

All reactions were carried out under inert atmosphere. When required, solvents were dried via standard techniques.

NMR spectra were recorded on a Bruker Avance III 400 MHz spectrometer using CDCl<sub>3</sub> (Cambridge Isotope Laboratories, Inc.) as solvent. Elemental analyses and Mass Spectrometry were performed in our laboratories at ITQB. (2S)-2-(1-Imidazolyl)-3-methylbutyl 4-Methylbenzenesulfonate (**A**) was synthesized according to literature procedure.<sup>[4]</sup> All other reagents are commercially available and were used as received.

### 7.5.2. Synthesis and characterisation

#### Synthesis of Cp-functionalised imidazolium salt (*R*)-21

To a solution of freshly distilled cyclopentadiene (600 mg, 9.1 mmol) in dried THF (10 mL) was added drop wise a solution of *n*-butyllithium (5.4 mL, 8.7 mmol, 1.6 M of a solution in hexanes) at -50°C, and the temperature was then allowed to rise to room temperature. After being stirred for 1h, a solution of (*S*)-**A** (560 mg, 1.8 mmol) in dried THF (10 mL) was added at -78°C. The reaction mixture was then stirred for 3

hours and the temperature was warmed up to  $-20^{\circ}\text{C}$ . Hexane (50 mL) was then added, followed by addition of brine (100 mL). The reaction mixture was extracted 3 times with hexane (50 mL) and the organic phase was dried and evaporated to dryness. The remaining oil was dissolved in acetone and iodomethane (0.5 mL, 9 mmol) was added at once. After being stirred overnight at room temperature, the reaction mixture was evaporated to dryness and the remaining solid/oil was washed several times with dry ether. The title compound (*R*)-**21** was isolated as a hygroscopic pale yellow solid (400 mg, 1.2 mmol, 64%).  $^1\text{H}$  NMR (400 MHz,  $\text{CDCl}_3$ ):  $\delta$  10.24 + 10.12 (2s, 1H,  $\text{CH}_{\text{Imid}}$ ), 7.52 (m, 1H,  $\text{CH}_{\text{Imid}}$ ), 7.39 + 7.27 (2m, 1H,  $\text{CH}_{\text{Imid}}$ ), 6.36-6.09 (4m, 3H,  $\text{CH}_{\text{Cp}}$ ), 4.63-4.65 (m, 1H,  $\text{CH}_{\text{(linker)}}$ ), 4.08+4.06 (2s, 3H,  $\text{NCH}_3$ ), 3.16-2.83 (2m, 4H,  $\text{CH}_{2(\text{Cp})} + \text{CH}_{2(\text{linker})}$ ), 2.28-2.15 (m, 1H,  $\text{CH}_{(\text{i-Pr})}$ ), 1.11-1.08 (m, 3H,  $\text{CH}_{3(\text{i-Pr})}$ ), 0.90-0.89 (m, 3H,  $\text{CH}_{3(\text{i-Pr})}$ ).  $\{^1\text{H}\}^{13}\text{C}$  NMR (100 MHz,  $\text{CDCl}_3$ ):  $\delta$  141.97 ( $\text{C}_{\text{Cp}}$ ), 140.6 ( $\text{C}_{\text{Cp}}$ ), 136.7 ( $\text{CH}_{\text{Imid}}$ ), 135.4 + 133.1 + 132.7 132.1 + 130.6 + 130.5 ( $\text{C}_{\text{Cp}}$ ), 123.3 ( $\text{CH}_{\text{Imid}}$ ), 121.2 ( $\text{CH}_{\text{Imid}}$ ), 66.7 ( $\text{CH}_{\text{linker}}$ ), 43.8 + 41.9 ( $\text{CH}_{2(\text{Cp})}$ ), 37.1 ( $\text{NCH}_3$ ), 33.45 + 33.19 + 32.95 + 32.75 ( $\text{CH}_{2(\text{linker})} + \text{CH}_{(\text{i-Pr})}$ ), 19.7 + 19.14 + 18.9 ( $\text{CH}_{3(\text{i-Pr})}$ ).

### Synthesis of iridium **22** and rhodium **23** complexes – general procedure

The ligand precursor (*R*)-**21** (1 eq) was treated with  $\text{Ag}_2\text{O}$  (1.2 eq.) and the mixture was heated under reflux in 1,2-dichloroethane for 1h. Then,  $[\text{M}(\mu\text{-Cl})(\text{cod})]_2$  (0.5 eq, M = Ir and Rh) was added, and the mixture was refluxed for 30 min, followed by addition of glacial acetic acid. After refluxing overnight, the suspension was filtered through Celite, the filtrate evaporated to dryness and KI (5 eq) and methanol were added to the remaining residue. The mixture was then refluxed for a further 1 h. After cooling, the solvent was removed in vacuum and the crude solid was purified by flash chromatography ( $\text{CH}_2\text{Cl}_2$ / acetone).

**Compound (R)-22**

Yield: 35%.  $^1\text{H}$  NMR (400 MHz,  $\text{CDCl}_3$ ):  $\delta$  6.87 (s, 1H,  $\text{CH}_{\text{Imid}}$ ), 6.79 (s, 1H,  $\text{CH}_{\text{Imid}}$ ), 5.65 + 5.37 + 5.27 (3s, 4H,  $\text{CH}_{\text{Cp}}$ ), 4.05 (s, 3H,  $\text{NCH}_3$ ), 3.80 (m, 1H,  $\text{CH}_{\text{(linker)}}$ ), 2.70 (dd, 1H,  $^2J_{\text{H-H}} = 15.4$  Hz,  $^3J_{\text{H-H}} = 5.2$  Hz,  $\text{CH}_2_{\text{(linker)}}$ ), 2.27 (dd, 1H,  $^2J_{\text{H-H}} = 15.4$  Hz,  $^3J_{\text{H-H}} = 3.3$  Hz,  $\text{CH}_2_{\text{(linker)}}$ ), 2.20 (m, 1H,  $\text{CH}_{(\text{i-Pr})}$ ), 1.06 (d, 3H,  $^3J_{\text{H-H}} = 6.9$  Hz,  $\text{CH}_3_{(\text{i-Pr})}$ ), 0.82 (d, 3H,  $^3J_{\text{H-H}} = 6.6$  Hz,  $\text{CH}_3_{(\text{i-Pr})}$ ).  $\{^1\text{H}\}$   $^{13}\text{C}$  NMR (100 MHz,  $\text{CDCl}_3$ ):  $\delta$  137.9 ( $\text{C}_{\text{NHC}}$ ), 121.5 ( $\text{CH}_{\text{Imid}}$ ), 120.9 ( $\text{CH}_{\text{Imid}}$ ), 92.2 ( $\text{CH}_{\text{Cp}}$ ), 90.1 ( $\text{CH}_{\text{Cp}}$ ), 87.5 ( $\text{C}_{\text{Cp}}$ ), 73.3 ( $\text{CH}_{\text{Cp}}$ ), 72.8 ( $\text{CH}_{\text{Cp}}$ ), 68.9 ( $\text{CH}_{\text{(linker)}}$ ), 43.4 ( $\text{NCH}_3$ ), 29.8 ( $\text{CH}_{(\text{i-Pr})}$ ), 23.2 ( $\text{CH}_2_{\text{(linker)}}$ ), 20.1 ( $\text{CH}_3_{(\text{i-Pr})}$ ), 17.5 ( $\text{CH}_3_{(\text{i-Pr})}$ ).

**Compound (R)-23**

Yield: 30%.  $^1\text{H}$  NMR (400 MHz,  $\text{CDCl}_3$ ):  $\delta$  6.99 (s, 1H,  $\text{CH}_{\text{Imid}}$ ), 6.85 (s, 1H,  $\text{CH}_{\text{Imid}}$ ), 5.82 + 5.74 + 5.3 + 5.21 (4s, 4H,  $\text{CH}_{\text{Cp}}$ ), 3.99 (m, 4H,  $\text{NCH}_3$  +  $\text{CH}_{\text{(linker)}}$ ), 2.75 (dd, 1H,  $^2J_{\text{H-H}} = 15.4$  Hz,  $^3J_{\text{H-H}} = 5.1$  Hz,  $\text{CH}_2_{\text{(linker)}}$ ), 2.48 (dd, 1H,  $^2J_{\text{H-H}} = 15.4$  Hz,  $^3J_{\text{H-H}} = 3.5$  Hz,  $\text{CH}_2_{\text{(linker)}}$ ), 2.25 (m, 1H,  $\text{CH}_{(\text{i-Pr})}$ ), 1.07 (d, 3H,  $^3J_{\text{H-H}} = 7.4$  Hz,  $\text{CH}_3_{(\text{i-Pr})}$ ), 0.81 (d, 3H,  $^3J_{\text{H-H}} = 6.0$  Hz,  $\text{CH}_3_{(\text{i-Pr})}$ ).  $\{^1\text{H}\}$   $^{13}\text{C}$  NMR (100 MHz,  $\text{CDCl}_3$ ):  $\delta$  156.1 ( $^1J_{\text{Rh-C}} = 54.1$  Hz,  $\text{C}_{\text{NHC}}$ ), 122.1 ( $\text{CH}_{\text{Imid}}$ ), 121.8 ( $\text{CH}_{\text{Imid}}$ ), 96.1 ( $\text{CH}_{\text{Cp}}$ ), 95.6 ( $\text{C}_{\text{Cp}}$ ), 94.0 ( $\text{CH}_{\text{Cp}}$ ), 81.4 ( $^1J_{\text{Rh-C}} = 6.6$  Hz,  $\text{CH}_{\text{Cp}}$ ), 80.8 ( $^1J_{\text{Rh-C}} = 6.4$  Hz,  $\text{CH}_{\text{Cp}}$ ), 69.0 ( $\text{CH}_{\text{(linker)}}$ ), 44.23 ( $\text{NCH}_3$ ), 30.1 ( $\text{CH}_{(\text{i-Pr})}$ ), 23.8 ( $\text{CH}_2_{\text{(linker)}}$ ), 20.1 ( $\text{CH}_3_{(\text{i-Pr})}$ ), 17.8 ( $\text{CH}_3_{(\text{i-Pr})}$ ).

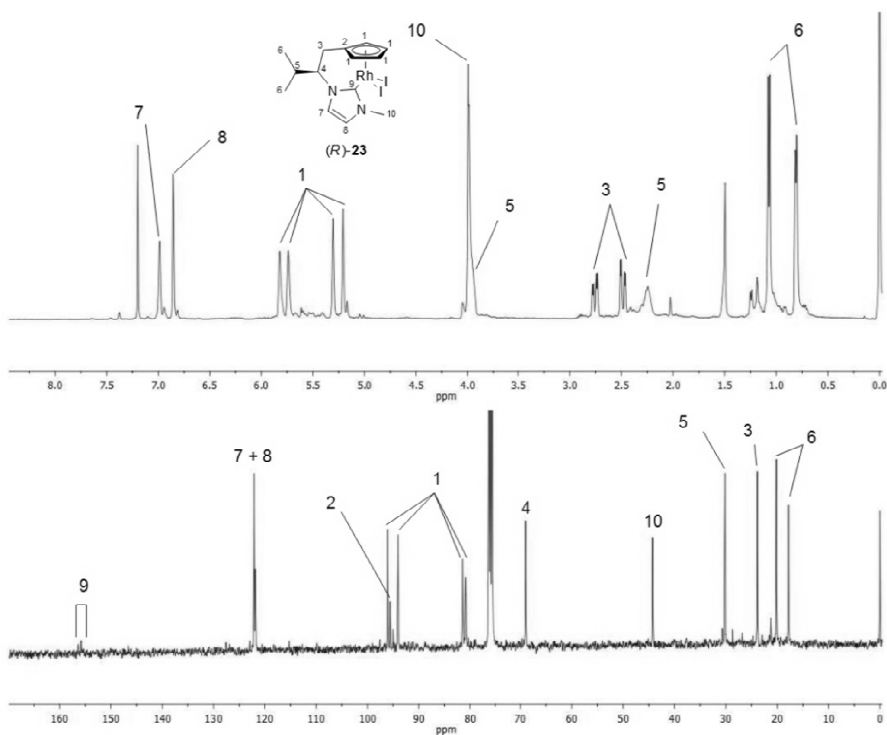
**7.6. Acknowledgements**

We wish to acknowledge M. C. Almeida and Dr. A. Coelho for providing data from the Mass Spectrometry Services at ITQB. The Bruker Avance III 400 MHz spectrometer is part of the National NMR Network and was purchased in the framework of the National Program for Scientific Re-equipment, contract REDE/1517/RMN/2005, with funds from POCI 2010 (FEDER) and Fundação para a Ciência e a Tecnologia (FCT).

## 7.7. References

- [1] R. L. Halterman, *Chem. Rev.* **1992**, 92, 965.
- [2] H. Butenschon, *Chem. Rev.* **2000**, 100, 1527.
- [3] Q. Huang, Y. Qian, *Synthesis* **1987**, 1987, 910.
- [4] U. Nagel, C. Diez, *Eur. J. Inorg. Chem.* **2009**, 2009, 1248.
- [5] C. Diez, U. Nagel, *Appl. Organomet. Chem.* **2010**, 24, 509.
- [6] A. P. da Costa, M. Sanaú, E. Peris, B. Royo, *Dalton Trans.* **2009**, 6960.
- [7] A. P. da Costa, M. Viciano, M. Sanaú, S. Merino, J. Tejada, E. Peris, B. Royo, *Organometallics* **2008**, 27, 1305.
- [8] S. P. Downing, P. J. Pogorzelec, A. A. Danopoulos, D. J. Cole-Hamilton, *Eur. J. Inorg. Chem.* **2009**, 1816.

## 7.8. Supporting information



**Figure 7.6.** (a)  $^1\text{H}$  NMR (400 MHz,  $\text{CDCl}_3$ , 300K) and (b)  $\{^1\text{H}\}^{13}\text{C}$  NMR (100 MHz,  $\text{CDCl}_3$ , 300K) spectra of complex (R)-23.

---

# 8.

## FINAL DISCUSSION

---

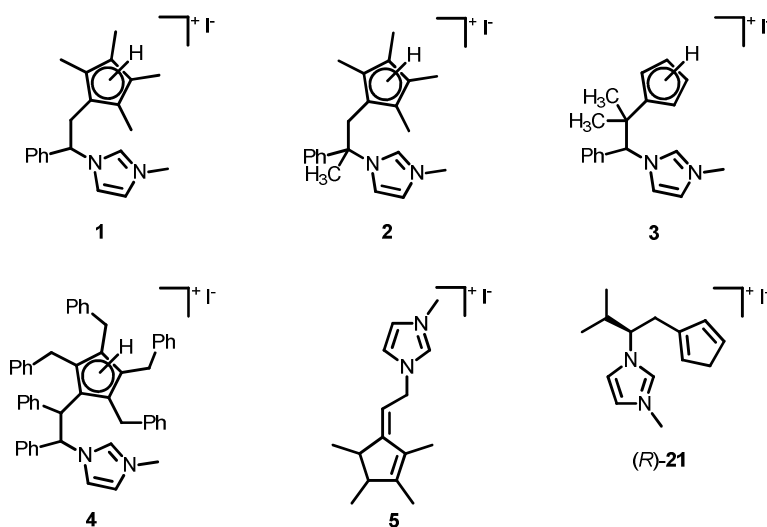
|      |   |     |
|------|---|-----|
| 8.1. | Overview  | 135 |
| 8.2. | Synthesis of Cp-NHC proligands  | 137 |
| 8.3. | Synthesis of metal complexes and their applications in catalysis                  | 139 |
|      | 8.3.1. Synthesis of metal complexes containing the Cp-functionalised NHC ligands, | 139 |
|      | 8.3.2. Synthesis of chiral-at-metal complexes,                                    | 142 |
|      | 8.3.3. Catalysis,   | 143 |
| 8.4. | Conclusions and outlook   | 148 |

Cyclopentadienyl-Functionalised N-Heterocyclic Carbenes:  
Synthesis, Coordination to Mo, Ru, Rh and Ir and Catalytic Applications.

---

## 8.1. Overview

This thesis describes the synthesis of a family of Cp'-functionalised imidazolium salts, depicted in Figure 8.1. The basic architectural design consists of an ethylene linker between the Cp' ring and the N-methyl imidazolium moiety. Different substituents have been introduced in the cyclopentadienyl ring and the linker with the aim to fine tune the electronic and steric properties of the ligand.



**Figure 8.1.** Cp'-functionalised imidazolium salts.

The Cp'-functionalised imidazolium salts were successfully coordinated to Mo, Ru, Rh and Ir, affording a manifold of complexes ranging from half-sandwich with chelating Cp'-functionalised NHC ligand to homo-bimetallic complexes with bridging Cp-NHC ligands, as shown in Figure 8.2. The half-sandwich complexes with chelating Cp'-functionalised NHC ligands were studied in homogeneous catalytic processes, such as olefin epoxidation (Mo); transfer hydrogenation, N-alkylation of amines and  $\beta$ -alkylation of alcohols (Ir) and isomerisation of allylic alcohols (Ru). For the molybdenum and ruthenium complexes, the

preparation of the differently substituted cyclopentadienyls Cp, Cp\* and Cp<sup>Bz</sup> provided a smooth change in the electronic properties of the complexes with implication in catalysis.

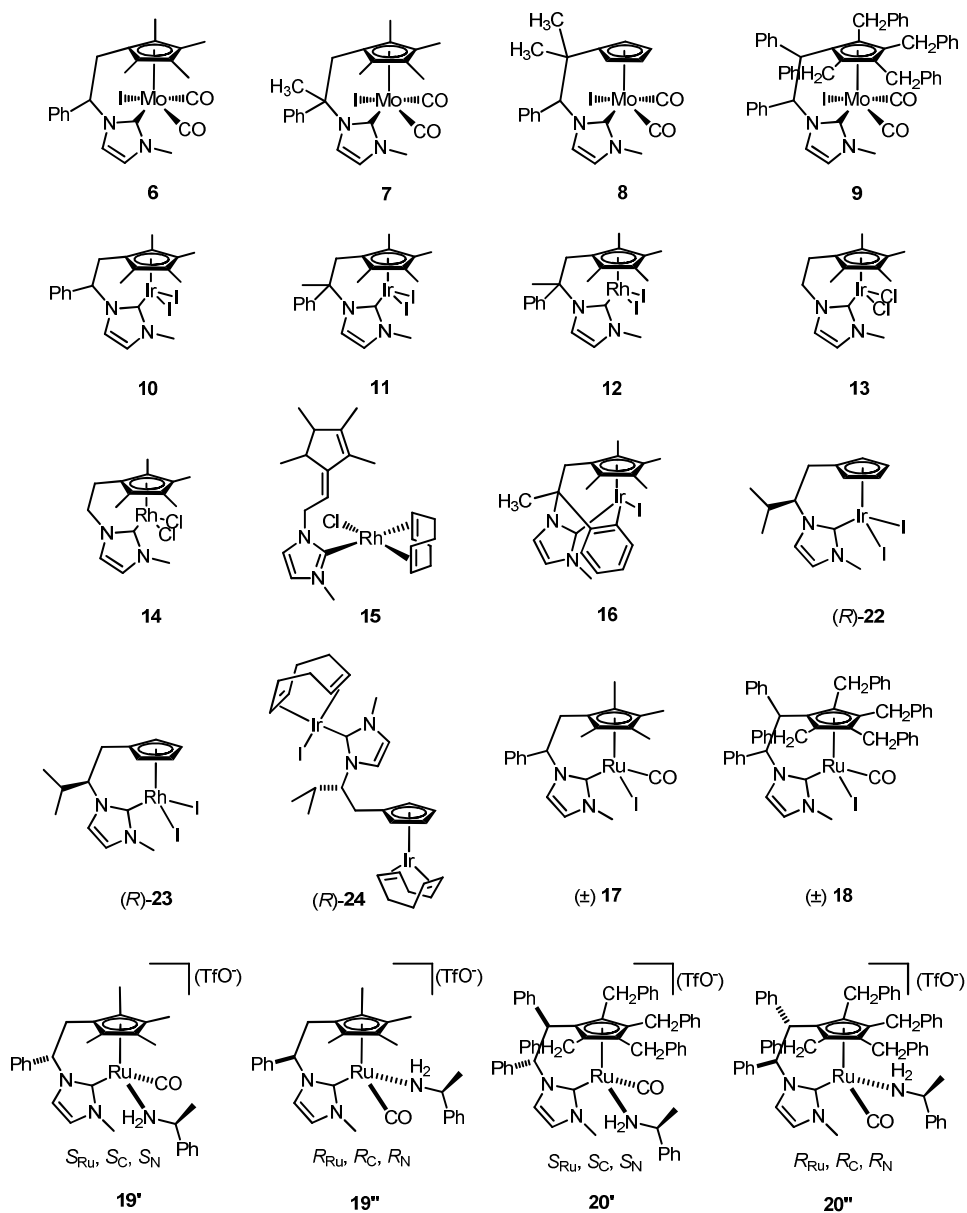


Figure 8.2. Organometallic complexes synthesised.

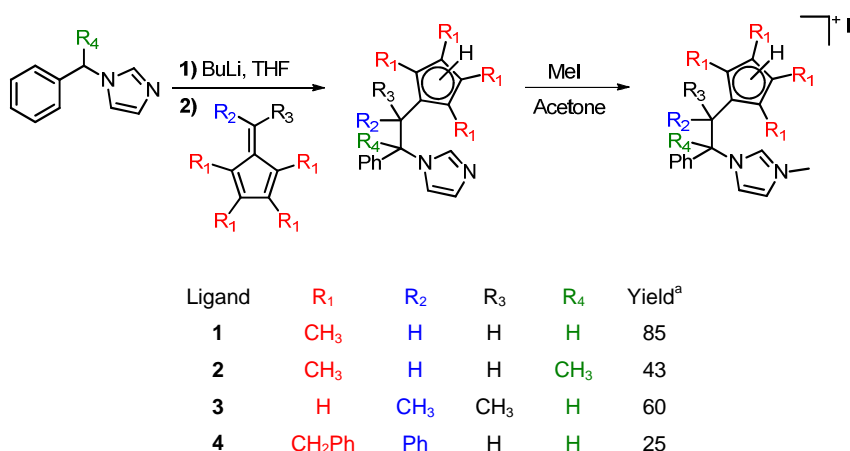


## 8.2. Synthesis of Cp-NHC proligands

The Cp'-functionalised imidazolium salts were synthesised following three different synthetic approaches:

### (i) The fulvene route

The pro-ligands **1**, **3** and **4** were synthesised by deprotonation at the methylene group of 1-benzylimidazole with *n*-butyl lithium, followed by reaction with the corresponding fulvene and treatment with MeOH. Subsequent reaction with iodomethane affords the imidazolium salts in good overall yields, as depicted in Scheme 8.1. This route allows the preparation of a series of Cp'-functionalised imidazolium salts tuning both steric and electronic properties of the Cp' ring.

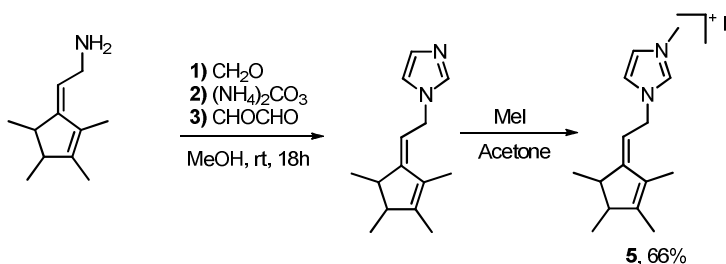


**Scheme 8.1.** Synthesis of proligands **1-4**. <sup>a</sup> Overall yield, based on imidazole.

### (ii) The Cp\*-amine route

The condensation of 2-(2,3,4,5-tetramethylcyclopentadienyl)ethylamine with glyoxal, formaldehyde and ammonium carbonate, followed by quaternization with iodomethane provides a simple and straight-forward

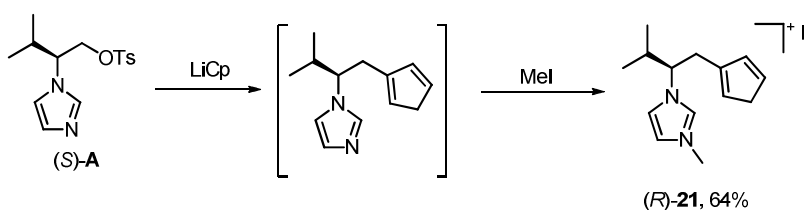
approach to Cp\*-functionalised imidazolium salts. The imidazolium iodide **5** was isolated in 66% overall yield, as depicted in Scheme 8.2. The one pot reaction and easy purification of the final product are the major advantages of this synthetic strategy. However, the isolation of the exocyclic isomer of the cyclopentadiene ring might hamper the coordination of this ligand precursor.



Scheme 8.2. Synthesis of **5**.

### (iii) The L-valinol route

We developed a synthetic approach towards enantiomerically pure Cp-functionalised imidazolium salt (*R*)-**21**, depicted in Scheme 8.3. The L-valinol derivative, imidazole tosylate **A**, was reacted with lithium cyclopentadienyl followed by quaternization with iodomethane to afford the enantiomerically pure pro-ligand **21** in 64% overall yield. The reaction proceeded smoothly towards the products without extensive purification steps needed, apart from extraction and precipitation.



Scheme 8.3. Synthesis of (*R*)-**21**.

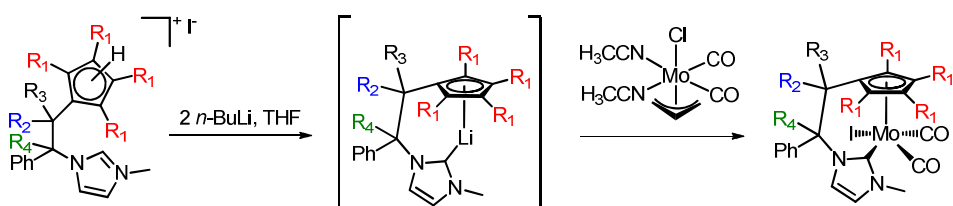
## 8.3. Synthesis of metal complexes and their application in catalysis

### 8.3.1. Synthesis of metal complexes containing the Cp'-functionalised NHC ligands

The Cp'-functionalised imidazolium salts were coordinated following four different strategies depending on the metal centre:

#### (i) Deprotonation by a strong base

Deprotonation of the imidazolium salt with a strong base affords the free carbene, which can coordinate to the desired metal fragment. This strategy was used for the coordination of Cp'-functionalised NHC ligands to molybdenum, as depicted in Scheme 8.3. Both the cyclopentadiene and imidazolium rings were simultaneously deprotonated with two equivalents of *n*-butyl lithium, affording the lithium cyclopentadienyl imidazolylidene, which reacted *in situ* with  $[\text{MoCl}(\eta^3\text{-C}_5\text{H}_5)(\text{CO})_2(\text{NCCH}_3)_2]$  yielding complexes **6-9**.



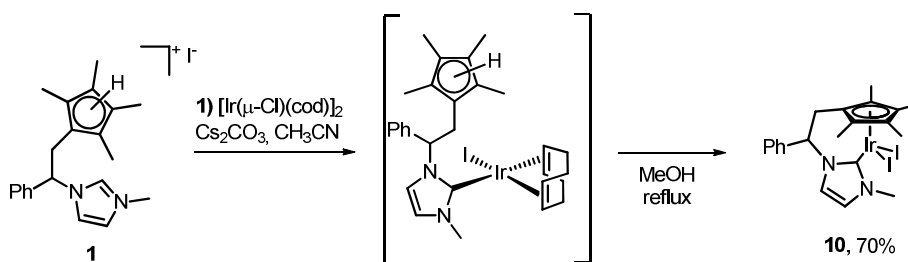
| Ligand | R <sub>1</sub>     | R <sub>2</sub>  | R <sub>3</sub>  | R <sub>4</sub>  | Complex | Yield (%) |
|--------|--------------------|-----------------|-----------------|-----------------|---------|-----------|
| 1      | CH <sub>3</sub>    | H               | H               | H               | 6       | 77        |
| 2      | CH <sub>3</sub>    | H               | H               | CH <sub>3</sub> | 7       | 55        |
| 3      | H                  | CH <sub>3</sub> | CH <sub>3</sub> | H               | 8       | 48        |
| 4      | CH <sub>2</sub> Ph | Ph              | H               | H               | 9       | 63        |

Scheme 8.4. Synthesis of complexes **6-9**.

## (ii) *In situ* deprotonation by weak base

The coordination of imidazolium salt to late transition metals can be achieved by reaction with a weak base. This strategy was used to coordinate the imidazolium salt **1** to Ir. As depicted in Scheme 8.5, the imidazolium salt was reacted with  $[\text{Ir}(\mu\text{-Cl})(\text{cod})]_2$  in the presence cesium carbonate followed by refluxing methanol to afford complex **10** with the chelating ligand.

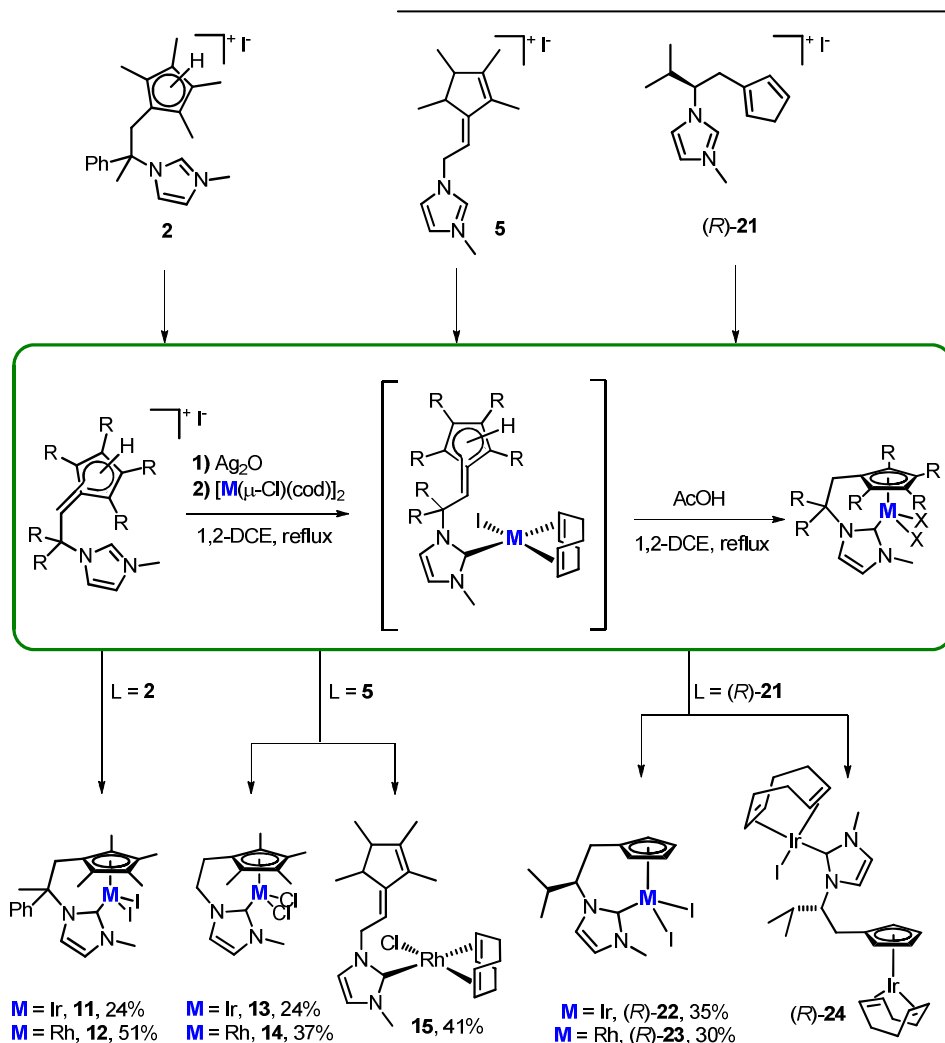
Although we made no attempts to isolate any intermediate of the reaction, it is reasonable to assume that the NHC fragment coordinates to Ir in the weak basic media, while C-H activation of the cyclopentadiene occurs in refluxing methanol.



Scheme 8.5. Synthesis of the Ir complex **10**.

## (iii) Transmetalation from preformed silver-NHCs

The reaction of an imidazolium salt with  $\text{Ag}_2\text{O}$  affords the Ag-NHC adduct, which can transmetallate the carbene to a variety of transition metals. This strategy was used in the coordination of imidazolium salts **2**, **5** and (*R*)-**21** to rhodium and iridium affording the metal complexes **11-15** and **22-24**, as shown in Scheme 8.6. The *in situ* pre-formed Ag-NHC complexes were transmetalated to  $[\text{M}(\mu\text{-Cl})(\text{cod})]_2$  ( $\text{M} = \text{Ir}, \text{Rh}$ ), followed by acid-promoted C-H activation of the cyclopentadiene moiety. For the imidazolium salt **5**, the Rh(I)-intermediate **15** was isolated and characterised.

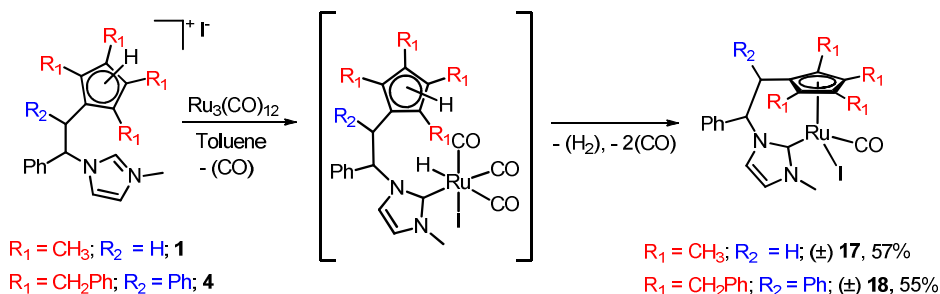


Scheme 8.6. Synthesis of complexes 11-15 and 22-24.

**(iv) Oxidative addition**

Imidazolium salts can coordinate to electron-rich metals by oxidative addition, affording the corresponding M-NHC complexes. This strategy was applied for the coordination of Cp'-functionalised imidazolium salts **1** and **4** to ruthenium, as depicted in Scheme 8.7. The corresponding imidazolium salts were reacted with  $\text{Ru}_3(\text{CO})_{12}$  cluster in refluxing toluene, affording complexes **17** and **18**.

Probably, the first step of the reaction is the oxidative addition of the imidazolium salt to the Ru(0) center, followed by hydrogen release to afford the half-sandwich complexes with the chelating ligand.

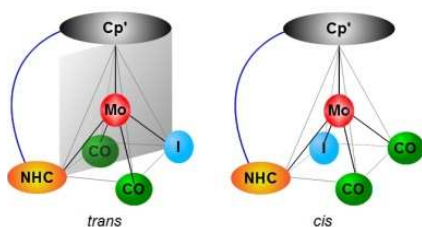


**Scheme 8.7.** Synthesis of complexes **17** and **18**.

### 8.3.2. Synthesis of chiral-at-metal complexes

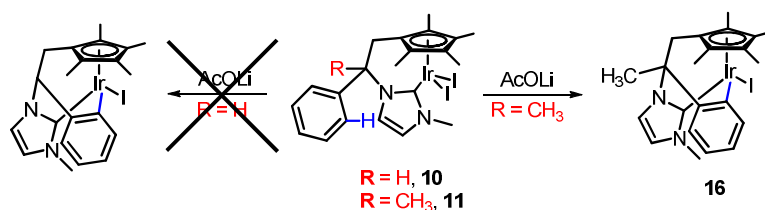
We successfully isolated chiral-at-metal Cp'-functionalised NHC complexes of molybdenum, iridium and ruthenium. However, both the molybdenum and iridium chiral-at-metal complexes were isolated as racemic mixtures. The ruthenium complexes were separated to afford enantiomerically pure chiral-at-metal complexes.

For the molybdenum complexes, the *cis* isomer is chiral, while the *trans* isomer has a symmetry plane containing the Mo, I and C<sub>NHC</sub> atoms (Figure 8.3).



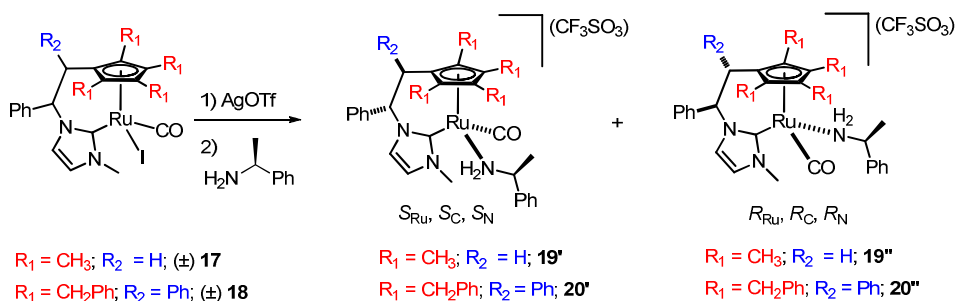
**Figure 8.3.** Isomers of the molybdenum complexes.

The isolated (Cp'-NHC)IrX<sub>2</sub> complexes are not chiral-at-metal, although the intra-molecular C-H activation afforded the chiral-at-metal *ortho*-metallated complex **16**, as shown in Scheme 8.8. For the cyclometallation to occur, the phenyl group must be oriented close to the metal centre; therefore the less sterically hindered complex **10** did not react under the same reaction conditions.



**Scheme 8.8.** Intramolecular C-H activation reactivity of complexes **10** and **11**.

The coordination of Cp'-functionalised NHC ligands to ruthenium afforded racemic mixtures of compounds **17** and **18**. The abstraction of the iodide ligand and coordination of an enantiomerically pure amine proceeded smoothly towards the formation of only two diastereoisomers, as shown in Scheme 8.9. The diastereoisomers were successfully separated by preparative thin-layer chromatography, although in low yields.

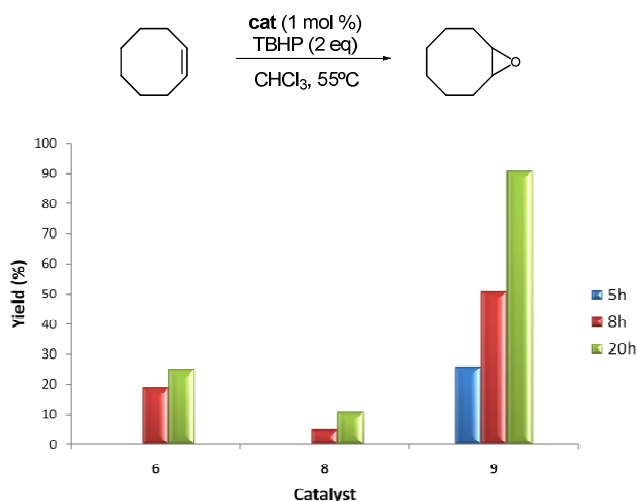


**Scheme 8.9.** Synthesis of enantiomerically pure ruthenium complexes **19** and **20**.

### 8.3.3. Catalysis

The molybdenum complexes **6**, **8** and **9** were tested in the catalytic epoxidation of *cis*-cyclooctene using *tert*-butylhydroperoxide as oxidant.

The results showed that the change in the electronic and steric properties of the Cp' moiety clearly influences the catalytic activity of the organometallic complex. The Cp<sup>Bz</sup>-functionalised complex **9** was the most active catalyst, affording 91% yield of the corresponding epoxide after 20 hours of reaction. The catalytic results are summarised in Figure 8.4.



**Figure 8.4.** Cyclooctene catalytic epoxidation with complexes **6**, **8** and **9**. Reaction conditions: 55°C in CHCl<sub>3</sub>. Catalyst : cyclooctene : TBHP ratio of 1 : 100 : 200.

The ruthenium compounds **17** and **18** were tested in the catalytic isomerization of allylic alcohols. Again, the results showed that the electronic and steric properties of the Cp' moiety influence the catalytic activity of the catalysts. The more sterically crowded complex **18**, shows very low activity, while **17** is very active both in THF or H<sub>2</sub>O. The activity of the catalyst **17** in H<sub>2</sub>O was high, although we needed to increase the temperature to 75°C (reactions in THF are performed at 55°C), for which full conversions were achieved even with catalyst loadings as low as 0.2 mol % (entries 2, 7, 10, 11 and 12). The catalytic results are summarised in Table 8.1.



**Table 8.1.** Catalytic isomerisation of allylic alcohols.<sup>a</sup>

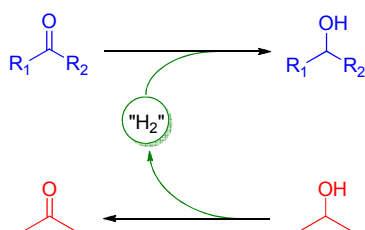
| Entry | Substrat | Cat. <sup>b</sup> | Cat. Load (mol%) | Solv.            | T (°C) | t (h) | Yield (%) <sup>c</sup> |
|-------|----------|-------------------|------------------|------------------|--------|-------|------------------------|
| 1     |          | <b>17</b>         | 1                | THF              | 55     | 1     | 99                     |
| 2     |          | <b>17</b>         | 0.2              | H <sub>2</sub> O | 75     | 2     | 99                     |
| 3     |          | <b>17</b>         | 1                | THF              | rt     | 6     | 99                     |
| 4     |          | <b>17</b>         | 1                | THF              | 55     | 3     | 99                     |
| 5     |          | <b>17</b>         | 1                | THF              | 75     | 0.33  | 99                     |
| 6     |          | <b>18</b>         | 1                | THF              | 55     | 24    | 20                     |
| 7     |          | <b>17</b>         | 0.2              | H <sub>2</sub> O | 75     | 4     | 99                     |
| 8     |          | <b>17</b>         | 1                | THF              | 55     | 3     | 99                     |
| 9     |          | <b>18</b>         | 1                | THF              | 55     | 24    | 25                     |
| 10    |          | <b>17</b>         | 0.2              | H <sub>2</sub> O | 75     | 4     | 99                     |
| 11    |          | <b>17</b>         | 0.2              | H <sub>2</sub> O | 75     | 4     | 99                     |
| 12    |          | <b>17</b>         | 0.2              | H <sub>2</sub> O | 75     | 24    | 20                     |
| 13    |          | <b>17</b>         | 1                | THF              | 55     | 24    | 60                     |

<sup>a</sup> Reactions carried out with 0.4 mmol of substrate in 0.5 mL of THF or 4 mL H<sub>2</sub>O. <sup>b</sup> Activated by Ag(O<sub>3</sub>SCF<sub>3</sub>), 10 min at rt. <sup>c</sup> Yield determined by <sup>1</sup>H NMR.

The iridium complexes **10** and **13** were studied in hydrogen borrowing catalysis, such as transfer hydrogenation (**10**),  $\beta$ -alkylation of secondary alcohols (**10** and **13**) and N-alkylation of amines (**10** and **13**).

Complex **10** is active in the catalytic transfer hydrogenation of both aliphatic and aromatic ketones even at low catalyst loadings. The high turnover numbers (TONs) obtained indicate that the catalyst is stable under the reaction conditions used. The catalytic results are summarised in Table 8.2.

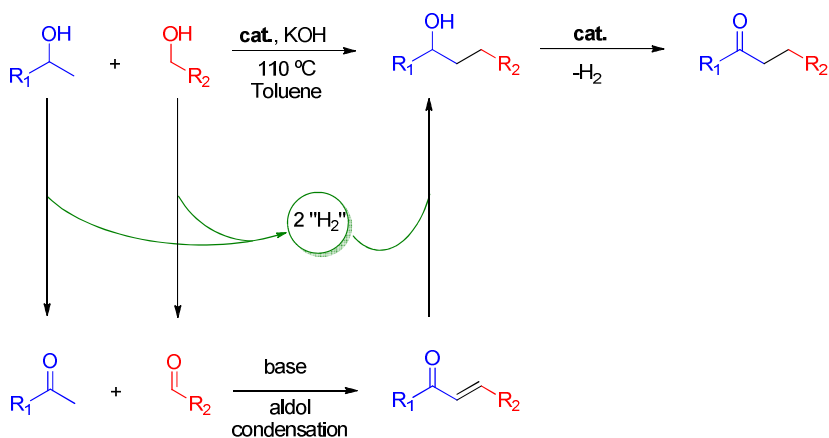
**Table 8.2.** Catalytic transfer hydrogenation.<sup>a</sup>



| entry | catalyst  | substrate     | % cat | t (h) | TON  | % yield |
|-------|-----------|---------------|-------|-------|------|---------|
| 1     | <b>10</b> | acetophenone  | 0.1   | 5.5   | 990  | >99     |
| 2     | <b>10</b> | cyclohexanone | 0.1   | 2.5   | 870  | 87      |
| 3     | <b>10</b> | cyclohexanone | 0.1   | 4.5   | 990  | >99     |
| 4     | <b>10</b> | cyclohexanone | 0.01  | 20    | 9900 | >99     |
| 5     | <b>10</b> | benzophenone  | 0.1   | 2     | 130  | 13      |
| 6     | <b>10</b> | benzophenone  | 0.1   | 8     | 990  | >99     |

<sup>a</sup> 2 mmol of ketone, KOH (10 mL, 0.2M in *i*-PrOH), T = 80 °C. Yields determined by <sup>1</sup>H NMR spectroscopy.

Complexes **10** and **13** are active in the  $\beta$ -alkylation of secondary alcohols even at low catalyst loadings (1 mol%). Aromatic primary alcohols gave better selectivity than aliphatic alcohols to the desired alcohols, and also needed shorter reaction times to achieve full conversions. Dehydrogenation of the resulting alcohol to the corresponding ketone is observed when the catalytic reaction is kept for longer reaction times (see entries 5, 6 and 7, 8). The results are summarised in Table 8.3.

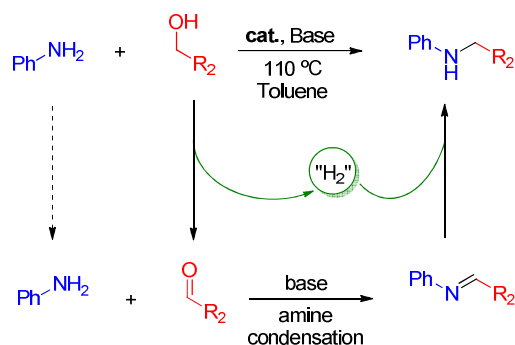
**Table 8.3.**  $\beta$ -alkylation of secondary alcohols with primary alcohols.<sup>a</sup>

| entry | catalyst  | R <sub>1</sub> | R <sub>2</sub>                       | t (h) | % conv | % alcohol | % ketone |
|-------|-----------|----------------|--------------------------------------|-------|--------|-----------|----------|
| 1     | <b>10</b> | Ph             | Ph                                   | 3     | 70     | 100       | 0        |
| 2     | <b>10</b> | Ph             | Ph                                   | 6     | 90     | 100       | 0        |
| 3     | <b>10</b> | Ph             | Ph                                   | 9     | >95    | 100       | 0        |
| 4     | <b>10</b> | Ph             | Ph                                   | 24    | >99    | 100       | 0        |
| 5     | <b>10</b> | Ph             | 4-Cl(C <sub>6</sub> H <sub>4</sub> ) | 6     | 87     | 100       | 0        |
| 6     | <b>10</b> | Ph             | 4-Cl(C <sub>6</sub> H <sub>4</sub> ) | 9     | 100    | 50        | 50       |
| 7     | <b>10</b> | Ph             | Pr                                   | 3     | 100    | 80        | 20       |
| 8     | <b>10</b> | Ph             | Pr                                   | 6     | 100    | 50        | 50       |
| 9     | <b>13</b> | Ph             | Ph                                   | 3     | 70     | 100       | 0        |
| 10    | <b>13</b> | Ph             | Ph                                   | 6     | 80     | 100       | 0        |
| 11    | <b>13</b> | Ph             | Ph                                   | 24    | >99    | 100       | 0        |

<sup>a</sup> 1 mmol of primary and secondary alcohol, 1 mmol (100 mol%) of KOH, 0.3 mL of toluene, 1 mol % cat., T = 110 °C. Conversions and yields determined by <sup>1</sup>H NMR spectroscopy.

Complex **10** was able to facilitate the alkylation of aniline with aliphatic and aromatic primary alcohols in moderate to good yields. Complex **13** was tested for the alkylation of aniline with benzyl alcohol. These results are summarised in Table 8.4.

**Table 8.4.** N-alkylation of aniline with primary alcohols.<sup>a</sup>



| entry          | catalyst  | alcohol        | base               | t (h) | % yield |
|----------------|-----------|----------------|--------------------|-------|---------|
| 1 <sup>b</sup> | <b>10</b> | benzyl alcohol | KOH                | 9     | 54      |
| 2              | <b>10</b> | benzyl alcohol | KOH                | 25    | 67      |
| 3              | <b>10</b> | benzyl alcohol | KOH                | 45    | 76      |
| 4              | <b>10</b> | benzyl alcohol | KO <sup>t</sup> Bu | 16    | 85      |
| 5              | <b>10</b> | 1-butanol      | KO <sup>t</sup> Bu | 16    | 47      |
| 6              | <b>10</b> | 1-butanol      | KO <sup>t</sup> Bu | 24    | 55      |
| 7              | <b>13</b> | benzyl alcohol | KO <sup>t</sup> Bu | 17    | 93      |

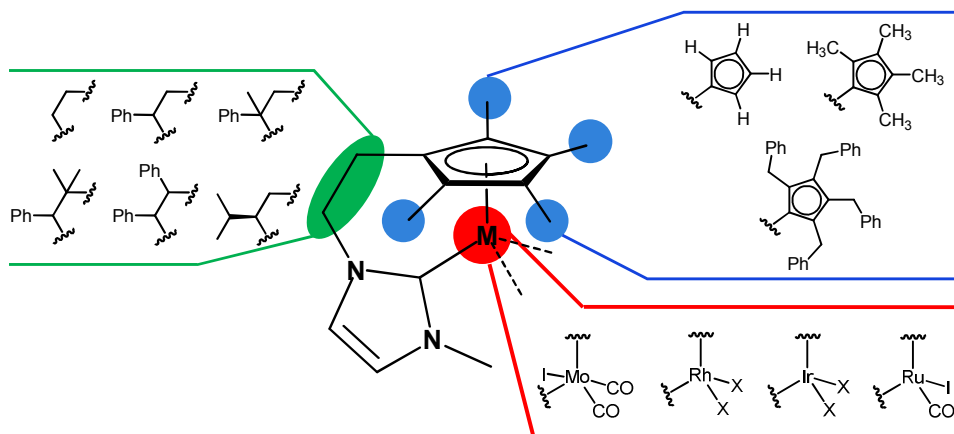
<sup>a</sup> 2mmol of aniline and alcohol, 2 mmol (100 mol %) of base, 0.3 mL of toluene, 0.75 mol % cat., T = 110 °C. Yields determined by <sup>1</sup>H NMR. <sup>b</sup> 50 mol % base and 2.5 mol % of catalyst.

## 8.4. Conclusions and outlook

In this thesis we describe the synthesis of a series of Cp'-functionalised imidazolium salts, featuring topological variations of the linker between the two moieties and both electronic and steric control of the cyclopentadienyl group. The imidazolium salts were coordinated to Mo, Rh, Ir and Ru, affording an array of new organometallic complexes, as outlined in Figure 8.5.

The new metal complexes were successfully applied as catalysts in a variety of organic transformations, such as: olefin epoxidation (Mo);

transfer hydrogenation, N-alkylation of amines and  $\beta$ -alkylation of alcohols (Ir) and allyl alcohol isomerization (Ru).



**Figure 8.5.** Cp'-functionalised NHCs: coordination to Mo, Ru, Rh and Ir.

Currently, our research groups are focused in two topics: (i) the study of the asymmetric induction in catalytic processes by using the enantiomerically pure complexes (*R*)-**22** and (*R*)-**23** as catalysts; and (ii) the coordination of these type of ligands to other metal centers, namely to first row transition metals.

ITQB-UNL | Av. da República, 2780-157 Oeiras, Portugal  
Tel (+351) 214 469 100 | Fax (+351) 214 411 277

[www.itqb.unl.pt](http://www.itqb.unl.pt)